# ELUCIDATING THE ROLE OF THE TGF-β SUPERFAMILY SIGNALING IN PULMONARY VASCULAR CELL PROLIFERATION

By

Kit Yee Chu

A DISSERTATION

Submitted to
Michigan State University
in partial fulfillment of the requirements
for the degree of

Biochemistry and Molecular Biology – Doctor of Philosophy

2023

## ABSTRACT

Pulmonary arterial hypertension is a fatal disease characterized by the remodeling of the pulmonary vasculature. The aberrant proliferation of pulmonary arterial endothelial cells and smooth muscle cells is the primary factor contributing to vascular obstruction and the development of plexiform lesions. It is known that germline mutations in BMPR2 (~70%), ALK1, BMP9, and BMP10 are associated with both familial PAH and idiopathic PAH, indicating that TGF-β signaling plays a significant role in PAH. Even in the absence of BMPR2 mutations, there is a decrease in BMPR2 signaling and an increase in TGF-β signaling. Therefore, the imbalance of BMPR2/TGF-β signaling may contribute to the pathogenesis of PAH. However, the molecular mechanisms behind the imbalance of BMPR2/TGF-β signaling that result in the proliferation of pulmonary vasculature cells are still not fully understood. The fact that TGF-growth factors can interact with multiple TGF-type II receptors or that different growth factors can bind to the same receptors makes TGF signaling more complex. In this dissertation, I concentrate on TGF-β signaling focusing on two major aspects. One of my hypotheses is that mutations in the BMPR2 gene may alter their binding affinity to growth factors, changing their preference for binding and possibly triggering a signaling switch. The pro-proliferative status in pulmonary artery endothelial cells and pulmonary arterial smooth muscle cells could arise from these changes in PAH. In this dissertation, I aim to explore the interactions between the TGF-β growth factors and the TGF-β Type II receptor BMPR2, as well as compare the growth factor binding sites of Type II receptors. Furthermore, I intend to examine the impact of BMPR2 mutations identified in PAH patients on receptor binding interactions and elucidate the role of TGF-β signaling in pulmonary arterial endothelial cell proliferation. This will enhance our understanding of the mechanistic role of TGF-β signaling in PAH.

## ACKNOWLEDGMENTS

I would like to express my deepest appreciation and gratitude to all those who provided invaluable support, guidance, and encouragement throughout my PhD year. This accomplishment would not have been possible without their contributions. First and foremost, I thank my advisor, Dr. Erik Martinez-Hackert. I am grateful to have you as my PI. You provided great support, valuable feedback, and immense knowledge. I will always remember the one important sentence you said, “Look at the data!!!” Your guidance and expertise were instrumental in shaping my research and making me into an independent scientific researcher who always strives for the highest standards.

I am also grateful to my committee members, Dr. Amy Ralston, Dr. Brian Schutte, Dr. Bill Henry, and Dr. John Lapres, who provided valuable insights, suggestions, and expertise throughout the process. Your input shaped my critical thinking about being a scientist.

I would like to express my gratitude to the present and past lab members, including Dr. Senem Aykul, Dr. Viji Thamilselvan, Dr. Anjali Malik, Amber Crawford, Nina Aitas, and Madelynn Herber. The lab dynamic is awesome, and I enjoy working with each and every one of them. In particular, Amber always brings in delicious and beautifully decorated cakes and cookies (cream cheese frosting is the best), which provides a great energy boost for every day in the lab.

I also want to thank the DO/PhD program, Dr. Brian Schutte, and Michelle Volker for their constant support and help to ensure that my journey in the program goes smoothly. Your efforts are greatly appreciated, and I always felt secure being part of this big, warm DO/PhD family.

I would like to express my gratitude to the biochemistry department and its staff, who supported me in countless ways throughout my PhD journey, making me feel welcome here. Firstly, I want to thank Dr. David Arnosti, who always cares about students and arranges pizza "parties"

for us. I also want to thank Jessica for assisting me with tuition issues and Pappan for helping me with technical issues and printing my posters, as well as for his valuable time chatting with me in the hallway.

Furthermore, I want to express my gratitude to table tennis, which has been a significant part of my life. Thanks to table tennis, I have had the opportunity to meet many amazing people from all over the world, and it has become an excellent stress reliever for me. Whenever I feel stressed and encounter difficulties, I turn to the words of my idol, Ma Long. He is the one who taught me to keep fighting, never give up, and pursue my passions.

I am also deeply grateful to my family and friends for their unconditional love, support, and patience throughout this journey. To my parents, who have always believed in me and encouraged me to follow my dreams, even though I don't have a job yet. I also want to thank the friends I met at Michigan State, including Ana-Maria Raicu, whom I met during the BMS interview and decided to eat donuts with during comprehensive exam preparation at the library. She has been the biggest support during these six years, and without her, grad school probably would be a lot different. I am very fortunate to have AM as my best friend ever. I am also very grateful to have friends like Aiko Turmo, Basma Klump, and Mariia Mikhova, who wrote furiously with me, and my amazing DO/PhD cohorts, Brad Ryva, Nick Giacobbi, Alan Halim, Melissa Meschkewitz, Megan Russ, Nick Chargo, and John Baker, without whom I could not survive med school. Thank you all for keeping me sane during school, and I love you all!

Finally, I would like to thank my cute doggie, Loki, who is the best dog ever and a very patient boy, even though I sometimes don't have time to play ball with him and always drag him to study with me and stay up with me for late nights. Once again, I am deeply grateful to everyone

who has contributed to the successful completion of my PhD journey. Your support has made all the difference.

## TABLE OF CONTENTS

## LIST OF ABBREVIATIONS

| | |
|---|---|
| ActRIIA | Activin receptor type IIA |
| ALK1 | Activin receptor-like kinase 1 |
| AMH | Anti-Müllerian hormone |
| BiMAb | Bimagrumab |
| BMP | Bone morphogenetic protein |
| BMP10 | Bone morphogenetic proteins-10 |
| BMP9 | Bone morphogenetic proteins-9 |
| BMPR2 | Bone morphogenetic protein receptor type II |
| BrdU | Bromodeoxyuridine |
| BRE | BMP responsive element |
| CaSR | Extracellular calcium-sensing receptor |
| CHO | Chinese hamster ovary |
| CM | Conditioned medium |
| ECM | Extracellular matrix |
| EGFR | Epidermal growth factor receptor |
| EMEM | Eagle's minimum essential medium |
| ENG | Endoglin |
| ER | Endoplasmic reticulum |
| ET-1 | Endothelin-1 |
| FGF-2 | Fibroblast growth factor-2 |
| FSH | Follicle-stimulating hormone |
| GBD | GF-binding domain |

| | |
|---|---|
| GDF11 | Growth differentiation factor 11 |
| GFs | Growth factors |
| HEK293 | Human embryonic kidney 293 |
| HMVEC-LBl | Human microvascular endothelial cells |
| HHT | Hereditary hemorrhagic telangiectasia |
| IgG1 | Immunoglobulin G1 |
| LH | Luteinizing hormone |
| LTBPs | Latent TGF-β binding proteins |
| MCT | Monocrotaline |
| mPAP | mean pulmonary artery pressure |
| NCS | noncrystallographic symmetry |
| NO | nitric oxide |
| PAECs | Pulmonary arterial endothelial cells |
| PAH | Pulmonary arterial hypertension |
| PASMCs | Pulmonary arterial smooth muscle cells |
| PDGF | Platelet-derived growth factor |
| PVR | pulmonary vascular resistance |
| qPCR | quantitative real-time PCR |
| RT | Room temperature |
| RU | responsive units |
| SBE | SMAD binding element |
| SEC | size-exclusion chromatography |
| SLC | Small latent complex |

| | |
|---|---|
| SPR | surface plasmon resonance |
| SU5416 | Sugen 5416 |
| TGF-β | Transforming growth factor beta superfamily |
| VEGF | Vascular endothelial growth factor |

# CHAPTER 1

# INTRODUCTION

## HUMAN BLOOD CIRCULATION: PULMONARY CIRCULATION AND CARDIOVASCULAR CIRCULATION

The human circulation system is crucial for the transport of blood throughout the body, providing nutrients and oxygen to the body's tissues and organs and removing waste products such as carbon dioxide. The circulatory system consists of the heart, blood vessels (arteries, veins, and capillaries), and blood. The blood circulatory system operates as a highly integrated network. Therefore any disruption or dysfunction in one part of the system can have far-reaching consequences for the body's overall health, disrupting homeostasis and potentially leading to a range of health problems. There are two major circulations: pulmonary circulation and cardiovascular circulation [1]. Pulmonary circulation is responsible for the transport of deoxygenated blood from the heart to the lungs and gas exchange happens in the lung and oxygenated blood goes back to the heart and that is when cardiovascular circulation begins [2]. These two circulation system works in coordination to ensure that oxygenated blood is delivered to the body's tissues while also ensuring that carbon dioxide is eliminated from the body.

In pulmonary circulation, deoxygenated blood is pumped from the right ventricle of the heart to the lungs via the pulmonary artery. Once in the lungs, the blood is oxygenated through gas exchange with the air in the lungs. Oxygenated blood then returns to the heart via the pulmonary veins, entering the left atrium and subsequently the left ventricle, out of the aorta, where it is then pumped out to the rest of the body through the systemic circulation [2]. Once the oxygenated blood left the heart through the aorta. It travels via arteries to different body tissues and organs. When they reached certain organs, the size of the arteries will become narrower until it becomes capillaries, which are small, thin-walled blood vessels that allow for the exchange of nutrients, oxygen, and waste products between the blood and the body's tissues. Capillaries then merge to

form veins, which carry deoxygenated blood back to the heart (Fig 1.1).

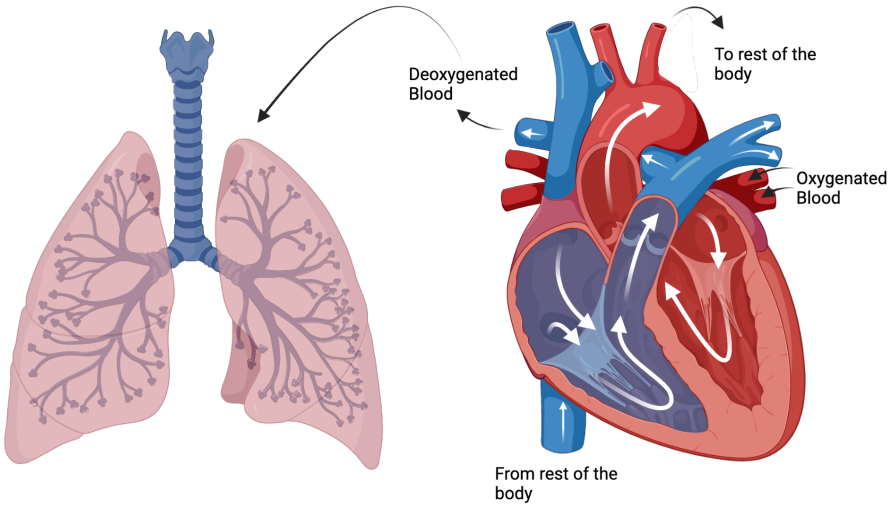


Figure 1.1: Overview of human blood circulation. Pulmonary circulation transports deoxygenated blood from the heart to the lungs for oxygenation and then returns oxygen-rich blood back to the heart. Cardiovascular circulation proceeds as oxygenated blood travels from the heart through the aorta to the rest of the body, supplying nutrients and removing waste from organs. Created with BioRender.com.

Overall, the circulatory system is crucial for maintaining homeostasis, Any disruption to this system can have significant consequences for the body's overall health. Diseases that affect the circulatory system include atherosclerosis, peripheral artery disease, and congestive heart failure, while pulmonary embolism and pulmonary arterial hypertension are examples of diseases affecting pulmonary circulation [3]. It's worth noting that these diseases can affect both circulations, given their interconnectivity. Symptoms and risk factors vary for each disease, but all require prompt diagnosis and treatment to prevent further complications. Pulmonary arterial hypertension, for instance, is a progressive and life-threatening condition that often leads to heart failure and requires a lung transplant [3]. As a result, there is ongoing research aimed at better understanding the disease's causes, improving diagnostic tools, and finding more effective treatments for patients.

## PULMONARY ARTERIAL HYPERTENSION

### Significance of PAH

Pulmonary arterial hypertension (PAH) is a severe and progressive condition characterized by high blood pressure in the pulmonary arteries, which can lead to right-sided heart failure and death. PAH is one of the five subgroups of pulmonary hypertension and has an aggressive nature, low survival rate, and few treatment options [4, 5]. It has significant morbidity and mortality rates, with a median survival of approximately 2.8 years after diagnosis if left untreated [6]. PAH can occur as an idiopathic condition or as a secondary complication of other medical conditions, such as connective tissue diseases, HIV infection, portal hypertension, and congenital heart diseases. Other risk factors include exposure to certain drugs and toxins such as recreational drugs, such as cocaine and methamphetamines [7].

The global prevalence of PAH is about 1% with an incidence of 2-5 per million adults. Unfortunately, the numbers are still rising [8]. PAH can affect individuals of all ages, there are significant differences in the incidence, prevalence, and median survival of PAH. Individuals between the ages of 30 and 60 years old are the most common age group that is being diagnosed [9]. There has been an increased number of elderly people being diagnosed with heart failure becomes a leading cause that's affecting around 10% of elderly aged 65 years or older [10]. There is also a huge number of children each year that are being diagnosed with PAH. The annual incidence of PAH in children ranged from 25.7-32.6 per million population, and the prevalence ranged from 4.8-8.1 per million population [11]. The median survival of children with PAH is poor compared to that of adults, with a median survival of 8 months for children not treated with targeted drugs after diagnosis of PAH compared to 2.8 years for adults. This difference may be related to a greater genetic load and delayed treatment in children with atypical initial symptoms. Despite the

difference in prevalence and incidence in age difference, there is also a difference in the sex ratio, the female-to-male ratio is approximately 3.6:1 in adults with PAH. In recent years, with the clinical application of targeted drugs and optimization of treatment strategies, the 3-year survival rate of idiopathic PAH can reach 75.1%, and the 5-year survival rate of PAH patients has increased from about 20% to more than 50%. Overall, a study reported that survival rates had improved over time, with patients diagnosed in 2010-2014 having better survival rates than those diagnosed in 2000-2004 (3-year survival rate of 83.1% vs. 69.6%) [12]. While there have been significant advancements in the treatment of PAH, there are still some challenges associated with recent therapies. Many improve patients' life quality, but they may not necessarily improve long-term outcomes such as survival or disease progression. Therefore despite improvements in survival rates, PAH remains a progressive and ultimately fatal disease for many patients. Therefore, there is a continued need for research into new therapies and a better understanding of the underlying mechanisms of the disease.

**Diagnostic tools**

The latest gold standard for diagnosing pulmonary hypertension is a resting mean pulmonary artery pressure (mPAP) of ≥25 mmHg (1 mmHg = 0.133 kPa), measured by right heart catheter at rest at sea level. It can also be defined as an mPAP with exercise >30 mm Hg [4]. For diagnosing pulmonary arterial hypertension, there is an additional criterion that the pulmonary arterial wedge pressure must be >15 mm Hg and pulmonary vascular resistance (PVR), requiring that it be 2 or 3 Wood units [13]. For screening and diagnosis, there are non-invasive and invasive ways. Often times, doppler echocardiography is a commonly used modality for screening and managing PAH [14, 15]. It can measure several parameters including PAP, tricuspid regurgitation, and right ventricular size and function. Essentially, it is a type of ultrasound imaging that uses

high-frequency sound waves to evaluate the blood flow through the heart and blood vessels. Patients exhibit elevated PAP, often accompanied by increased right ventricular wall thickness and right atrial chamber enlargement which can all be detected by doppler echocardiography. Other non-invasive measurements include Chest X-ray and pulmonary function tests. With all the non-invasive methods, it aids in the screening and management of PAH. The downside of these methods is the lack of accuracy and specificity of diagnosis. Right heart catheterization is the gold standard for diagnosing PAH, and it is an invasive procedure that involves inserting a catheter into the right side of the heart to measure various pressures, including pulmonary artery pressure, cardiac output, and pulmonary capillary wedge pressure [16]. This technique provides accurate and reliable information about the severity of PAH, which can help guide treatment decisions. However, due to its invasive nature, it carries potential risks, such as bleeding and infection. Therefore, it is typically reserved for patients with confirmed or suspected PAH who are being considered for lung transplantation or other advanced therapies. Another modality that can be used by clinicians to better assess the severity of PAH and monitor the progression of the disease is chest CT. Since it requires a higher radiation dose compared to other imaging tests like echocardiography, low-dose chest CT has emerged as an alternative that can show the fine structure of lung tissue and better reflect changes in the mediastinum, lung parenchyma, interstitial lung, and cardiac function. Out of all the different modalities of diagnosing PAH, we cannot neglect the clinic presentation as it is equally important. Therefore, a thorough clinical evaluation, including history taking, a good physical examination with the tests mentioned above are all needed in making an accurate diagnosis.

**Clinical presentation**

Symptoms of PAH can very nonspecific. It can be challenging to diagnose because its

symptoms can overlap with those of other cardiovascular and respiratory conditions. Syncope is a common symptom of PAH, but also presents in patients with hypotension, cardiac arrhythmias and various neurological disorder. Data has shown that about 16% of patients develop syncope within two years of symptom onset, while only 18% are diagnosed with PAH based on syncope after two years [17]. The most common symptoms of PAH are exertional dyspnea followed by chest discomfort, leg edema and fatigue. In addition to the common symptoms mentioned, patients with PAH may also experience dizziness, lightheadedness, and fainting episodes. These symptoms may occur due to decreased cardiac output and reduced oxygen delivery to the brain. Patients with PAH may also have a dry cough or cough up blood, which can be a sign of underlying pulmonary hypertension. As the disease progress, the patient might develop right-sided heart failure, which can cause edema, ascites, and abdominal distention. This indicates that patients are in an advanced stage of the disease [18]. PAH can also affect the functioning of the liver and the kidneys, leading to abdominal discomfort, decreased appetite, and weight loss. Patients may also experience right upper quadrant pain due to liver enlargement caused by blood congestion. The swelling in the legs and ankles can progress to involve the entire lower extremities, and in severe cases, it can involve the trunk and upper extremities as well. The quality of life of patients can also be affected as patients can develop depression and anxiety [19, 20]. Patients may feel isolated and helpless due to the chronic nature of the disease and the lack of a cure. This can have a significant impact on their emotional well-being and social functioning. Therefore, it is important to recognize the symptoms of PAH early and provide appropriate treatment to improve the patient's quality of life. With the variability of clinical presentation among PAH patients, but they all share a common underlying pathology. Understanding the pathological features of PAH can provide valuable insights into the disease mechanisms and highlight the importance of early diagnosis and treatment.

**Pathological features**

PAH is characterized by the proliferation of endothelial and smooth muscle cells in the walls of the pulmonary arteries, resulting in the narrowing of the vessel lumen [21]. Despite extensive research, the exact mechanisms underlying cell proliferation and pulmonary vascular remodeling remain unclear. The pulmonary arteries are composed of three layers: adventitia, media and intima. In PAH, the intimal layer becomes thick and fibrotic, and the media layer undergoes hypertrophy, leading to a reduction in the diameter of the arterial lumen (Fig 1.2). In severe cases, plexiform lesions can develop, which are clusters of abnormal blood vessels formed within the pulmonary vasculature, contributing to increased resistance to blood flow and right heart failure. Endothelial dysfunction and cell proliferation are the two major pathological features leading to the development of pulmonary vascular remodeling [21]. Dysfunction in endothelial cells can lead to a reduction of nitric oxide (NO) and the release of pro-inflammatory factors and reactive oxygen species, as well as the production of extracellular matrix proteins, such as collagen and fibronectin, contributing to vascular remodeling [22]. PAH involves multiple cellular and molecular mechanisms, and it is believed that growth factors, cytokines, and hypoxia are involved in cell proliferation and endothelial dysfunction in PAH. Studies have shown that the downregulation of BMPR2, a type 2 receptor in the transforming growth factor beta superfamily, relates to the abnormal proliferation and migration of endothelial and smooth muscle cells in PAH. However, the exact mechanisms of BMPR2 downregulation in PAH are not completely understood, but it is thought to involve genetic mutations, epigenetic changes, and environmental factors such as hypoxia and inflammation. Current research continues to investigate ways to restore BMPR2 signaling in PAH as a potential therapeutic strategy.

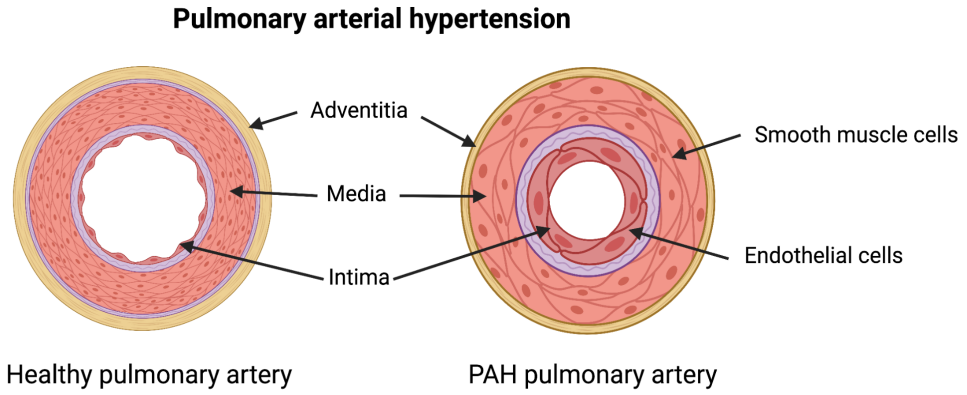


Figure 1.2: Pulmonary vascular remodeling in PAH pulmonary artery. The pulmonary artery has three layers: adventitia, media, and intima. The media layer primarily consists of smooth muscle cells, while the intima layer is mainly composed of endothelial cells. In PAH, both endothelial and smooth muscle cells become proliferative, leading to the formation of plexiform lesions and hypertrophy of the media layer, which results in the narrowing of the arterial lumen. Created with BioRender.com.

## Current treatment

Over the past decades, the treatment options for PAH have improved drastically, but there is still no cure for the disease. The goals of current treatments are to manage symptoms, slow disease progression, and improve the patient's quality of life. Medication includes vasodilators, common ones are prostacyclin analogs, endothelin receptor antagonists, phosphodiesterase type 5 and calcium channel blockers, to name a few. [7]. They aid to dilate the blood vessels and reduce the pressure within the pulmonary arteries. Diuretics including Furosemide, Spironolactone and Hydrochlorothiazide are often prescribed. They usually help to reduce water retention in the body and therefore can ease the workload on the heart. Besides medication aimed at alleviating symptoms, lung transplantation is often considered for PAH patients who have not responded to other treatment options or whose disease has progressed to an advanced stage. It can improve patients' quality of life and long-term survival. It is a high-risk surgery and not all PAH patients are candidates for lung transplant. There are several factors that need to be assessed to ensure a successful transplantation. This includes the severity of the disease, age and psychosocial factors.

Typically lung transplant is reserved for patients with severe, end-stage PAH and since it is a high-risk surgery, it requires a multidisciplinary team of experts, including pulmonologists, surgeons, and transplant coordinators to evaluate suitable candidates. After a lung transplant, patients improve their exercise capacity and reduced symptoms. However, there are potential complications during post-operative recovery such as infection and organ rejection. Therefore, usually it requires comprehensive pre-transplant assessments to minimize risks.

**Clinical trials**

Continual clinical trials are necessary to advance the development of optimal treatment strategies for PAH patients. Currently, Sotatercept is an investigational drug undergoing Phase III clinical trial, called PULSAR, as a potential treatment option for PAH [23]. Sotatercept is a fusion protein consisting of the extracellular domain of activin receptor type IIA (ActRIIA) linked to the immunoglobulin G1 (IgG1) Fc domain. It works by binding to and neutralizing members of the TGF-β growth factors, such as activin A and growth differentiation factor 11 (GDF11), which are known to be upregulated in the pulmonary vasculature of PAH patients. In the PULSAR trial, PAH patients were randomized to receive either sotatercept or placebo, in addition to their standard PAH therapies, over a specific period. The study found that sotatercept led to significant improvements in hemodynamics and 6-minute walk distance compared to placebo, suggesting that it may be a promising treatment option for PAH [24, 25].

Despite numerous clinical trials and available treatment options, more research is required to gain a deeper understanding of the pathophysiological mechanisms underlying PAH is essential for the advancement of more effective treatments in the future.

**Study models for PAH research**

Both *in vitro* and *in vivo* models are widely used to study PAH, these models enable

researchers to investigate the underlying mechanisms, potential therapeutic targets, and treatment strategies for PAH.

***In vitro* models**

Pulmonary arterial endothelial cells (PAECs) and smooth muscle cells (PASMCs) are the two most common *in vitro* models for studying PAH since they are the two key cell types in the pulmonary vasculature and their dysfunctions contributes greatly to the pulmonary vascular remodeling. Other studied cell type includes fibroblasts, macrophages, T-cells, B-cells, cardiomyocytes and even stem cells like endothelial progenitor cells and mesenchymal stem cells. PAECs form the inner layer of the pulmonary arteries. They regulate vascular tone by producing vasodilatory substances, such as NO and prostacyclin, and vasoconstrictors, such as endothelin-1 (ET-1) [26]. Endothelial dysfunction in PAH can lead to the release of many cytokines, increase production of vasoconstrictors and release of growth factors that stimulate PASMC proliferation and migration. PASMCs form the medial layer of the pulmonary arteries, they can contract or relax in response to different stimuli. Excessive growth of PASMCs will lead to the thickening of the arterial walls and narrowing of the vessel lumen. Researchers often cultured these cells for studying their cell proliferation, migration and apoptosis under different treatments. They can also knock down or knock in specific genes or induce hypoxia in those cell types. These models allow us to answer various fundamental questions.

Other *in vitro* models include pulmonary artery organoids. Basically, these 3D structures mimic the complex microenvironment in the human body and therefore provide more physiological relevant. For example, one study has adapted the 3D cell culture technique for culturing PASMCs, and they constructed a novel 3D model of the vascular media layer to study pulmonary vasculature remodeling [27].

### *In vivo* models

Researchers utilize heavily on mice and rats for investigating the in *vivo* progression of PAH, including its impact on pulmonary vascular remodeling, right ventricular function, and overall survival. Researchers can create genetically modified animal models with altered expression of specific genes, especially in PAH, it is important to study BMPR2 mutations and other associated mutations *in vivo*. In order to study the pathology of PAH, first researchers need to induce PAH in mice or rats. Several methods can be used such as monocrotaline injection, chronic hypoxia exposure, or genetic manipulation. The two common mouse models are the SUGEN 5416/hypoxia-induced and the monocrotaline (MCT)- induced PAH model. For the SUGEN 5416/hypoxia-induced PAH model, mice are exposed to the combination of a vascular endothelial growth factor (VEGF) receptor antagonist, Sugen 5416 (SU5416) and chronic hypoxia for an extended period, typically 3-4 weeks. The reduced oxygen levels can cause pulmonary vasoconstriction and increased pulmonary vascular resistance [28]. The MCT model involves the administration of monocrotaline, a toxic metabolite that causes damage to the pulmonary vascular endothelium. This can lead to inflammation, and increase vascular permeability [29, 30]. The mechanism of how monocrotaline affects the endothelium is still being investigated. One possible hypothesis is that MCT can bind and activate extracellular calcium-sensing receptors (CaSR). One study has shown that knockdown of CaSR inhibited MCT-induced cell injury indicating that MCT could activate CaSR to trigger endothelial damage, and eventually develops PAH [31]. These two models aim at mimicking the phenotype of human PAH, and creating the pulmonary arterial remodeling condition, which includes smooth muscle cell proliferation, endothelial cell dysfunction, and extracellular matrix alterations.

There are large animal models, such as pigs and dogs [32]. Although this is a less common

approach to studying PAH. The benefit of having big animal models is that they have similar anatomy, physiology and response to therapies, making them valuable for preclinical evaluation of novel treatments.

Overall, *In vitro* models allow the study of molecular mechanisms and test potential treatments with great control, on the other hand, *in vivo* models provide a holistic view of PAH. And in this dissertation, I will be utilizing PAECs to study the molecular mechanism of TGF-β signaling for cell proliferation.

### Genetic mutation in PAH

PAH is classified into familial and idiopathic types. Familial PAH is a rare, inherited form of the disease caused by genetic mutations, with BMPR2 being the most common mutation found in patients, though other mutations such as ALK1, ENG, BMP9 and BMP10 have also been identified [33]. In contrast, idiopathic PAH is the most common form of PAH, accounting for approximately 40% of cases. All of these genetic mutations belong to the transforming growth factor beta superfamily (TGF-β), suggesting that TGF-β signaling plays a significant role in the development and progression of PAH.

## TRANSFORMING GROWTH FACTOR-β SUPERFAMILY

### Transforming growth factor-β superfamily

Transforming growth factor-β is a family of secreted, multi-functional proteins that play crucial roles in regulating various cellular processes, including cell growth, differentiation, proliferation, migration, and apoptosis. In humans, TGF-β superfamily consists of a sophisticated network composed of more than 35 distinct growth factors (GFs), 7 "Type I" (ALK1, ALK2, ALK3, ALK4, ALK5, ALK5, ALK6 and ALK7) and 5 "Type II" (BMPR2, ActRIIA, ActRIIB,

TGFβRII and AMHR2) transmembrane kinase receptors, 5 R-SMAD transcriptional effectors (SMAD1, SMAD2, SMAD3, SMAD5 and SMAD8), along with a diverse range of co-receptors, antagonists, and intracellular regulatory molecules, like Cripto-1, Endoglin, betaglycan and BAMBI [34] (Fig 1.3).

| > 35 GFs | Type I receptors | Type II receptors | R-SMADs |
|---|---|---|---|
| BMP4, | ALK1, | BMPR2, | SMAD1, |
| BMP7 | ALK2, | ActRIIA, | SMAD2, |
| BMP9, | ALK3, | ActRIIB, | SMAD3, |
| BMP10, | ALK4, | TGFβRII, | SMAD5, |
| GDF11, | ALK5, | AMHRII | SMAD8 |
| GDF8, | ALK6, | | |
| Activin A, | ALK7 | | |
| Activin B, | | | |
| Nodal, | | | |
| TGF-β1, etc | | | |

Figure 1.3: The overview of the TGF-β superfamily. TGF-β superfamily consists of over 35 distinct growth factors (GFs), seven type I receptors, five type II receptors and five R-SMADs. Different GFs have their own distinct functions.

The growth factors are widely expressed in different tissues, and their functions vary depending on the cell types. Activins, for example, are highly expressed in the ovaries and testes, and they regulate the secretion of follicle-stimulating hormone (FSH) and luteinizing hormone (LH) in the pituitary gland [35]. Nodal, on the other hand, is important in embryonic development and it is found to be expressed in the embryonic tissues where it establishes the left-right asymmetry [36]. Due to its diverse range of activities, impaired TGF-β signaling has been strongly linked to a variety of developmental conditions, including cardiovascular and fibrotic disorders, autoimmune diseases, infectious diseases, and cancer. There has been extensive research on TGF-β signaling over the decades, leading to a significant increase in our understanding of this complex

pathway. However, due to its multifaceted nature, there is still much to uncover in terms of its full biological and pathological roles.

The discovery of TGF-β dates back to the early 1980s. In 1982, two independent research groups led by Michael Sporn and Anita Roberts at the National Cancer Institute (NCI), and Harold Moses and Joanne Massague at the Vanderbilt University School of Medicine discovered and characterized factors in different cell lines. [37, 38] They used conditioned media from cultured cells and tested its ability to stimulate the growth of fibroblasts, which led to the identification of a novel protein with growth-promoting activity distinct from previously known growth factors. They purified this protein using chromatographic techniques and characterized its biological activity, naming it transforming growth factor-beta. As molecular biology techniques advanced, researchers were able to clone cDNAs encoding TGF-β proteins. This allowed them to identify additional TGF-β isoforms (TGF-β1, TGF-β2, and TGF-β3) with distinct yet structurally similar amino acid sequences and they were found to have different tissue distributions and biological activities. Subsequently, researchers were able to identify two types of serine/threonine kinase receptors, Type I and Type II TGF-β receptors and SMAD proteins which are essential intracellular signaling molecules for TGF-β signaling transduction. Over the years, researchers have identified additional TGF-β family members, such as bone morphogenetic proteins, activins, and inhibins. With the advancement in technologies and ongoing research, our comprehension of TGF-β signaling is enhanced, laying the foundation for the development of targeted therapies for a range of diseases.

**TGF- β signaling pathways**

The TGF-β family consists of two functional subgroups: one includes three TGF-β isoforms, activins, nodals, and some growth and differentiation factors, while the other subgroup,

known as the bone morphogenetic protein group, consists of all BMPs and the majority of GDFs [39]. A typical TGF-β growth factor (GFs) comprises three domains: a signal peptide, a prodomain, and a mature domain. TGF-β GFs are synthesized as precursor proteins containing a signal peptide, a prodomain, and a mature domain (Fig 1.4, top panel). The signal peptide directs the protein through the secretory pathway into the endoplasmic reticulum (ER). In the ER, the signal peptide is cleaved, and the prodomain and mature domain form a complex called the small latent complex (SLC). The SLC is then secreted from the cell and binds to latent TGF-β binding proteins (LTBPs) in the extracellular matrix (ECM). Eventually, the biologically active form usually presents as a dimeric mature domain linked by disulfide bonds [40]. Typically, ligands adopt a hand-like structure, as they comprise two sets of antiparallel β-strands and loops that create finger-like extensions. A three-turn α-helix forms the heels of the hand. Within the sequence, there are nine cysteines; eight of them form four intrachain disulfide bonds, while the ninth forms an interchain disulfide bond with another subunit, stabilizing the dimeric structure [41, 42]. TGF-β signaling initiates by GF binding to the type II TGF-β receptor on the cell surface, which leads to the recruitment and transphosphorylation of the type I TGF-β receptor. This forms a heterotetrameric receptor complex. Upon activation, the type I receptor phosphorylates receptor-regulated Smads (R-Smads) at their C-terminal serine residues. R-SMAD can be group into two major TGF-β signaling branches: SMAD 2/3 and SMAD 1/5/8 [39]. R-Smads also associate with a common mediator Smad (Co-Smad), Smad4, which form the R-Smad/Co-Smad complex. This complex subsequently translocate to the nucleus, activating the transcription of target genes such as PAI-1, Smad 7, COL1A1, MMPs, Osterix, Msx1, and Id-1. Additionally, there are inhibitory Smads (Smad 6 and Smad 7) that inhibit the interaction of R-Smads with type I receptor, thus preventing the potentiation of the signaling. As mentioned, TGF-β signaling can be divided into Smad1/5/8

and Smad2/3 signaling pathways (Fig 1.5). Typically, BMPs/GDFs transmit their signaling through SMAD 1/5/8 signaling pathway while TGF-β/activin/nodal usually transmit their signaling through SMAD 2/3 signaling pathway. It is remarkable that there are over 35 distinct TGF-β GFs, and each GF binds to specific type I and type II receptors, activate either SMAD 1/5/8 or SMAD 2/3 signaling pathway, and elicit a diverse range of biological effects. Apart from the canonical SMAD-mediated pathways, TGF-β can also initiate various noncanonical signaling cascades, including MAPK, Akt and NF-κB pathways, further enhancing the complexity of TGF-β signaling [43, 44].

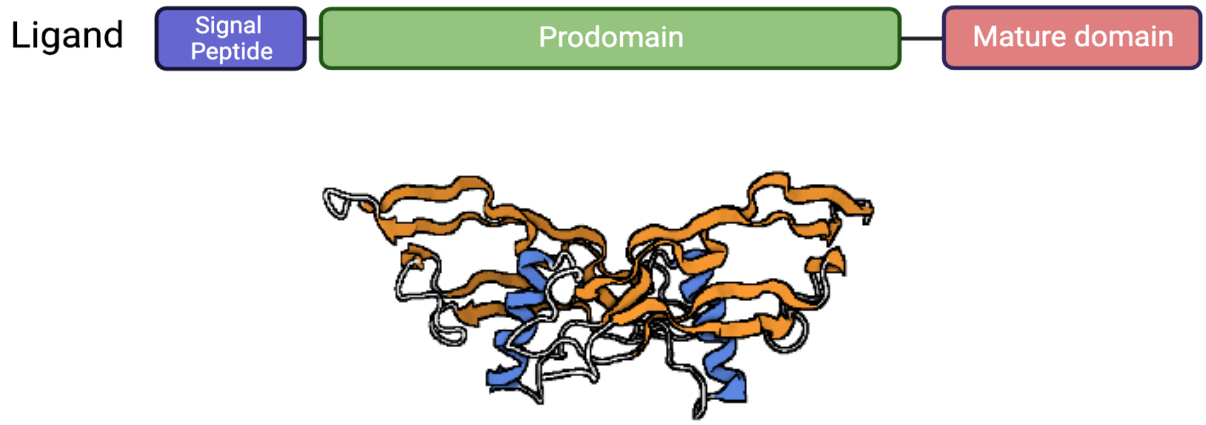


Figure 1.4: Structure of a ligand. Upper panel: A typical ligand consists of a signal peptide (purple), a prodomain (light green), and a mature domain (orange-pink). Lower panel, the crystal structure of BMP9 (PDB: 1ZKZ) serves as a representative example of a TGF-β ligand. Ligands are usually present as a dimer that consists of two sets of antiparallel β-strands and loops (orange) and a three-turn α-helix (blue). Created with BioRender.com.

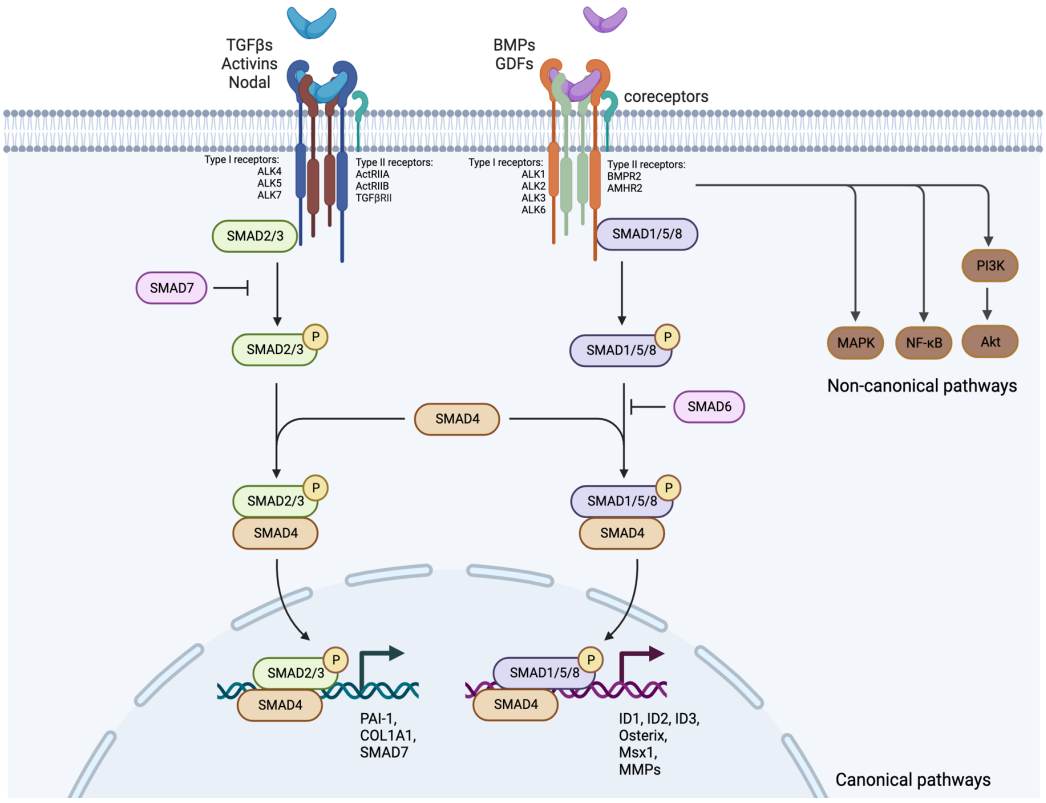


Figure 1.5: The overview of TGF-β signaling. The TGF-β superfamily comprises 33 growth factors (GFs), which are further divided into subgroups: BMPs and GDFs as one group, and TGF-βs, Activins, and Nodal as another. There are two canonical signaling pathways: SMAD 2/3 and SMAD 1/5/8 signaling pathways. The pathways are initiated when a GF binds to two type I receptors and two type II receptors at the cell surface. The TGF-β signaling pathway utilizes 7 type I receptors and 5 type II receptors. Upon the formation of the ligand-receptor signaling complex, signal transduction commences by phosphorylating R-Smad (SMAD 2/3 or SMAD 1/5/8). The R-Smads then bind to a co-Smad, SMAD 4, to form an R-Smad/Co-Smad complex. This complex subsequently translocates into the nucleus, where it interacts with other transcription factors to initiate the transcription of target genes such as PAI-1, COL1A1, ID1, and MMPs, among others. Co-receptors and inhibitory Smads (SMAD 6 or 7) also contribute to the regulation of TGF-β signaling. There are also co-receptors and inhibitory Smads (SMAD 6 or 7) for the regulation of TGF-β signaling. TGF-β family GFs can signal through either canonical or non-canonical pathways, which include Akt, MAPK, and NF-κB pathways. The numerous growth factors, receptors, co-receptors, inhibitors, and non-canonical pathways involved introduce multiple layers of complexity to TGF-β signaling. Created with BioRender.com.

## BMP signaling pathway

Bone morphogenetic proteins are a subgroup of the TGF-β superfamily. So far, there are more than 20 BMPs have been identified and they are further categorized into subgroups based on their structural and functional similarities like BMP2/4, BMP9/10 and GDF8/GDF11 [45]. Like all other TGF-β growth factors, BMPs bind to the heteromeric complex of two type I and two type II receptors. Type I receptors like ALK1, ALK2, and ALK3 and type II receptors like BMPR2,

ActRIIA and ActRIIB are the common receptors known to bind to BMPs. Following receptor activation, the signaling cascade proceeds to induce the SMAD 1/5/8 signaling branch and initiate gene transcription. BMPs regulate the transcription of a wide range of target genes, depending on the cellular context and the specific BMP growth factors involved. There are some well-known targeted genes of BMP signaling, including inhibitors of DNA binding (IDs), which are involved in the regulation of cell differentiation, cell-cycle progression, and tissue development. Osterix, a zinc finger transcription factor involved in osteoblast differentiation and bone formation and Msx genes that play a major role in embryonic development, particularly in the limb and craniofacial patterning. Dysregulation of BMP signaling has been associated with numerous pathological conditions, such as skeletal disorders, cancer, and pulmonary arterial hypertension. Notably, BMPR2, a receptor within the BMP signaling pathway, has been identified as mutated in PAH patients. Understanding BMPR2 signaling and its interaction with TGF-β growth factors is essential to gain insight into the molecular mechanisms driving disease progression.

**TGF- β growth factors: BMP9 and BMP10**

Bone morphogenetic proteins-9 (BMP9) and Bone morphogenetic proteins-10 (BMP10) are TGF-β growth factors that belong to the BMP family. They share numerous structural and functional similarities. Their mature domains have high sequence homology and they are both key regulators of diverse biological processes such as angiogenesis, organogenesis, and tissue differentiation. They bind to ALK1 and BMPR2 and induce SMAD 1/5/8 signaling. Despite extensive research on BMP9 and BMP10, their roles in vascular maintenance are still not fully understood.

BMP9, also known as Growth Differentiation Factor-2, is primarily synthesized in the liver and released into circulation as an active mature dimer. However, BMP9 expression has also been

detected in other tissues including the heart, lungs, kidneys, and skeletal muscles. Studies have shown that the mature, active form of BMP9 circulates in the bloodstream at plasma concentrations ranging from 2 to 12 ng/mL. Also, it is found that circulating BMP9 consistently activates Smad1/5/8 signaling in endothelial cells [46]. Similarly, BMP10 is also important for vascular homeostasis and blood vessel formation. BMP10 is predominantly expressed in the heart, particularly during embryonic development and in the early postnatal period. It plays a crucial role in heart development, including the formation and maturation of trabeculae, which are muscular ridges found in the ventricles. In addition to its expression in the heart, BMP10 has been detected in other tissues such as the lungs and similar to BMP9, it circulates in the bloodstream as well [47]. Recent studies have revealed that mutations in BMP9 and BMP10 are present in some patients with PAH. Dysregulated BMP9 and BMP10 signaling could contribute to the pathological vascular remodeling observed in PAH, but the exact role of BMP9 and BMP10 in PAH remains unclear. Overall, the presence of mutations in BMPR2, BMP9, and BMP10 in PAH patients suggests that BMP signaling plays a significant role in the pathogenesis of PAH.

**TGF-β signaling in cell proliferation**

Cell proliferation is a fundamental biological process that involves the growth, division, and reproduction of cells. In order for the cell to proliferate, it has to undergo cell cycle, which entails a series of events for cell division. It consists of four main phases: G1, synthesis, G2, and mitosis phase. During the G1 phase, the cell grows and carries out its normal functions. In the S phase, DNA synthesis occurs, and the cell duplicates its genetic material. The G2 phase allows the cell to continue growing and prepare for division, while the M phase is the actual process of cell division. Each step has many regulations and is controlled by signaling pathways and cell cycle checkpoints. TGF-β family plays a big role in the regulation of cell proliferation, depending on

different cell contexts, TGF-β signaling can either suppress or induce cell proliferation [48]. Many studies showed evidence of TGF-β leading to cell arrest in endothelial cells, epithelial cells, and hematopoietic cells. [49, 50] One has shown that in epithelial cells, TGF-β causes cell cycle arrest at G1 phase through the repression of expression of certain growth-promoting transcription factors and the induction of expression of specific CDK inhibitors. TGF-β suppresses c-Myc and cell differentiation inhibitors ID1, 2 and 3. These directly prevent cells from entering the S phase [51]. On the other hand, TGF-β also has a proliferative effect on different cell types. For example, in smooth muscle cells, TGF-β can induce platelet-derived growth factor (PDGF) [52]. In renal fibroblasts, it is found that TFG-β can induce the expression of basic fibroblast growth factor-2 (FGF-2) [53]. The distinct opposing cell proliferation effect of TGF-β depends on the activation of different downstream signaling. It is well-established that TGF-β signaling plays a crucial role in cell proliferation and survival under both physiological and pathological conditions. However, the exact molecular mechanism underlying these observations remains unclear.

## TGF-β signaling in PAH

### BMPR2 mutations

Bone morphogenetic protein receptor type II (BMPR2) is a member of the TGF-β superfamily receptor. Heterozygous mutations in the BMPR2 gene are detected in 80% of familial cases and 20% of idiopathic cases (Fig 1.7). It is autosomal dominant and the prevalence of BMPR2 mutations in all cases is estimated to be around 10-20% since the mutation is incompletely penetrant, meaning that not everyone with the mutation will exhibit symptoms of the disease [54, 55]. To date, more than 300 mutations in the BMPR2 gene have been identified in individuals with PAH. These mutations can occur at various locations within the gene and can affect the function of the BMPR2 protein in different ways [56]. There are different types of mutations found along

the BMPR2 gene including missense, nonsense, frameshift, and splice site mutation (Fig 1.6). Some BMPR2 mutations are associated with a higher risk of developing PAH and a more severe course of the disease, while others may have a milder impact on disease development and progression. For example, one study showed that truncated mutations are associated with an earlier age of onset of PAH and a worse prognosis. Other studies have shown that a specific BMPR2 mutation called the R899X mutation, is associated with a more severe form of PAH [57]. Because of the low prevalence, the presence of BMPR2 mutation does not necessarily mean that a person will develop PAH. However, it does increase the risk as the mutation may interact with other factors like environmental, or lifestyle factors that increase the likelihood of developing PAH.

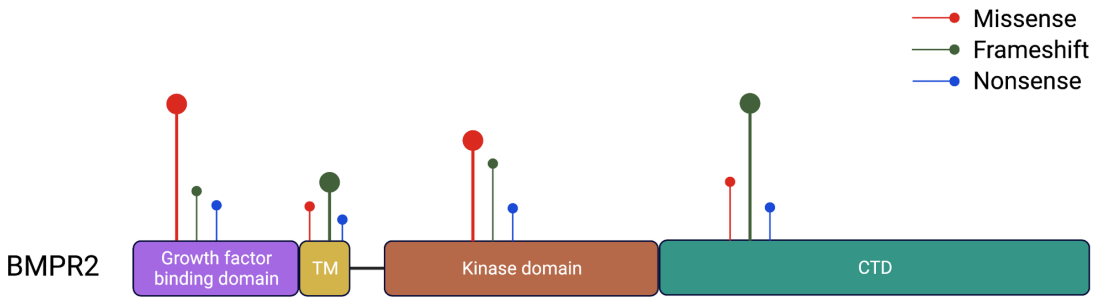


Figure 1.6: Mapping the mutations on the BMPR2 gene. Approximately 300 mutations have been identified throughout the BMPR2 gene, including missense (red stick), frameshift (green stick), and nonsense (blue stick) mutations. The distribution of these mutation types varies across different domains. In both the growth factor binding domain and the kinase domain, the majority of mutations are missense (red stick) mutations. Meanwhile, the transmembrane (TM) domain and the C-terminal domain (CTD) predominantly carry frameshift mutations. Created with BioRender.com.

**Other mutations in the TGF-β family**

Activin receptor-like kinase 1 (ALK1) is a type I serine/threonine kinase receptor that belongs to the TGF-β superfamily. ALK1 is involved in BMP signaling pathways and is able to form signaling complexes with BMPR2. Although ALK1 mutations account for a relatively small percentage of cases of pulmonary arterial hypertension (PAH), studies have shown that patients with ALK1 mutations are typically diagnosed at a younger age compared to patients with other

mutations carrier. Additionally, patients with ALK1 mutations tend to have better hemodynamic status than other PAH patients, but they do not respond well to vasodilator treatment [58].

BMP9 and BMP10 are members of the bone morphogenetic protein (BMP) family, which are growth factors that belong to the TGF-β superfamily. They play a big role in vascular development and angiogenesis. Mutations of both growth factors are found in patients with heritable and idiopathic PAH. One study has shown that BMP10 is associated with an earlier onset and more rapid progression of the disease [59] (Fig 1.7).

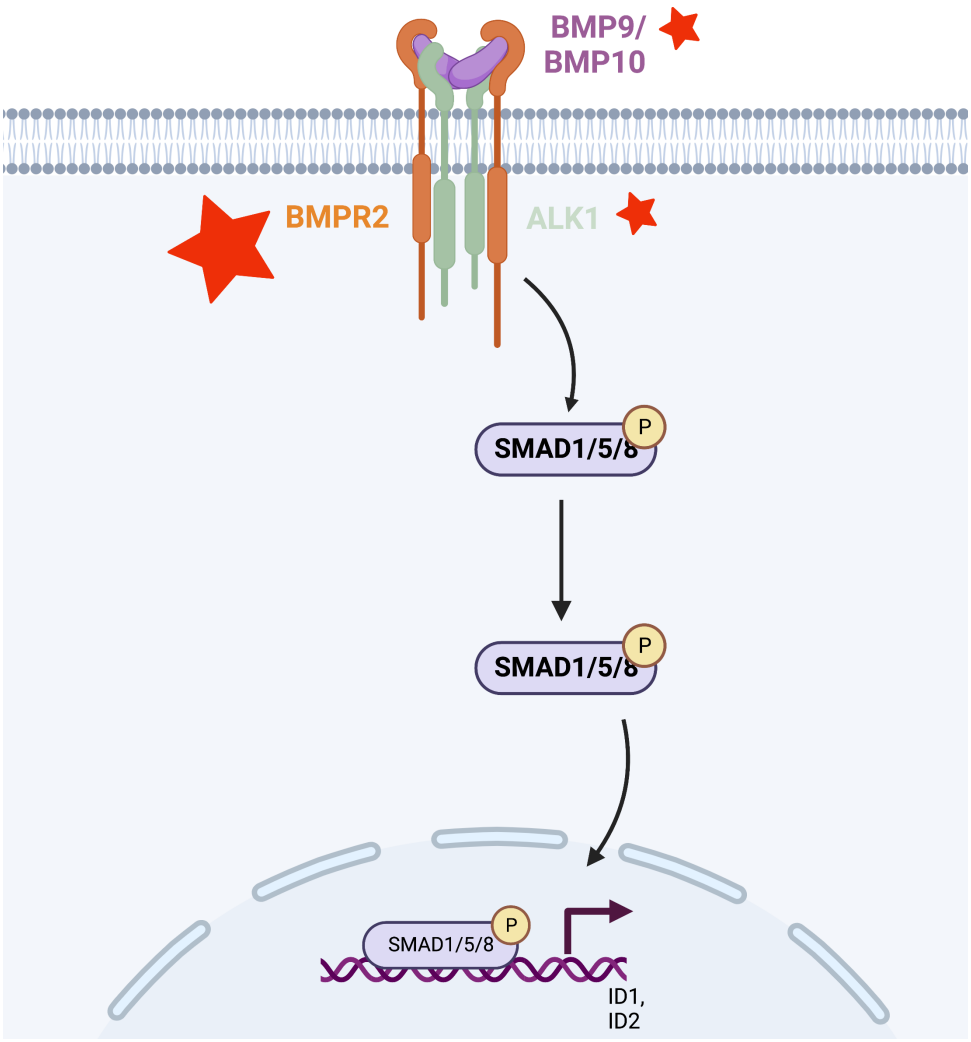


Figure 1.7: Mutations of genes are found along the BMP signaling pathway. The majority of mutations are identified in the BMPR2 gene, and some are found in the genes of BMP9, BMP10 and ALK1. These genes encode the signaling molecules that belong to the BMP signaling pathway. Created with Biorender.com.

Endoglin (ENG) encodes a transmembrane glycoprotein that is primarily expressed on proliferating vascular endothelial cells and plays a crucial role in the regulation of vascular development, angiogenesis, and tissue repair [60]. It acts as a co-receptor for TGF-β superfamily. ENG mutations account for a small percentage of PAH cases, with estimates ranging from 1% to 5% of cases [54, 55]. Dysfunction in the BMP signaling pathway contributes to the development of PAH. Mutations are detected ranging from growth factors, receptors and coreceptors. Therefore, targeting this signaling pathway may represent a promising therapeutic strategy for the treatment of PAH.

**DISSERTATION OVERVIEW**

There has been substantial growth in PAH research. Patients with PAH often exhibit nonspecific symptoms, leading to delayed diagnosis. At present, no curative treatments for PAH exist, with lung transplant being the only limited option for patients with severe PAH. It is widely known that TGF-β signaling is a major contributing factor to PAH pathogenesis, and numerous literatures have investigated its role in the disease. Over 300 mutations have been identified in the BMPR2 gene in PAH patients. Because of its low penetrance, whether all mutations are pathogenic has yet to be discovered. In addition, there is a knowledge gap regarding the connection between the reduction of BMPR2 signaling and the aberrant growth of pulmonary arterial endothelial cells and smooth muscle cells. The aim of this dissertation is to elucidate the role of TGF-β signaling in PAECs proliferation. In Chapter 2, I demonstrate the interaction between BMPR2 and TGF-β GFs and how BMPR2 mutations, found in PAH patients, impact this GFs-BMPR2 interaction. In Chapter 3, I examine which TGF-β growth factors induce PAEC proliferation and investigate the potential alterations in receptor binding when BMPR2 levels are reduced. In Chapter 4, I conclude

by summarizing the findings presented in this dissertation, as well as discussing potential future research directions.

## REFERENCES


1. Alexander, R.S., *The general physiology of heart and circulation.* Phys Ther Rev (1948), 1950. **30**(11): p. 452-61.

2. Suresh, K. and L.A. Shimoda, *Lung Circulation.* Compr Physiol, 2016. **6**(2): p. 897-943.

3. Brittain, E.L. and A.R. Hemnes, *Introduction to Review Series on Pulmonary Vascular Disease and Right Ventricular Heart Failure.* Circ Res, 2022. **130**(9): p. 1362-1364.

4. Sahay, S., *Evaluation and classification of pulmonary arterial hypertension.* J Thorac Dis, 2019. **11**(Suppl 14): p. S1789-S1799.

5. Emmons-Bell, S., et al., *Prevalence, incidence, and survival of pulmonary arterial hypertension: A systematic review for the global burden of disease 2020 study.* Pulm Circ, 2022. **12**(1): p. e12020.

6. Hoeper, M.M., *Definition, classification, and epidemiology of pulmonary arterial hypertension.* Semin Respir Crit Care Med, 2009. **30**(4): p. 369-75.

7. Xiao, Y., et al., *Pathological Mechanisms and Potential Therapeutic Targets of Pulmonary Arterial Hypertension: A Review.* Aging Dis, 2020. **11**(6): p. 1623-1639.

8. Galie, N., et al., *2015 ESC/ERS Guidelines for the diagnosis and treatment of pulmonary hypertension: The Joint Task Force for the Diagnosis and Treatment of Pulmonary Hypertension of the European Society of Cardiology (ESC) and the European Respiratory Society (ERS): Endorsed by: Association for European Paediatric and Congenital Cardiology (AEPC), International Society for Heart and Lung Transplantation (ISHLT).* Eur Heart J, 2016. **37**(1): p. 67-119.

9. Levine, D.J., *Pulmonary arterial hypertension: updates in epidemiology and evaluation of patients.* Am J Manag Care, 2021. **27**(3 Suppl): p. S35-S41.

10. Hoeper, M.M., et al., A global view of pulmonary hypertension. Lancet Respir Med, 2016. 4(4): p. 306-22.

11. Li, L., et al., *Pulmonary arterial hypertension in the USA: an epidemiological study in a large insured pediatric population.* Pulm Circ, 2017. **7**(1): p. 126-136.

12. Galie, N., et al., *2015 ESC/ERS Guidelines for the Diagnosis and Treatment of Pulmonary Hypertension.* Rev Esp Cardiol (Engl Ed), 2016. **69**(2): p. 177.

13. Badesch, D.B., et al., *Diagnosis and assessment of pulmonary arterial hypertension.* J Am Coll Cardiol, 2009. **54**(1 Suppl): p. S55-S66.

14. Bonderman, D., et al., *Non-invasive algorithms for the diagnosis of pulmonary hypertension.* Thromb Haemost, 2012. **108**(6): p. 1037-41.

15. Hur, D.J. and L. Sugeng, *Non-invasive Multimodality Cardiovascular Imaging of the Right Heart and Pulmonary Circulation in Pulmonary Hypertension.* Front Cardiovasc Med, 2019. **6**: p. 24.

16. Rosenkranz, S. and I.R. Preston, *Right heart catheterisation: best practice and pitfalls in pulmonary hypertension.* Eur Respir Rev, 2015. **24**(138): p. 642-52.

17. Zugurov, I.K., et al., *Surgical treatment of chronic thromboembolic pulmonary hypertension in combination with a left anterior descending artery myocardial bridge: A case report.* Front Cardiovasc Med, 2022. **9**: p. 1061665.

18. Ruopp, N.F. and B.A. Cockrill, *Diagnosis and Treatment of Pulmonary Arterial Hypertension: A Review.* JAMA, 2022. **327**(14): p. 1379-1391.

19. Talwar, A., et al., *Dyspnea, depression and health related quality of life in pulmonary arterial hypertension patients.* Journal of Exercise Rehabilitation, 2015. **11**(5): p. 259-265.

20. Zhou, X., et al., *Anxiety and depression in patients with pulmonary arterial hypertension and chronic thromboembolic pulmonary hypertension: Results from a Chinese survey.* Experimental and Therapeutic Medicine, 2020. **19**(4): p. 3124-3132.

21. Jia, Z., et al., *Pulmonary Vascular Remodeling in Pulmonary Hypertension.* J Pers Med, 2023. **13**(2).

22. Kurakula, K., et al., *Endothelial Dysfunction in Pulmonary Hypertension: Cause or Consequence?* Biomedicines, 2021. **9**(1).

23. Elliott, C.G., *Genetics of pulmonary arterial hypertension.* Clin Chest Med, 2013. **34**(4): p. 651-63.

24. Austin, E.D. and J.E. Loyd, *Heritable forms of pulmonary arterial hypertension.* Semin Respir Crit Care Med, 2013. **34**(5): p. 568-80.

25. Austin, E.D., J.A. Phillips, III, and J.E. Loyd, *Heritable Pulmonary Arterial Hypertension Overview*, in *GeneReviews((R))*, M.P. Adam, et al., Editors. 1993: Seattle (WA).

26. Gamou, S., et al., *Genetics in pulmonary arterial hypertension in a large homogeneous Japanese population.* Clin Genet, 2018. **94**(1): p. 70-80.

27. Sztrymf, B., et al., *Clinical outcomes of pulmonary arterial hypertension in carriers of BMPR2 mutation.* Am J Respir Crit Care Med, 2008. **177**(12): p. 1377-83.

28. Girerd, B., et al., *Clinical outcomes of pulmonary arterial hypertension in patients carrying an ACVRL1 (ALK1) mutation.* Am J Respir Crit Care Med, 2010. **181**(8): p. 851-61.

29. Eyries, M., et al., *Widening the landscape of heritable pulmonary hypertension mutations in paediatric and adult cases.* Eur Respir J, 2019. **53**(3).

30. Pousada, G., et al., *Mutational and clinical analysis of the ENG gene in patients with pulmonary arterial hypertension.* BMC Genet, 2016. **17**(1): p. 72.

31. Xiao, R., et al., Monocrotaline Induces Endothelial Injury and Pulmonary Hypertension by Targeting the Extracellular Calcium-Sensing Receptor. J Am Heart Assoc, 2017. 6(4).

32. Hoeper, M.M., et al., *Phase 3 Trial of Sotatercept for Treatment of Pulmonary Arterial Hypertension.* N Engl J Med, 2023.

33. Yung, L.M., et al., *ACTRIIA-Fc rebalances activin/GDF versus BMP signaling in pulmonary hypertension.* Sci Transl Med, 2020. **12**(543).

34. Joshi, S.R., et al., *Sotatercept analog suppresses inflammation to reverse experimental pulmonary arterial hypertension.* Sci Rep, 2022. **12**(1): p. 7803.

35. Chester, A.H. and M.H. Yacoub, *The role of endothelin-1 in pulmonary arterial hypertension.* Glob Cardiol Sci Pract, 2014. **2014**(2): p. 62-78.

36. Morii, C., et al., *3D in vitro Model of Vascular Medial Thickening in Pulmonary Arterial Hypertension.* Front Bioeng Biotechnol, 2020. **8**: p. 482.

37. Vitali, S.H., et al., *The Sugen 5416/hypoxia mouse model of pulmonary hypertension revisited: long-term follow-up.* Pulm Circ, 2014. **4**(4): p. 619-29.

38. Wilson, D.W., et al., *Mechanisms and pathology of monocrotaline pulmonary toxicity.* Crit Rev Toxicol, 1992. **22**(5-6): p. 307-25.

39. Wu, X.H., et al., *Experimental animal models of pulmonary hypertension: Development and challenges.* Animal Model Exp Med, 2022. **5**(3): p. 207-216.

40. Okada, M., et al., *Establishment of canine pulmonary hypertension with dehydromonocrotaline. Importance of larger animal model for lung transplantation.* Transplantation, 1995. **60**(1): p. 9-13.

41. Martinez-Hackert, E., A. Sundan, and T. Holien, *Receptor binding competition: A paradigm for regulating TGF-beta family action.* Cytokine Growth Factor Rev, 2021. **57**: p. 39-54.

42. Namwanje, M. and C.W. Brown, *Activins and Inhibins: Roles in Development, Physiology, and Disease.* Cold Spring Harb Perspect Biol, 2016. **8**(7).

43. Brennan, J., D.P. Norris, and E.J. Robertson, *Nodal activity in the node governs left-right asymmetry.* Genes Dev, 2002. **16**(18): p. 2339-44.

44. Moses, H.L., et al., *Transforming growth factor production by chemically transformed cells.* Cancer Res, 1981. **41**(7): p. 2842-8.

45. Roberts, A.B., et al., *Purification and properties of a type beta transforming growth factor from bovine kidney.* Biochemistry, 1983. **22**(25): p. 5692-8.

46. Weiss, A. and L. Attisano, *The TGFbeta superfamily signaling pathway.* Wiley Interdiscip Rev Dev Biol, 2013. **2**(1): p. 47-63.

47. Walton, K.L., et al., *Two distinct regions of latency-associated peptide coordinate stability of the latent transforming growth factor-beta1 complex.* J Biol Chem, 2010. **285**(22): p. 17029-37.

48. Daopin, S., et al., *Crystal structure of transforming growth factor-beta 2: an unusual fold for the superfamily.* Science, 1992. **257**(5068): p. 369-73.

49. Goebel, E.J., et al., *Structural biology of the TGFbeta family.* Exp Biol Med (Maywood), 2019. **244**(17): p. 1530-1546.

50. Hata, A. and Y.G. Chen, *TGF-beta Signaling from Receptors to Smads.* Cold Spring Harb Perspect Biol, 2016. **8**(9).

51. Chaikuad, A. and A.N. Bullock, *Structural Basis of Intracellular TGF-beta Signaling: Receptors and Smads.* Cold Spring Harb Perspect Biol, 2016. **8**(11).

52. Yadin, D., P. Knaus, and T.D. Mueller, *Structural insights into BMP receptors: Specificity, activation and inhibition.* Cytokine Growth Factor Rev, 2016. **27**: p. 13-34.

53. David, L., et al., *Identification of BMP9 and BMP10 as functional activators of the orphan activin receptor-like kinase 1 (ALK1) in endothelial cells.* Blood, 2007. **109**(5): p. 1953-61.

54. Chen, H., et al., *Overexpression of bone morphogenetic protein 10 in myocardium disrupts cardiac postnatal hypertrophic growth.* J Biol Chem, 2006. **281**(37): p. 27481-91.

55. Zhang, Y., P.B. Alexander, and X.F. Wang, *TGF-beta Family Signaling in the Control of Cell Proliferation and Survival.* Cold Spring Harb Perspect Biol, 2017. **9**(4).

56. Takehara, K., E.C. LeRoy, and G.R. Grotendorst, *TGF-beta inhibition of endothelial cell proliferation: alteration of EGF binding and EGF-induced growth-regulatory (competence) gene expression.* Cell, 1987. **49**(3): p. 415-22.

57. Tucker, R.F., et al., *Growth inhibitor from BSC-1 cells closely related to platelet type beta transforming growth factor.* Science, 1984. **226**(4675): p. 705-7.

58. Planas-Silva, M.D. and R.A. Weinberg, *The restriction point and control of cell proliferation.* Curr Opin Cell Biol, 1997. **9**(6): p. 768-72.

59. Battegay, E.J., et al., *TGF-beta induces bimodal proliferation of connective tissue cells via complex control of an autocrine PDGF loop.* Cell, 1990. **63**(3): p. 515-24.

60. Strutz, F., et al., *TGF-beta 1 induces proliferation in human renal fibroblasts via induction of basic fibroblast growth factor (FGF-2).* Kidney Int, 2001. **59**(2): p. 579-92.

# CHAPTER 2

# TYPE II BMP AND ACTIVIN RECEPTORS BMPR2 AND ACVR2A SHARE A CONSERVED MODE OF GROWTH FACTOR RECOGNITION

Work presented in this chapter has been published as:

Chu, K.-Y., Malik, A., Thamilselvan, V., & Martinez-Hackert, E. (2022). Type II BMP and activin receptors BMPR2 and ACVR2A share a conserved mode of growth factor recognition. Journal of Biological Chemistry, 298(7), 102076. https://doi.org/10.1016/j.jbc.2022.102076.

## ABSTRACT

BMPR2 is a type II Transforming Growth Factor (TGF)-β family receptor that is fundamentally associated with pulmonary arterial hypertension (PAH) in humans. BMPR2 shares functional similarities with the type II activin receptors ACVR2A and ACVR2B, as it interacts with an overlapping group of TGF-β family growth factors (GFs). However, how BMPR2 recognizes GFs remains poorly understood. Here, we solved crystal structures of BMPR2 in complex with the GF activin B and of ACVR2A in complex with the related GF activin A. We show that both BMPR2 and ACVR2A bind GFs with nearly identical geometry using a conserved hydrophobic hot spot, while differences in contacting residues are predominantly found in loop areas. Upon further exploration of the GF-binding spectrum of the two receptors, we found that although many GFs bind both receptors, the high-affinity BMPR2 GFs comprise BMP15, BMP10, and Nodal, whereas those of ACVR2A are activin A, activin B, and GDF11. Lastly, we evaluated GF-binding domain BMPR2 variants found in human PAH patients. We demonstrate that mutations within the GF-binding interface resulted in loss of GF binding, while mutations in loop areas allowed BMPR2 to retain the ability to bind cognate GFs with high affinity. In conclusion, the in vitro activities of BMPR2 variants and the crystal structures reported here indicate biochemically relevant complexes that explain how some GF-binding domain variants can lead to PAH.

## INTRODUCTION

Cells communicate to regulate development, maintenance, and regeneration of tissues throughout the lifespan of all multicellular organisms (1). Transforming Growth Factor-β (TGF-β) signaling pathways provide a means for such cell-to-cell communication and tissue fate specification in animals (2–4). Their role in tissue formation, maintenance, and repair is

fundamentally linked with clinically relevant pathologies, including cardiovascular diseases, musculoskeletal disorders, and cancers, making TGF-β pathways key targets for clinical intervention (5, 6). In mammals, TGF-β pathways comprise over 35 secreted growth factors (GFs), seven "type I" and five "type II" serine/ threonine transmembrane kinase receptors, five R-SMAD transcription factors, and many additional accessory factors, including coreceptors, antagonists, and cotranscription factors (7). At the most basic level, TGF-β pathways are activated when a dimeric GF forms a signaling complex with both receptor types, triggering a phosphorylation cascade from receptors to R-SMADs that results in R-SMAD–mediated transcriptional responses (2, 3). Among type II receptors, TGFβR2 and AMHR2 only interact functionally with a select number of GFs, whereas ACVR2A, ACVR2B, and BMPR2 are promiscuous and can form signaling and nonsignaling complexes with an overlapping group of over 30 GFs, including homodimeric and heterodimeric activins, inhibins, bone morphogenetic proteins (BMPs), growth and differentiation factors (GDFs), Nodal, and Lefty (8–11). Structural and biochemical studies have revealed that the GF binding domain (GBD) of both type I and type II receptors adopt a similar, "three-finger toxin fold", where the "fingers" refer to three pairs of antiparallel β-strands that form an extended β-sheet (12, 13). However, in spite of their significant structural homology, receptors interact with GFs in distinct ways (14). Among type II receptors, TGFβR2 binds GFs via an outer β-strand (15, 16). By contrast, ACVR2A and ACVR2B contact GFs via a conserved hydrophobic hot spot localized at the center of the β-sheet (17–21). AMHR2 also binds its cognate GF via a centrally located hydrophobic hot spot but uses a distinct set of aliphatic amino acids that confers AMHR2 its unique specificity (22). Less is known about BMPR2. Structures of unbound BMPR2 have been solved (23). Combined with mutagenesis data (24, 25), they indicate that BMPR2 interacts with GFs like ACVR2A/B. Yet despite this knowledge, many questions about

the molecular basis of BMPR2-GF recognition, specificity determination, and interacting GFs remain unanswered (23, 26–30). Notably, mutations in the BMPR2 gene are profoundly associated with pulmonary arterial hypertension (PAH) (31), a highly morbid disorder characterized by vascular remodeling with progressive obliteration of the lung microvascular system (32, 33). Loss-of-function BMPR2 variants are the most common genetic factor in hereditary forms of PAH, implicating deficient BMPR2 signaling in its pathogenesis (34). Nonetheless, missense mutations in the BMPR2-GBD have also been identified (31). What role these variants play in PAH pathogenesis is unclear. To determine how BMPR2 and its GBD variants interact with GFs, we solved the crystal structure of BMPR2-GBD in complex with activin B, a GF that can bind BMPR2 (28, 35) and that signals via BMPR2 in some cell types (29, 36). To identify molecular differences in GF recognition, we solved the structure of ACVR2A-GBD in complex with activin A and compared how the two receptors interact with these homologous GFs. To establish GF–receptor affinity and activity preferences, we tested binding of different GFs to soluble BMPR2-Fc and ACVR2A-Fc fusion proteins and evaluated the inhibitory potency of these fusion proteins against their targets. Finally, to define the consequences of BMPR2-GBD mutations identified in PAH patients, we evaluated how variants impact the receptor–GF interaction.

## RESULTS

### BMPR2 and ACVR2A employ an analogous GF-binding mode

Figure 2.1 shows the crystal structures of BMPR2-GBD– activin B and ACVR2A-GBD–activin A complexes. We obtained crystals of the complexes by combining purified GF with approximately 1.2 M excess purified receptor GBD. All proteins were expressed individually in Chinese hamster ovary (CHO) cells, purified to homogeneity, and deglycosylated as needed. We collected diffraction data to a resolution of 3.45 Å and 3.14 Å, respectively, and solved both

structures by molecular replacement and multiple rounds of manual rebuilding. For the ACVR2A complex, we used previous crystal structures as search models (37). We solved the BMPR2 complex by placing the activin B protomer structure predicted by AlphaFold (38) first. We then positioned a BMPR2 model lacking loop regions manually and improved its placement with rigid body refinement (23). Notably, previous structures and AlphaFold models were essential for building and refinement of the BMPR2 complex as the resolution of these crystals was limited (For Data collection and refinement statistics, see Table S2.1, for examples of electron density see Figs. 2.S1 and 2.S2). The asymmetric unit of the BMPR2 complex comprised three receptor and three GF protomers, where all biological dimers were related by crystallographic symmetry. The asymmetric unit of the ACVR2A complex contained four receptor and four GF protomers, where all biological dimers were related by noncrystallographic symmetry (NCS). BMPR2 binds activin B at its "knuckle epitope" (Fig 2.1A) (39), a convex surface on the GF that is formed by a set of antiparallel β-strands or "fingers" (40). This binding mode is similar to that between ACVR2A/B and other GFs, as can be seen both in the ACVR2A-activin A structure shown here (Fig 2.1B) and other ACVR2A/B complexes (17–21). One significant difference between the two complexes is the relative orientation of GF protomers within a GF dimer (Fig 2.1, A and B). These differences can be attributed to flexibility of the activin dimer interface, which leads activin A to adopt a closed conformation and activin B an extended conformation. BMPR2 adopts the three-finger toxin fold seen in other TGF-β family receptors with minor variations in β-strand length, flexibility, and orientation (Fig 2.1, C and D). Its GF binding interface is similar to that of ACVR2A and consists of a concave surface that harbors a hydrophobic hot spot containing three conserved aromatic residues, Y67, W85, and F115, at its center (Fig 2.1, C and D). The buried surface areas of the BMPR2–activin B and ACVR2A–activin A complexes are 710 $Å^2$ and 658 $Å^2$, respectively (Table

2.1).

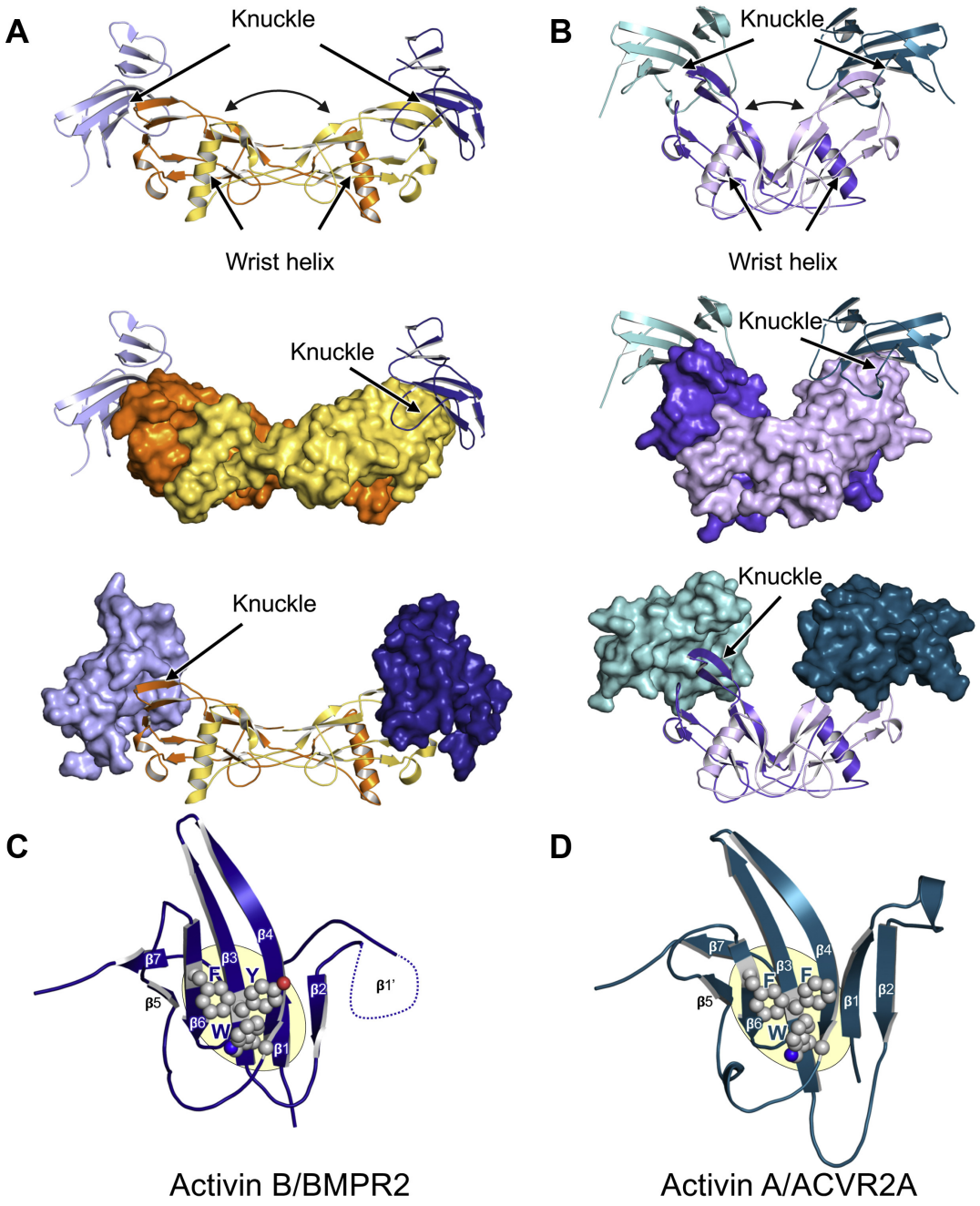


Figure 2.1: Crystal structures of the BMPR2–activin B and ACVR2A–activin A complexes. A, BMPR2–activin B complex. Activin B protomers are colored gold and orange, and BMPR2 GBD protomers are shown in dark and light blue. B, ACVR2A–activin A complex. Activin A protomers are colored light and dark purple, and ACVR2A GBD protomers are shown in light and dark teal. The top panels show all moieties as ribbon diagrams, and the middle panels show surface representations of the GF moiety. The bottom panels show surface representations of the receptors. Arrows point out the knuckle epitope where receptors interact with GFs. C, BMPR2 and D, ACVR2A as seen in complex with their respective GFs. β-strands are labeled to emphasize the "three-finger toxin fold". The "fingers" are formed by β1–β2 (finger 1), β3–β4 (finger 2), and β5–β6 (finger 3). Conserved hydrophobic patch residues are shown as spheres. BMP, bone morphogenetic protein; GBD, GF-binding domain; GF, growth factor.

**GF dimer shape is determined by 'wrist helix' positioning**

GFs are homodimeric or heterodimeric proteins. Protomers are often described as having a hand-like shape, as they contain two sets of antiparallel β-strands with finger-like extensions (the "fingers") that protrude from a central α-helix (the "wrist helix") (Fig 2.2A) (40). Activins exhibit significant flexibility in the wrist helix position (Fig 2.2A). The relative orientation of the two protomers within the dimer varies significantly in these and other activin structures as a result (Fig 2.1, A and B). This flexibility can be explained by the lose tethering of the wrist helix to the rest of the protomer polypeptide chain, as loops connecting the wrist helix to the finger region are mostly disordered in both activin B and activin A structures. Notably, the relative orientation of wrist helix dictates the overall dimer shape as it packs into the concave finger surface of the opposing protomer. The structures presented here, thus, provide additional evidence that the dimer structure of activin class ligands is flexible and that the wrist helix can exist in multiple conformations, leading to significant variability in dimer conformation. We speculate that such conformational plasticity could enable activins to bind two type II receptors with high affinity, even as their relative orientation on the membrane fluctuates. The buried surface area of the GF dimer is substantial (Table 2.1), as has been observed (13, 14), and mainly involves interactions between the wrist helix of one protomer and the inward facing finger surface of the opposite protomer. We also observed a second, substantial interface, which results in the formation of a GF hexamer (Fig 2.2B). While this contact forms part of a crystallographic interaction, its size could hint at the existence of a higher order activin B oligomer. Notably, type I receptors interact with the wrist helix at the GF dimer interface (Fig 2.2C) (18, 20, 21, 39) and this feature is occluded in the hexameric activin B complex. Thus, activin B may not be able to interact with type I receptors in the form observed here. In addition, the orientation of the wrist helix in this complex is unique

compared with homologous GFs that are bound to type I receptors (18, 20, 21), indicating activin B must acquire a different conformation from that observed here to bind type I receptors in the same way as other GFs.

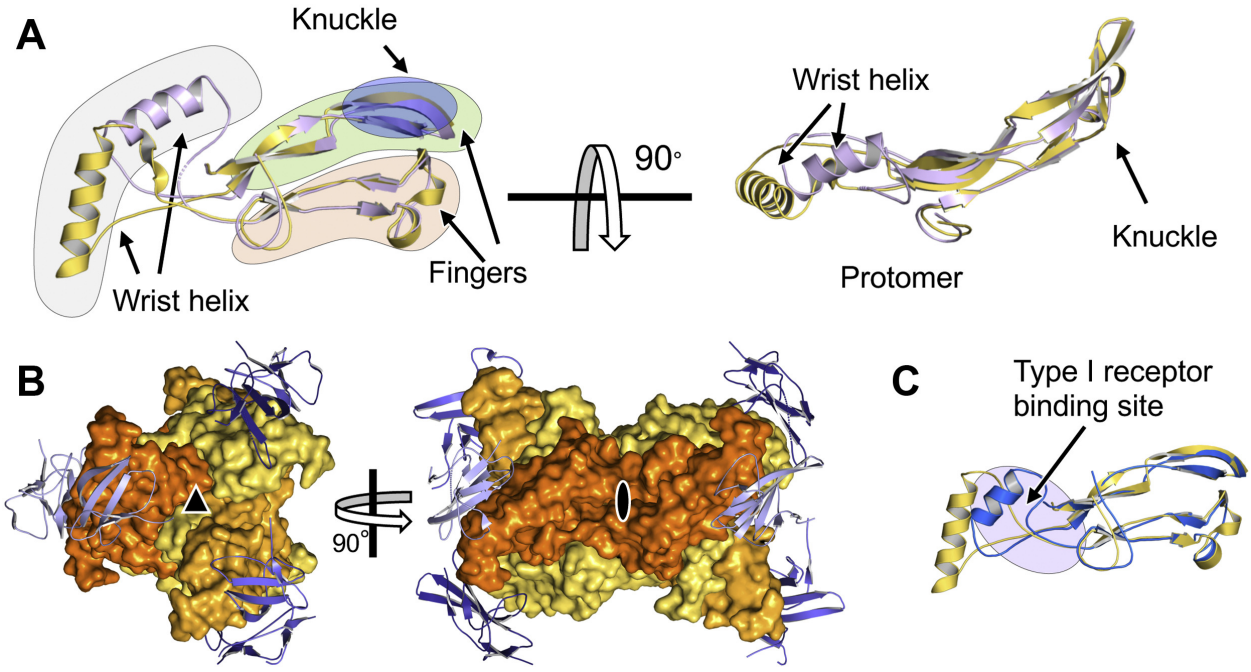


Figure 2.2: GF conformations. *A*, superposition of activin B (*gold*) and activin A (*light purple*) protomers. Previously defined features of the GF structure are highlighted, including the fingers, the wrist helix, and the Figure 2.2 (cont'd) knuckle epitope. Activin B and A have highly superimposable structures. However, the wrist helix adopts GF specific conformations. *Left* and *right panels* represent orthogonal orientations. *B*, activin B forms a higher order, hexameric complex through crystal contacts. The *left panel* shows a noncrystallographic pseudo-threefold axis. The *right panel* shows a crystallographic two-fold axis that generates the biological dimer. *C*, GDF-11 (*blue*) from the GDF-11–ACVR2B–ALK5 signaling complex (6MAC) is superimposed on activin B (*gold*). The Type I receptor-binding site near the wrist helix is highlighted by the *purple circle*. The wrist helix acquires a distinct orientation in the hexameric-signaling complex. GDF, growth and differentiation factor; GF, growth factor.

Table 2.1: Protein-protein interaction surface analysis

| Protein 1 | Protein 2 | Interaction | Copy # | BSA (Å$^2$) | σBSA (Å$^2$) |
|---|---|---|---|---|---|
| Activin B–BMPR2 complex | | | | | |
| INHBB | INHBB | GF dimer | 2 | 1518 | 24 |
| INHBB | BMPR2 | GF-receptor | 3 | 710 | 65 |
| INHBB | INHBB | Lattice | 2 | 1041 | 138 |
| Activin A–ACVR2A complex | | | | | |
| INHBA | INHBA | GF dimer | 2 | 1346 | 9 |
| INHBA | ACVR2A | GF-receptor | 4 | 658 | 17 |

**Abbreviations: BSA, buried surface area; σBSA, SD BSA.**

**Conserved hydrophobic hot spot and variable loops form GF interaction site**

Superposition of the activin A/activin B finger region shows that BMPR2 and ACVR2A bind the knuckle region with nearly identical contacts and orientations (Fig 2.3A) (41). This conclusion is supported by the near perfect superposability of the central receptor β-strands after alignment of the GF moiety. Gray areas of the GF-interaction surface further highlight shared surface elements recognized by both receptors. Nevertheless, receptors appear to have distinct laterality preferences for GF binding. The interface area indicates in general terms that the BMPR2-interaction surface is weighted toward the right side of the GF and the ACVR2A-interaction surface is weighted toward the left side of the GF. The inserted view of the binding interface underscores this preference. Structural superposition of the two receptors further indicates that the laterality preference could result from extended loops that vary in length and placement by receptor (Fig 2.3B). Thus, BMPR2 has three extended loops linking strands β1–β2, β4–β5, and β5–β6 (blue circles), whereas ACVR2A has one extended loop linking strands β2–β3 (green circle). Although these loops are flexible and partially disordered in the BMPR2 structure, they are mostly within contact distance of the GF and, thus, can provide a significant number of unique contacts. Extended BMPR2 loops are generally in position to contact the right side and top of the GF (blue), whereas the extended ACVR2A loop connecting strands β2 and β3 can contact the left side of the GF. However, it is also possible that the laterality bias observed here partly results from limited diffraction. Analysis of the BMPR2–activin B and ACVR2A–activin A interfaces (Fig 2.3, C and D) reveals that most interacting residues are conserved and hydrophobic, with four aliphatic residues and a proline forming the central contact site on activin B and activin A and three aromatic residues forming the hydrophobic hot spot on BMPR2 and ACVR2A. Based on its conservation, we speculate that the aromatic hot spot underlies GF-binding promiscuity of

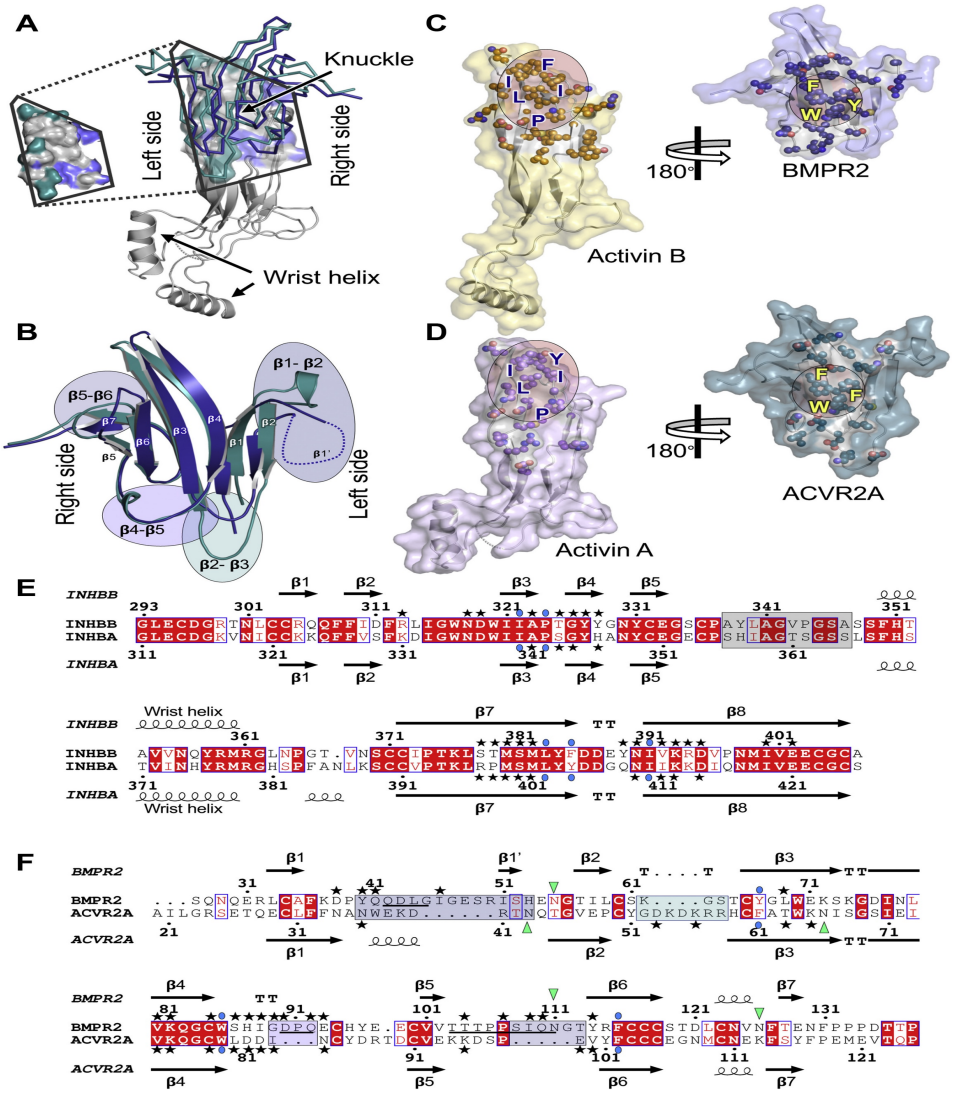


Figure 2.3: The receptor–GF interaction. A, superposition of the GF fingers shows the orientation of BMPR2 (blue) and ACVR2A (teal) on their respective GF is analogous. The interaction surface reveals some areas are contacted by both receptors (gray), whereas others are closer to BMPR2 (blue) or ACVR2A (teal). The inset highlights contact area preferences. B, least squares superposition of BMPR2 (blue) and ACVR2A (teal). Main chain atoms of β-strands 3 and 4 were used in the alignment. β-strands and loops connecting anti-parallel β-strands (i.e., finger loops) are labeled. Finger loops correspond to most variable sequences in BMPR2 and ACVR2A. Circles show finger loops, with blue circles highlighting the longer BMPR2 loops and the green circle highlighting the longer ACVR2A loop. With exception of the β1–β2 loop, longer loops generally lead to more GF contacts. C, BMPR2–activin B complex. Activin B and BMPR2 are shown as yellow and blue surfaces, respectively. D, ACVR2A–activin A complex. Activin A and ACVR2A are shown as purple and teal surfaces, respectively. The views in (C) and (D) correspond to the orientation in (A), with the GF on the left side and the receptor rotated by 180 degrees on the right side. Contact areas are highlighted by the red circles. All residues within contact distance are shown as atoms. The main aliphatic GF and hydrophobic receptor contact residues are also labeled. E, sequence alignment of activin B and activin A. These GFs share 64.3% sequence identity over 115/116 amino acids. F, sequence alignment of BMPR2 and ACVR2A. In both alignments, red areas indicate sequence identity. Stars indicate residues that are within contact distance of their interacting partner. Blue circles denote conserved contact residues labeled in (C) and (D). Contact residues were identified using the PISA (60). Squares (colored as in B) highlight loop areas with significant variability in sequence and disorder in structures. Green triangles show receptor GBD N-glycosylation sites. BMP, bone morphogenetic protein; GBD, GF-binding domain; GF, growth factor.

the two receptors and ACVR2B. In contrast to the central, hydrophobic hot spot, peripheral residues are less conserved and enriched in polar or charged amino acids. Structure-based sequence alignments (42) of the two GFs (Fig 2.3E) and receptors (Fig 2.3F) further indicate that contact residues are conserved in position but not in sequence, with loops providing most unique contacts. Notably, loop residues immediately following strand β4 (i.e., BMPR2 86–92 and ACVR2A 80–84) contribute extensively to the GF interaction. As these residues are not conserved between the two receptors, we speculate that they could have a key role in establishing receptor selectivity.

**BMPR2 exhibits conformational plasticity and binds a distinct set of GFs**

Crystals obtained here contained multiple GF–receptor complexes in the asymmetric unit, allowing us to evaluate the dynamic nature of the various components. Superposition of the GFs indicates GF protomers have a relatively fixed structure, as they are nearly identical except for the activin A wrist helix orientation (Fig S2.3). Similarly, receptor positioning on the GF did not diverge much between BMPR2 and ACVR2A with respect to the placement of contact residues and orientation of the contacting β-strands, indicating a significant degree of functional and structural conservation in the receptor–GF interaction (Fig S2.4). In addition, the different ACVR2A structures were completely superimposable, indicating that the conformational flexibility of the ACVR2A GBD is limited (Fig S2.5A). By contrast, BMPR2 exhibited significant variability in loop regions and in areas that were not directly involved contacting the GF (Figs. 4A and S5B), possibly reflecting the intermediate-binding affinity of BMPR2 for activin B (28) and the conformational plasticity of the GF-free BMPR2 structures (23). In fact, loop conformations in the GF-free structure would preclude GF binding, supporting the idea that these loops adopt distinct conformations in the GF-free and GF-bound forms (Fig 2.4B) (23). Notably, these mobile loops are shorter and generally better ordered in the GF-bound ACVR2A, where they contribute

significantly to the GF interaction (Fig 2.4C). Our findings together with previous structural analysis, therefore, indicate that the BMPR2 GBD is inherently flexible and dynamic. This idea is further supported by the higher average B-factor of BMPR2 (~175 Å2) relative to activin B (~115 Å2) in this complex. Although BMPR2 and ACVR2A utilize a similar GF-binding mode and employ a conserved set of GF-interacting residues, they have distinct GF-binding specificities (8, 28, 43). To better define GF utilization by the two receptors, we evaluated binding of several GFs that have been shown to interact with BMPR2 (28, 29, 35, 36). We were able to obtain good estimates of binding rates and equilibrium-binding constants using single injection surface plasmon resonance at room temperature and we carried out titrations over several concentrations to confirm kinetic parameters for GFs that are relevant to this work (Figs. 4D and S6, Table 2.2). With exception of BMP8b and GDF11, all tested GFs bound soluble BMPR2 GBD-Fc. BMP10 and Nodal had the most stable interaction as indicated by their slow dissociation rate, while activin A, activin B, and BMP15 had similar interaction kinetics with fast association and dissociation rates. BMP7 presented a unique example as it dissociated from BMPR2 at a very fast rate. In contrast to BMPR2, ACVR2A GBD-Fc bound fewer of the tested GFs. They included BMP10, activin A, and activin B, as well as GDF11. Notably, the GF-binding spectrum of ACVR2A was more stratified, with activin A, activin B, and GDF11 forming extremely stable complexes (Table 2.2). These results support previous data showing that ACVR2A and BMPR2 bind an overlapping group of ligands (28); however, ACVR2A binds activin type GFs, including GDF11, with much higher affinity than other tested GFs. We note that a new BMP7 formulation from RnD systems likely accounts for differences with a previous study (28). To uncover functional consequences of the receptor–GF interaction, we tested the ability of the GBD-Fc fusions to inhibit signaling by activin A, activin B, and BMP10 (Fig 2.4E and Table 2.3). Using stably transfected human

embryonic kidney (HEK293) reporter cells, we found increasing concentrations of ACVR2A GBD-Fc–inhibited both activin A/B and BMP10 signaling, as indicated, respectively, by the reduced SMAD2/3 and SMAD1/5/8 responses. By contrast, BMPR2 GBD-Fc inhibited BMP10 but not activin A or activin B signaling. This result may appear surprising, as both receptor fusions bind the four GFs with appreciable affinity. However, in the context of cells that express ACVR2A and are grown at 37 °C, BMPR2-Fc may not bind activins with high enough affinity to compete with the much higher affinity ACVR2A interaction. Along the same lines, BMPR2 GBD-Fc inhibited 5 nM BMP10 with greater potency than ACVR2A GBD-Fc (34.7 and 187.0 nM, respectively, Table 2.3), although both receptor fusions bind BMP10 with similar affinities (Table 2.2) (20, 28). These results indicate how GF signaling could be affected by cell-specific receptor levels (44, 45).

Table 2.2: SPR-based GF-receptor-binding rates

| Binding parameters | BMP7 | BMP8b | BMP10 | BMP15 | GDF11 | Nodal | ActA | ActB |
|---|---|---|---|---|---|---|---|---|
| BMPRII-Fc (single) | | | | | | | | |
| $k_a$ | 5.2E+05 | *NB* | 9.1E+04 | 3.3E+05 | *NB* | 4.2E+04 | 3.7E+05 | 7.9E+05 |
| $k_d$ | 7.1E-03 | *NB* | 1.9E-04 | 2.1E-03 | *NB* | 1.4E-04 | 3.6E-03 | 1.8E-03 |
| $K_D$ | 1.3E-08 | *NB* | 2.1E-09 | 6.3E-09 | *NB* | 3.2E-09 | 9.6E-09 | 2.3E-09 |
| SD $K_D$ | 4.4E-09 | *NB* | 2.8E-10 | 1.0E-09 | *NB* | 2.8E-11 | 1.5E-09 | 2.5E-10 |
| ACVR2A-Fc (single) | | | | | | | | |
| $k_a$ | *NB* | *NB* | 3.6E+05 | *NB* | 3.5E+06 | *NB* | 2.1E+06 | 1.4E+06 |
| $k_d$ | *NB* | *NB* | 3.5E-04 | *NB* | 1.8E-04 | *NB* | 1.9E-04 | 7.4E-05 |
| $K_D$ | *NB* | *NB* | 1.0E-09 | *NB* | 5.2E-11 | *NB* | 9.0E-11 | 5.3E-11 |
| SD $K_D$ | *NB* | *NB* | 3.0E-10 | *NB* | 8.3E-12 | *NB* | 4.3E-12 | 1.0E-11 |

| | BMPRII-Fc (titration) | | ACVR2A-Fc(titration) | |
|---|---|---|---|---|
| | ActB | BMP10 | ActA | ActB |
| $k_a$ | 8.8E+05 | 2.3E+04 | 6.0E+05 | 6.1E+06 |
| $k_d$ | 6.2E-04 | 5.5E-05 | 1.2E-05 | 9.7E-06 |
| $K_D$ | 7.1E-10 | 2.4E-09 | 1.8E-11 | 1.6E-12 |
| $Chi^2$ | 0.93 | 0.15 | 1.72 | 1.93 |

**$k_a$ ($M^{-1}$ $s^{-1}$), $k_d$ ($s^{-1}$), $K_D$ (M), *NB*, no binding, single: single curve fit averages of two independent injections 80 nM GF injections, titration: global fit of 2.5 nM, 5.0 nM, 10.0 nM, 20.0 nM, and 40.0 nM GF injections.**

Table 2.3: Inhibitory potency of Fc Fusions

| Receptor | BMP10 | Activin B |
|---|---|---|
| BMPRII-Fc | 3.5E-08 | *NI* |
| ACVR2A-Fc | 18.7E-08 | 1.4E-08 |

**$IC_{50}$ (M), *NI*, no inhibition.**

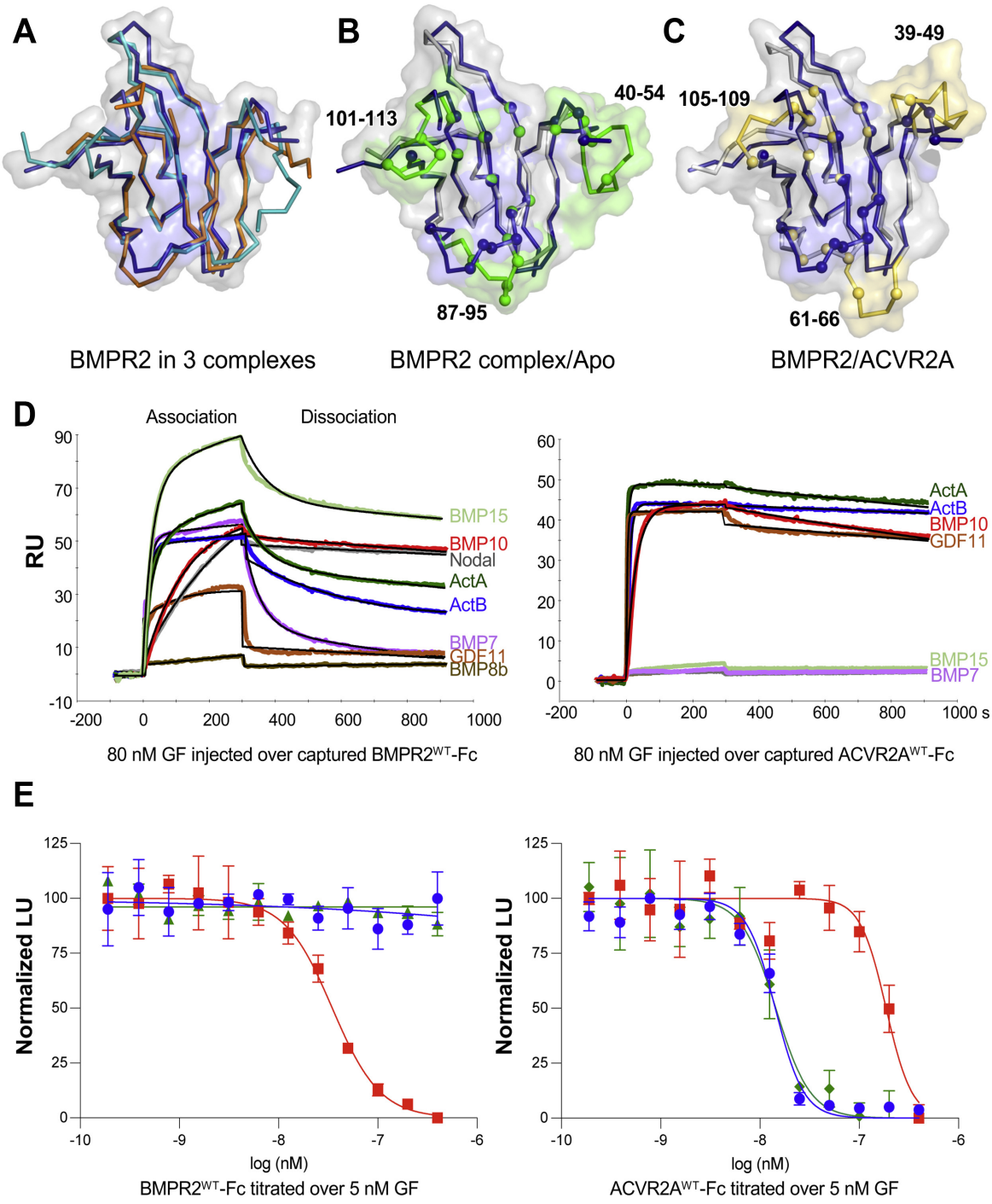


Figure 2.4: Structural and functional comparison of BMPR2 and ACVR2A. A, superposed noncrystallographic BMPR2 protomers shown as ribbons (blue, cyan, and orange). The surface of one protomer is shown in gray with the GF interaction surface colored blue. Disordered loops and variability in strand positioning indicate structural flexibility. B, superposed APO- (gray/green, 2HLQ) and GF- (blue) bound BMPR2 shown as ribbons. APO- and GF-bound BMPR2 surfaces are shown in gray with the GF interaction surface colored blue and ordered loops in the APO structure colored green. Cα atoms of contacting residues are shown as spheres, with GF-bound BMPR2 Cα atoms colored blue and the corresponding APO BMPR2 Cα atoms colored green. Loop regions are ordered in the APO structure (2HLQ) and the finger three loop (β4–β5, residues 87–95) undergoes a significant structural rearrangement upon GF binding. C, superposed GF-bound ACVR2A (gray/yellow) and BMPR2 (blue) shown as ribbons.

Figure 2.4 (cont'd).
BMPR2/ACVR2A surfaces are shown in gray with the GF interaction surface of BMPR2 colored blue and ACVR2A loops colored yellow. Cα atoms of the respective GF contacting residues are shown as spheres, with BMPR2 contact residues colored blue and ACVR2A contact residues colored yellow. The ACVR2A finger two loop (β2–β3, residues 61–66) extends relative to the BMPR2 and provides a distinct set of GF contacts. D, GF binding specificity determined by SPR. BMPR2-Fc (left panel) and ACVR2A-Fc (right panel) were captured on an SPR sensor chip. 80 nM activin A, activin B, Nodal, BMP7, BMP8b, BMP10, BMP15, or GDF11 were injected over the bound receptors. BMP10 and Nodal bind BMPR2 with high affinity as indicated by the slow dissociation rates. Samples are color coded as noted in the figure, black lines correspond to the fitted curved. E, GF inhibition by BMRP2-Fc and ACVR2A-Fc. Stably transfected HEK293 reporter cells were induced with 5 nM BMP10, activin B, or activin A. Increasing concentrations of BMRP2-Fc inhibit BMP10 (left panel). Increasing concentrations of ACVR2A-Fc inhibit BMP10, activin B (blue), or activin A (dark green) (right panel). Luciferase units are normalized to GF control (Normalized Luciferase Units, Normalized LU). The average of three biological replicates is shown with error bars representing SD. BMP, bone morphogenetic protein; GDF, growth and differentiation factor; GF, growth factor; HEK293, human embryonic kidney cells.

## Hydrophobic hot spot variants identified in PAH patients lack GF-binding activity

Several BMPR2 GBD missense mutations have been identified in PAH patients (Table 2.4) (31). Variants could be categorized as forming part of the GF interaction surface (orange), of peripheral loop areas (purple), or of the conserved disulfide core (Fig 2.5A). We produced multiple variants as Fc fusions using stably transfected CHO cells as described. We excluded disulfide core variants as they are expected to misfold. Purified variants were monodisperse as determined by size-exclusion chromatography (SEC) and eluted at a volume consistent with the expected molecular weight (Fig S2.7), indicating they were properly folded. Using SPR, we tested binding of variants to activin B and BMP10 (Figs. 5, B and C and S8). Variants that formed part of the GF interaction surface failed to bind BMP10 and activin B, as indicated by the absent SPR response (orange curves). These results provide direct evidence that the hydrophobic hot spot is critical for GF binding and that the crystal structure is biochemically relevant. By contrast, peripheral loop variants (purple curves) bound activin B and BMP10 with affinities that were comparable to those of the WT receptor (green curve), indicating that the contribution of these loops to GF binding affinity and specificity may be relatively modest and possibly indirect. Notably, variants that potentially have increased loop rigidity (G47D and S107P) exhibited a modest gain in binding

affinity relative to the WT receptor, as reflected in the lower equilibrium dissociation constant (KD, Table 2.5). To validate our SPR results, we tested BMP10 signaling inhibition by the different GBD-Fc variants using stably transfected HEK293 reporter cells. Consistent with the SPR data in Figure 2.5C, we found that peripheral loop variants inhibited BMP10 signaling (Fig 2.5D), whereas interaction surface variants did not (Fig 2.5E). Three variants (G47D, Q92H, and S107P) inhibited BMP10 signaling with significantly greater potency than WT BMPR2 GBD-Fc (Table 2.5). Notably, PAH is generally assumed to be caused by BMPR2 loss of function. We show here that most GBD variants fit that model. However, we identify four variants that retain or gain GF binding activity, indicating that these variants either promote PAH pathogenesis by a distinct mechanism or that they are mischaracterized as pathogenic (Table 2.4)

Table 2.4: PAH mutations in BMPR2 GBD

| Mutation | Variant | Phenotype | Structural role | SPR binding | PMID |
|---|---|---|---|---|---|
| c.100T>C | C34R | Suspected | DS | - | 16429395 |
| c.125A>G | Q42R | Suspected | Periphery | Gain | 15358693 |
| c.140G>A | G47D | Suspected | Periphery | Normal | 15358693 |
| c.179G>A | C60Y | Suspected | DS | - | 11015450 |
| c.196T>C | C66R | Pathogenic | DS | - | 15055271 |
| c.197G>A | C66Y | Pathogenic | DS | - | 16429395 |
| c.200A>G | Y67C | Pathogenic | Central patch | Loss | 12358323 |
| c.203G>A | G68D | Pathogenic | Central patch | Loss | 16429395 |
| c.246A>C | Q82H | Suspected | Central patch | Loss | 12358323 |
| c.247G>A | G83R | Pathogenic | Central patch | Loss | 18356561 |
| c.276A>C | Q92H | Benign | Periphery | Gain | 16429395 |
| c.280T>C | C94R | Pathogenic | DS | - | 16429395 |
| c.295T>C | C99R | Pathogenic | DS | - | 16429395 |
| c.319T>C | S107P | Suspected | Periphery | Gain | 15358693 |
| c.350G>C | C117S | Pathogenic | DS | - | 16429395 |
| c.350G>A | C117Y | Pathogenic | DS | - | 11015450 |
| c.353G>A | C118Y | Suspected | DS | - | 16429395 |
| c.354T>G | C118W | Suspected | DS | - | 10973254 |
| c.367T>A | C123S | Pathogenic | DS | - | 16429395 |
| c.367T>C | C123R | Pathogenic | DS | - | 15358693 |

Orange: hydrophobic hot spot residues or residues near the hydrophobic hot spot. Purple: peripheral loop residues. Black: cysteines involved in disulfide bond formation are colored black. Abbreviation: DS, Disulfide Cysteine.

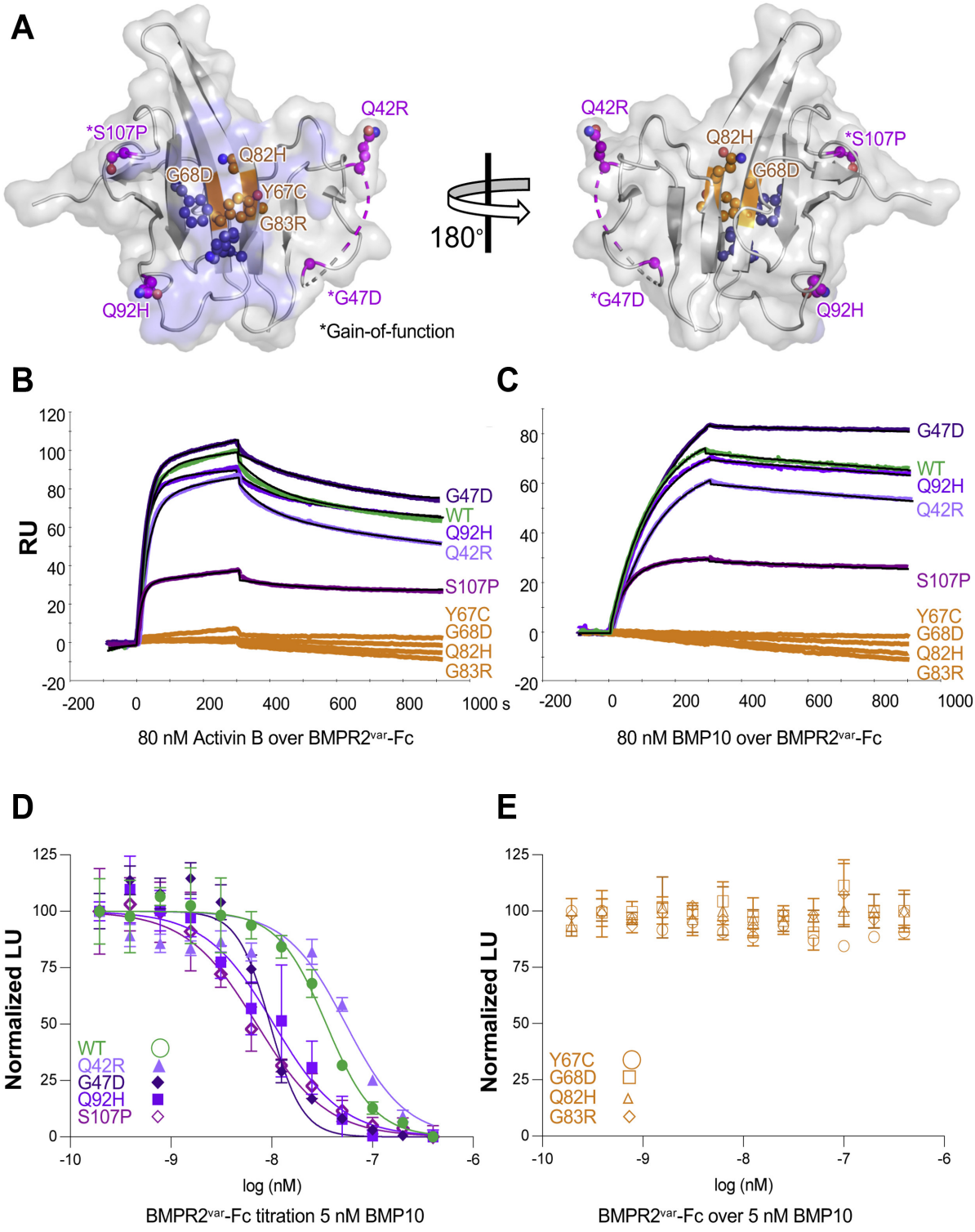


Figure 2.5: A, GF-bound BMPR2 GBD shown with residues mutated in PAH. Orange colored residues are near or form part of the hydrophobic hot spot. Magenta colored residues are on the periphery of the GF-binding interface. Asterisks mark gain-of-function variants. Dark purple colored residues form part of the hydrophobic hot spot. The blue surface corresponds to the GF-binding interface. Left and right panels are related by a 180-degree rotation. B and C, GF-binding properties of PAH variants analyzed by SPR. BMPR2-Fc variants were captured by an SPR sensor chip. 80 nM activin B (B) or BMP10 (C) were injected over the captured variants. WT BMPR2 is shown in green,

Figure 2.5 (cont'd).
sensograms corresponding to binding site variants are shown in orange, and sensograms corresponding to peripheral variants are shown in purple. All binding site variants lose their GF-binding function. By contrast, peripheral variants bind the two tested GFs similar to WT BMPR2. Samples are color coded as noted in the figure, black lines correspond to the fitted curved. D and E, GF inhibition by BMRP2-Fc variants. Stably transfected HEK293 reporter cells were induced with 5 nM BMP10. Increasing concentrations of BMRP2-Fc peripheral (D) and hot spot (E) were added. Peripheral variants Q42R, G47D, Q92H, and S107P inhibit BMP10 signaling, whereas binding site variants Y67C, G68D, Q82H, and G83R do not. Luciferase units are normalized to GF control (Normalized Luciferase Units, Normalized LU). The average of three biological replicates is shown with error bars representing SD. BMP, bone morphogenetic protein; GBD, GF-binding domain; GF, growth factor; HEK293, human embryonic kidney cells; PAH, pulmonary arterial hypertension.

## DISCUSSION

We have solved the crystal structures of the type II BMPR2 GBD in complex with activin B and of the type II activin Receptor ACVR2A in complex with activin A. We show that BMPR2 and activin type II receptors interact with GFs using a nearly identical mode of binding. Placement of the two receptors on their respective GFs is analogous in geometry, as central secondary structural elements of both type II receptors as placed on the GFs superpose well. Receptor–GF interactions are mostly preserved as both receptors contact a conserved set of aliphatic GF residues using a conserved set of aromatic residues that form a central hydrophobic hot spot. However, differences between receptors are also apparent. Most notably, the length and sequences of the loops that extend from the various “fingers” allow for unique receptor– GF contacts. These are weighted toward different sides of the GF, with BMPR2 favoring contacts with the right side of the GF and ACVR2A favoring the left side. In addition, BMPR2 residues 86 to 92 and ACVR2A residues 80 to 84, which form part of the loop connecting strands β4 and β5 and immediately follow the hydrophobic hot spot W85 (BMPR2) or W79 (ACVR2A), contribute significantly to the GF interaction but differ in sequence, highlighting a region that could account for differences in GF recognition between the two receptors. Collectively, these results indicate how receptors could acquire distinct specificities within the framework of a highly conserved, central interaction hot spot. Variations in peripheral loop residues could provide a platform of unique contacts to

establish receptor–GF binding selectivity. ACVR2A and BMPR2 can potentially interact with the same 30 GFs (8–11). Although their distinct biological functions indicate differences in their GF binding and signaling activities (46), questions about their GF-binding selectivity remain. Here, we demonstrated that the BMP15, BMP10, and Nodal are the highest affinity BMPR2 GFs. By contrast, activin A, activin B, and GDF11 are the highest affinity ACVR2A GF. Nevertheless, BMP10 also bound ACVR2A, and activins A and B also bound BMPR2 with considerable affinity, revealing a significant overlap in receptor utilization by these GFs. However, the faster dissociation rate of activins A and B from BMPR2 indicated that activin–BMPR2 complexes are less stable than activin ACVR2A complexes, providing a rationale for the preferential utilization of ACVR2A by activins. These observations were mirrored when analyzing signaling by the three GFs and their inhibition by the traps BMPR2-Fc and ACVR2A-Fc. Both traps inhibited BMP10, potentially reflecting the comparable binding affinity of BMPR2 and ACVR2A for BMP10. By contrast, only ACVR2A-Fc inhibited activin A and activin B, suggesting that the exceptionally high affinity of activins for ACVR2A could preclude their inhibition by the lower affinity interactor BMPR2 GBD-Fc at tested concentrations and temperatures. These observations indicate that in a physiological context, activins preferentially associate and signal via their high affinity receptors ACVR2A and ACVR2B. By contrast, BMPs could utilize the three type II receptors ACVR2A, ACVR2B, and BMPR2 equally as they associate with the three receptors with similar affinities. But activins could also signal via BMPR2 as shown previously, perhaps in cells that do not express ACVR2A/B (29, 36). The biological relevance of BMPR2 stems in part from its link to PAH (31). Over 250 mutations throughout the BMPR2 gene have been identified in PAH patients, including in the extracellular GBD region. Most PAH mutations result in loss of BMPR2 function or reduced BMPR2 levels. They include mutations in the GBD cysteines that form the

obligate cysteine disulfide core. However, missense mutations in the GBD of unknown consequence have also been identified. We generated these GBD variants and tested their ability to bind and/or inhibit signaling by activin B and BMP10. All mutations within the GF-binding interface resulted in loss of function, indicating that the crystal structure represents a biological complex. Y67C directly contacts the GF, highlighting the importance of the hydrophobic hot spot residues in GF binding. Other GF binding interface variants are adjacent in sequence or space to Y67C but point away from that site. That these variants fail to bind GF indicates that the overall integrity and shape of the GF-binding interface is critical for GF binding and may be modulated indirectly by amino acids that have a structural rather than functional role. By contrast, all loop variants bound activin B and BMP10, indicating that residues, which are distant in space from the hydrophobic hot spot, may only have a moderate functional significance. Notably, the fact that these variants bind BMPR2 could either indicate that these are misclassified as pathogenic or that they may cause PAH by an alternate mechanism. In fact, three variants gained function as indicated by a slower receptor–GF dissociation rate or by greater inhibitory potency. Two of these variants, G47D and S107P, may lead BMPR2 to have greater structural rigidity, possibly indicating that the inherent flexibility of the BMPR2 GBD may be linked with its overall lower GF-binding affinities. While testing these PAH variants in an in vitro signaling assay could clarify if they retain signaling activities, our ability to carry out these experiments is limited as BMP9/BMP10 signal strongly in most standard cell lines, including HepG2, A204, and HEK293 cells (28, 47–49). Overall, the structures and biochemistry presented here reveal how the type II TGF-β family receptor BMPR2 binds GFs. These structures demonstrate that ACVR2A, ACVR2B, and BMPR2 use a conserved mode of GF recognition and thus provide a molecular rationale for the promiscuous and shared GF-binding spectrum of the three receptors. But they also reveal interacting regions of low

homology that could account for GF selectivity. We further explored biochemical and in vitro activities of BMPR2 variants identified in PAH patients. Variants in the binding hot spot are not active, providing direct evidence that the crystal structure represents a biological complex and supporting the idea that BMPR2 loss of function is a key pathogenic mechanism in PAH. Strikingly, PAH variants in peripheral loop areas remained active. This observation either suggests that these variants are misclassified as pathogenic or that they could transform a signaling complex into a loss-of-function complex.

## EXPERIMENTAL PROCEDURES

### Receptor Fc fusions

Human BMPR2 cDNA (Q13873) and synthetic genes for human ACVR2A (P27037) and human IgG1-Fc were used to generate the receptor GBD-Fc fusions by two-step PCR. NCBI-protein accession numbers are shown in parentheses. Fusion constructs included the extracellular domains of human ACVR2A (1–120) or BMPR2 (1–138), a 20 amino acid linker containing TEV and enterokinase cleave sites, and a C-terminal Fc. The TEV site immediately followed the receptor GBD and the enterokinase site immediately preceded the Fc moiety. PAH variants were generated from the parental BMPR2-Fc construct via two-step PCR. Fusion proteins were expressed in stably transfected CHO cells and purified from conditioned medium (CM) using Protein A capture (MabSelect SuRe, Cytiva) as described (28) followed by SEC in PBS, pH 7.5. SEC removed aggregates ensuring that a monodisperse population of expected apparent molecular weight was used in all downstream studies. Purified proteins were stored at −80 °C.

### Growth factors

Human nodal (Q96S42), BMP7 (P18075), BMP15 (O95972), BMP8b (P34820), and

GDF11 (O95390) were obtained from R&D Systems or PeproTech. Activin A (P08476), activin B (Q53T31), and BMP10 (O95393) were produced in-house using stably transfected CHO cells. Activin A was captured from CM by Protein A affinity chromatography. BMP10 was captured from CM by Metal affinity chromatography (Excel, Cytiva). Both GF moieties were separated from the prodomain using Reversed Phase Chromatography (Resource RPC, Cytiva). Activin B was purified as described (50). GFs were lyophilized and stored at −80 C. NCBI-protein accession numbers are shown in parentheses.

**Crystallization**

Receptor GBD were cleaved from the Fc moiety by TEV protease (51, 52), resulting in fragments that consisted of residues 20 to 120 (ACVR2A) and 27 to 138 (BMPR2) followed by the TEV site. Fc was removed by protein A capture. Receptor GBDs were deglycosylated using Endo F3 or PNGase F, purified by SEC, dialyzed into Tris-buffered saline (pH 7.5), and stored at −80 C. GFs consisted of the full mature moiety, including residues 311 to 426 (activin A) and 293 to 407 (activin B). Both GFs fractions consisted 100% of disulfide linked dimers. For crystallization, GFs were resuspended in 4 mM HCl (RnD Systems, pH 2.4) and combined with 1.2 M excess receptor GBD. The buffer of the complexes was exchanged by centrifugation to 10 mM Tris–HCl, 40 mM NaCl, pH 8.0. The final concentration of the BMPR2–activin B and ACVR2A–activin A complexes was 11 mg/ml and 9 mg/ml, respectively. Crystallization conditions were identified using the JCSG+ screen (Qiagen). Diffraction quality crystals were obtained after optimizing conditions. BMPR2–activin B crystals were grown in 14% PEG 3K, 175 mM (NH4)2 SO4,

100 mM BisTris, pH 5.4. ACVR2A–activin A were grown in 17% PEG 3K, 100 NaCitrate, pH 5.8.

**Data collection**

Crystals for the BMPR2–activin B complex were crosslinked using glutaraldehyde (53), equilibrated in mother liquor containing 30% glycerol, and flash frozen in liquid nitrogen. A 3.45 Å dataset was collected at the Advanced Photon Source, beamline 21-ID-G. Molecular replacement using PHASER (54) placed three activin B protomers in the asymmetric unit. The activin B model was obtained from AlphaFold (38). The BMPR2 GBD (PDBid 2HLR/2HLQ, (23)) with loop regions deleted was placed manually onto one GF protomer, fitted with rigid body refinement, and extended by NCS. Crystals for the ACVR2A–activin A complex were equilibrated in 17% PEG 3K, 100 Na-formate, pH 4.5, and 30% glycerol. Data were processed and reduced with HKL2000 (55). A 3.20 Å dataset was collected on a Rigaku FR-E+ rotating anode generator at 100 K. Data were processed with MOSFLM and reduced with AIMLESS (56, 57). Molecular replacement with PHASER placed four receptor–GF complexes of the ACVR2B–activin A

crystal structure in the asymmetric unit (PDBid 1S4Y, (37)). Both structures were refined with PHENIX (58) using NCS restraints for equivalent residues. Manual building was performed in COOT (59). AlphaFold models and high resolution protomer structures were used to assist in model building. Electron density was continuous for all ACVR2A protomers. Activin A and activin B were generally well ordered except for loops connecting the wrist helix. BMPR2 was well defined in regions near the GF; however, loop regions were generally disordered. Water molecules were not placed in the final model. Contact maps and buried surface area values were calculated using the Protein Interfaces, Surfaces, and Assemblies server (60). Structural figures were prepared using PyMOL (61). Atomic coordinates and structure factor amplitudes were deposited in the Protein Data Bank (PDBid 7U5O, 7U5P). For data processing and refinement statistics, see Table S1.

**Surface plasmon resonance**

SPR experiments were performed using a BIAcore 3000. Experiments were carried out at 25 C in HBS/EPS (0.01 M Hepes, 0.5 M NaCl, 3 mM EDTA, 0.005% (v/v) Tween 20, pH 7.4) containing 0.1% bovine serum albumin as running buffer. The experimental flow rate was 50 µl/min. Approximately, 5000 to 7000 Response Units (RU) of Anti-human IgG (Fc) (Human antibody capture kit, Cytiva) were immobilized on three channels of a CM5 chip using amine-coupling chemistry. Approximately, 500 RU of purified BMPR2-Fc WT or BMPR2-Fc variants and 150 RU of purified ACVR2A-Fc were loaded on the experimental flow channels. A reference channel was monitored to account for nonspecific binding, drift, and bulk shifts. To identify ACVR2A- and BMPR2-interacting ligands, 80 nM activin A, activin B, BMP7, BMP8b, BMP10, BMP15, GDF11, and Nodal were injected over the WT receptors. To establish the binding activity of PAH variants, 80 nM BMP10 or activin B was injected over captured BMPR2-$Fc^{WT}$ or BMPR2-$Fc^{VAR}$. The single concentration approach allowed us to obtain an estimate of binding parameters. Injections were repeated two times. Titrations over several concentrations were used to confirm kinetic parameters for GFs and receptors that are relevant to this work. The antibody surface was regenerated to baseline after each binding cycle by injecting MgCl2. Sensograms were analyzed by double referencing. To obtain kinetic rate constants, the processed data were fitted to "1:1 binding model" using BiaEvaluation software. The equilibrium-binding constant KD was determined by calculating the ratio of binding rate constants kd/ka. Results are summarized in Table 1.

**Cell lines**

HEK293 were obtained from American Type Culture Collection. Cells were grown in Eagle's minimum essential medium (EMEM) supplemented with 10% fetal bovine serum and 1%

penicillin/streptavidin at 37 C under 5% humidified CO2 conditions as indicated. Passage 5 cells were transfected with the SMAD2/3 responsive reporter plasmid pGL4.48 (luc2P/SMAD binding element (SBE)/HYGRO) or the SMAD1/5/8 responsive reporter plasmid pGL4 (luc2P/2X BMP responsive element (BRE)/PURO) using lipofectamine 2000 and subjected to hygromycin B (50 µg/ml) or puromycin (0.5 µg/ml) selection. Passage 8 SBE reporter cell pools were cryopreserved. BRE reporter cells were subjected to clonal selection and single clones were cryopreserved at passage 11. Freshly thawed cells were passaged twice before seeding 96- well reporter assay plates.

**Reporter assays**

Fifty thousand SBE or 10,000 BRE reporter cells per well were seeded in 96-well plates and grown overnight in complete EMEM medium. After 24 h incubation, medium was replaced by assay medium (serum-free EMEM, 5 nM GFs and 0–400 nM receptor-Fc fusion). Assay medium was incubated at room temperature for 1 h before addition to cells. Luciferase expression was measured using a luciferase assay reagent after cells were incubated 16 h in assay medium. Firefly luciferase activity was measured using a FLUOstar Omega plate reader. Reporter gene assays were performed in triplicates and were repeated multiple times. Data presented is the mean of three independent measurements. Error bars represent the SD from three independent measurements. GraphPad Prism 9.3 was used for data fitting, analysis, and for generating graphs.

**Data availability**

Data and structures have been deposited at the Protein Data Bank (https://www.rcsb.org) and will be publicly released with publication. Accession numbers of the deposited structures are 7U5O and 7U5P.

**Acknowledgments**

We thank Senem Aykul for implementing activin B purification and Zahra Nossoni for assistance with synchrotron data collection. This research was funded by National Institute of General Medical Sciences, grant number R01 GM121499.

**Author contributions**

K.Y.C.,A.M.,V.T., and E. M.H. methodology; K.Y.C., A.M., V.T., and E.M.H. investigation; K.Y.C., A.M.,V.T., and E.M.H. formal analysis; K.Y.C.,A.M.,V.T., and E.M.H. resources; K.Y.C.,A.M.,V.T., and E.M.H. data curation; K.Y.C.,A.M.,V.T., and E.M.H. validation; E.M.H. conceptualization; E.M.H. supervision; E.M.H. project administration; E.M.H. writing original draft; E. M.-H. writing–review and editing; E. M.-H. visualization; E. M.-H. funding acquisition.

## REFERENCES


1. Perrimon, N., Pitsouli, C., and Shilo, B. Z. (2012) Signaling mechanisms controlling cell fate and embryonic patterning. Cold Spring Harb. Perspect. Biol. 4, a005975

2. Heldin, C. H., Miyazono, K., and Ten Dijke, P. (1997) TGF-beta signalling from cell membrane to nucleus through SMAD proteins. Nature 390, 465–471

3. Massague, J. (1998) TGF-beta signal transduction. Annu. Rev. Biochem. 67, 753–791

4. Huminiecki, L., Goldovsky, L., Freilich, S., Moustakas, A., Ouzounis, C., and Heldin, C. H. (2009) Emergence, development and diversification of the TGF-beta signalling pathway within the animal kingdom. BMC Evol. Biol. 9, 28

5. Santibanez, J. F., Quintanilla, M., and Bernabeu, C. (2011) TGF-beta/ TGF-beta receptor system and its role in physiological and pathological conditions. Clin. Sci. (Lond.) 121, 233–251

6. Miyazono, K., Kusanagi, K., and Inoue, H. (2001) Divergence and convergence of TGF-beta/BMP signaling. J. Cell. Physiol. 187, 265–276

7. Moustakas, A., and Heldin, C. H. (2009) The regulation of TGF-beta signal transduction. Development 136, 3699–3714

8. Martinez-Hackert, E., Sundan, A., and Holien, T. (2021) Receptor binding competition: a paradigm for regulating TGF-beta family action. Cytokine Growth Factor Rev. 57, 39–54

9. Mueller, T. D., and Nickel, J. (2012) Promiscuity and specificity in BMP receptor activation. FEBS Lett. 586, 1846–1859

10. Derynck, R., and Budi, E. H. (2019) Specificity, versatility, and control of TGF-beta family signaling. Sci. Signal. 12, eaav5183

11. Aykul, S., Corpina, R. A., Goebel, E. J., Cunanan, C. J., Dimitriou, A., Kim, H. J., et al. (2020) Activin A forms a non-signaling complex with ACVR1 and type II activin/BMP receptors via its finger 2 tip loop. Elife 9, e54582

12. Greenwald, J., Fischer, W. H., Vale, W. W., and Choe, S. (1999) Three-finger toxin fold for the extracellular ligand-binding domain of the type II activin receptor serine kinase. Nat. Struct. Biol. 6, 18–22

13. Hinck, A. P. (2012) Structural studies of the TGF-betas and their receptors - insights into evolution of the TGF-beta superfamily. FEBS Lett. 586, 1860–1870

14. Goebel, E. J., Hart, K. N., McCoy, J. C., and Thompson, T. B. (2019) Structural biology of the TGF-beta family. Exp. Biol. Med. 244, 1530–1546

15. Hart, P. J., Deep, S., Taylor, A. B., Shu, Z., Hinck, C. S., and Hinck, A. P. (2002) Crystal structure of the human TbetaR2 ectodomain–TGF-beta3 complex. Nat. Struct. Biol. 9, 203–208

16. Groppe, J., Hinck, C. S., Samavarchi-Tehrani, P., Zubieta, C., Schuermann, J. P., Taylor, A. B., et al. (2008) Cooperative assembly of TGF-beta superfamily signaling complexes is mediated by two disparate mechanisms and distinct modes of receptor binding. Mol. Cell 29, 157–168

17. Thompson, T. B., Woodruff, T. K., and Jardetzky, T. S. (2003) Structures of an ActRIIB:activin A complex reveal a novel binding mode for TGF-beta ligand:receptor interactions. EMBO J. 22, 1555–1566

18. Allendorph, G. P., Vale, W. W., and Choe, S. (2006) Structure of the ternary signaling complex of a TGF-beta superfamily member. Proc. Natl. Acad. Sci. U. S. A. 103, 7643-7648

19. Weber, D., Kotzsch, A., Nickel, J., Harth, S., Seher, A., Mueller, U., et al. (2007) A silent H-bond can be mutationally activated for high-affinity interaction of BMP-2 and activin type IIB receptor. BMC Struct. Biol. 7, 6

20. Townson, S. A., Martinez-Hackert, E., Greppi, C., Lowden, P., Sako, D., Liu, J., et al. (2012) Specificity and structure of a high affinity activin receptor-like kinase 1 (ALK1) signaling complex. J. Biol. Chem. 287, 27313–27325

21. Goebel, E. J., Corpina, R. A., Hinck, C. S., Czepnik, M., Castonguay, R., Grenha, R., et al. (2019) Structural characterization of an activin class ternary receptor complex reveals a third paradigm for receptor specificity. Proc. Natl. Acad. Sci. U. S. A. 116, 15505–15513

22. Hart, K. N., Stocker, W. A., Nagykery, N. G., Walton, K. L., Harrison, C. A., Donahoe, P. K., et al. (2021) Structure of AMH bound to AMHR2 provides insight into a unique signaling pair in the TGF-beta family. Proc. Natl. Acad. Sci. U. S. A. 118, e2104809118

23. Mace, P. D., Cutfield, J. F., and Cutfield, S. M. (2006) High resolution structures of the bone morphogenetic protein type II receptor in two crystal forms: implications for ligand binding. Biochem. Biophys. Res. Commun. 351, 831–838

24. Yin, H., Yeh, L. C., Hinck, A. P., and Lee, J. C. (2008) Characterization of ligand-binding properties of the human BMP type II receptor extracellular domain. J. Mol. Biol. 378, 191-203

25. Kirsch, T., Nickel, J., and Sebald, W. (2000) BMP-2 antagonists emerge from alterations in the low-affinity binding epitope for receptor BMPR-II. EMBO J. 19, 3314–3324

26. Liu, F., Ventura, F., Doody, J., and Massague, J. (1995) Human type II receptor for bone morphogenic proteins (BMPs): extension of the twokinase receptor model to the BMPs. Mol. Cell. Biol. 15, 3479–3486

27. Nohe, A., Hassel, S., Ehrlich, M., Neubauer, F., Sebald, W., Henis, Y. I., et al. (2002) The mode of bone morphogenetic protein (BMP) receptor oligomerization determines different BMP-2 signaling pathways. J. Biol. Chem. 277, 5330–5338

28. Aykul, S., and Martinez-Hackert, E. (2016) Transforming growth factorbeta family ligands can function as antagonists by competing for type II receptor binding. J. Biol. Chem. 291, 10792–10804

29. Olsen, O. E., Sankar, M., Elsaadi, S., Hella, H., Buene, G., Darvekar, S. R., et al. (2018) BMPR2 inhibits activin and BMP signaling via wild-type ALK2. J. Cell Sci. 131, jcs213512

30. Hiepen, C., Jatzlau, J., Hildebrandt, S., Kampfrath, B., Goktas, M., Murgai, A., et al. (2019) BMPR2 acts as a gatekeeper to protect endothelial cells from increased TGF-beta responses and altered cell mechanics. PLoS Biol. 17, e3000557

31. Garcia-Rivas, G., Jerjes-Sánchez, C., Rodriguez, D., Garcia-Pelaez, J., and Trevino, V. (2017) A systematic review of genetic mutations in pulmonary arterial hypertension. BMC Med. Genet. 18, 82

32. Thenappan, T., Ormiston, M. L., Ryan, J. J., and Archer, S. L. (2018) Pulmonary arterial hypertension: pathogenesis and clinical management. BMJ 360, j5492

33. Woodcock, C. C., and Chan, S. Y. (2019) The search for diseasemodifying therapies in pulmonary hypertension. J. Cardiovasc. Pharmacol. Ther. 24, 334–354

34. Orriols, M., Gomez-Puerto, M. C., and Ten Dijke, P. (2017) BMP type II receptor as a therapeutic target in pulmonary arterial hypertension. Cell. Mol. Life Sci. 74, 2979–2995

35. Kumar, R., and Knopf, J. (2017). In: World Intellectual Property Organization, ed. Bmprii Polypeptides and Uses Thereof, Acceleron Pharma, Inc, Cambridge, MA. US 2017 / 0291933, USPTO

36. Rejon, C. A., Hancock, M. A., Li, Y. N., Thompson, T. B., Hebert, T. E., and Bernard, D. J. (2013) Activins bind and signal via bone morphogenetic protein receptor type II (BMPR2) in immortalized gonadotrope-like cells. Cell Signal. 25, 2717–2726

37. Greenwald, J., Vega, M. E., Allendorph, G. P., Fischer, W. H., Vale, W., and Choe, S. (2004) A flexible activin explains the membrane-dependent cooperative assembly of TGF-beta family receptors. Mol. Cell 15, 485–489

38. Jumper, J., Evans, R., Pritzel, A., Green, T., Figurnov, M., Ronneberger, O., et al. (2021) Highly accurate protein structure prediction with AlphaFold, Nature 596, 583–589

39. Kirsch, T., Sebald, W., and Dreyer, M. K. (2000) Crystal structure of the BMP-2-BRIA ectodomain complex. Nat. Struct. Biol. 7, 492–496

40. Daopin, S., Piez, K. A., Ogawa, Y., and Davies, D. R. (1992) Crystal structure of transforming growth factor-beta 2: an unusual fold for the superfamily. Science 257, 369 - 373

41. Maiti, R., Van Domselaar, G. H., Zhang, H., and Wishart, D. S. (2004) SuperPose: a simple server for sophisticated structural superposition. Nucleic Acids Res. 32, W590–594

42. Pei, J., Kim, B. H., and Grishin, N. V. (2008) PROMALS3D: a tool for multiple protein sequence and structure alignments. Nucleic Acids Res. 36, 2295–2300

43. Yu, P. B., Beppu, H., Kawai, N., Li, E., and Bloch, K. D. (2005) Bone morphogenetic protein (BMP) type II receptor deletion reveals BMP ligand-specific gain of signaling in pulmonary artery smooth muscle cells. J. Biol. Chem. 280, 24443–24450

44. Olsen, O. E., Wader, K. F., Hella, H., Mylin, A. K., Turesson, I., Nesthus, I., et al. (2015) Activin A inhibits BMP-signaling by binding ACVR2A and ACVR2B. Cell Commun. Signal. 13, 27

45. Antebi, Y. E., Linton, J. M., Klumpe, H., Bintu, B., Gong, M., Su, C., et al. (2017) Combinatorial signal perception in the BMP pathway.Cell 170, 1184–1196.e24

46. Yang, P., Troncone, L., Augur, Z. M., Kim, S. S. J., McNeil, M. E., and Yu, P B. (2020) The role of bone morphogenetic protein signaling in vascular calcification. Bone 141, 115542

47. Castonguay, R., Werner, E. D., Matthews, R. G., Presman, E., Mulivor, A. W.,Solban, N., et al. (2011) Soluble endoglin specifically binds bone morphogenetic proteins 9 and 10 via its orphan domain, inhibits blood vessel formation, and suppresses tumor growth. J. Biol. Chem. 286, 30034–30046

48. Tillet, E., Ouarne, M., Desroches-Castan, A., Mallet, C., Subileau, M., Didier, R., et al. (2018) A heterodimer formed by bone morphogenetic protein 9 (BMP9) and BMP10 provides most BMP biological activity in plasma. J. Biol. Chem. 293, 10963–10974

49. Hatsell, S. J., Idone, V., Wolken, D. M., Huang, L., Kim, H. J., Wang, L., et al. (2015) ACVR1R206H receptor mutation causes fibrodysplasia ossificans progressiva by imparting responsiveness to activin A. Sci. Transl. Med. 7, 303ra137

50. Schmelzer, C. H., Burton, L. E., Tamony, C. M., Schwall, R. H., Mason, A. J., and Liegeois, N. (1990) Purification and characterization of recombinant human activin B. Biochim. Biophys. Acta 1039, 135–141

51. Aykul, S., and Martinez-Hackert, E. (2016) New ligand binding function of human cerberus and role of proteolytic processing in regulating ligand-receptor interactions and antagonist activity. J. Mol. Biol. 428, 590–602

52. Aykul, S., and Martinez-Hackert, E. (2016) Determination of halfmaximal inhibitory concentration using biosensor-based protein interaction analysis. Anal. Biochem. 508, 97–103

53. Lusty, C. J. (1999) A gentle vapor-diffusion technique for cross-linking of protein crystals for cryocrystallography. J. Appl. Crystallogr. 32, 106–112

54. Bunkoczi, G., Echols, N., McCoy, A. J., Oeffner, R. D., Adams, P. D., and Read, R. J. (2013) Phaser.MRage: automated molecular replacement. Acta Crystallogr. D Biol. Crystallogr. 69, 2276–2286

55. Otwinowski, Z., and Minor, W. (1997) Processing of X-ray diffraction data collected in oscillation mode. Methods Enzymol. 276, 307–326

56. Battye, T. G., Kontogiannis, L., Johnson, O., Powell, H. R., and Leslie, A.G. (2011) iMOSFLM: a new graphical interface for diffraction-image processing with MOSFLM. Acta Crystallogr. D Biol. Crystallogr. 67, 271–281

57. Evans, P. R., and Murshudov, G. N. (2013) How good are my data and what is the resolution? Acta Crystallogr. D Biol. Crystallogr. 69, 1204–1214

58. Liebschner, D., Afonine, P. V., Baker, M. L., Bunkoczi, G., Chen, V. B., Croll, T. I., et al. (2019) Macromolecular structure determination using X-rays, neutrons and electrons: recent developments in Phenix. Acta Crystallogr. D Struct. Biol. 75, 861–877

59. Emsley, P., Lohkamp, B., Scott, W. G., and Cowtan, K. (2010) Features and development of Coot. Acta Crystallogr. D Biol. Crystallogr. 66, 486–501

60. Krissinel, E., and Henrick, K. (2007) Inference of macromolecular assemblies from crystalline state. J. Mol. Biol. 372, 774–797

61. The PyMOL Molecular Graphics System, Version 2.0, Schrödinger, LLC, New York

# APPENDIX

Table S2.1: Data collection and refinement statistics

| | BMPR2 – Activin B | ACVR2A-Activin A |
|---|---|---|
| **Data collection** | | |
| Source | LS-CAT 21-ID-G | Rigaku FR-E+ |
| Space group | $C2_1$ | $P2_12_12_1$ |
| Cell dimensions | | |
| *a*, *b*, *c* (Å) | 81.0, 115.65, 110.2 | 82.6, 82.5, 151.3 |
| α, β, γ (°) | 90.0, 100.9, 90.0 | 90.0, 90.0, 90.0 |
| Resolution (Å) | 60.34-3.45 (3.78-3.45) | 25.00-3.15 (3.20-3.15) |
| $R_{merge}$ | 0.092 (0.355) | 0.065 (0.473) |
| $I / \sigma I$ | 5.5 (2.8) | 22.8 (2.9) |
| Completeness (%) | 99.8 (100.0) | 95.4 (90.7) |
| Redundancy | 5.5 (2.8) | 22.8 (2.9) |
| **Refinement** | | |
| Resolution (Å) | 50.0-3.45 | 24.68-3.15 |
| No. reflections | 13115 (1288) | 17763 (1631) |
| $R_{work}$ / $R_{free}$ | 23.6/28.4 | 21.7/27.6 |
| No. atoms | | |
| Protein | 4388 | 6326 |
| Glycan | - | 116 |
| Water/ion | - | - |
| *B*-factors | | |
| Protein | 141.78 | 81.34 |
| r.m.s. deviations | | |
| Bond lengths (Å) | 0.003 | 0.004 |
| Bond angles (°) | 0.692 | 1.050 |
| Ramachandran | | |
| Favored | 93.13 | 93.61 |
| Outliers | 0.72 | 0.51 |
| Accession Number | 7U5O | 7U5P |

*Values in parentheses are for highest-resolution shell.

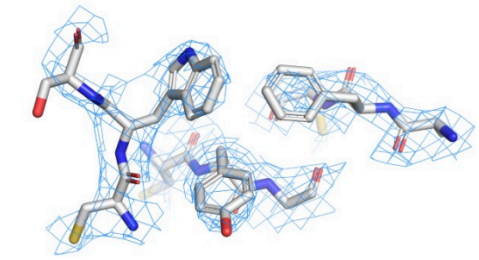

BMPR2 – Activin B

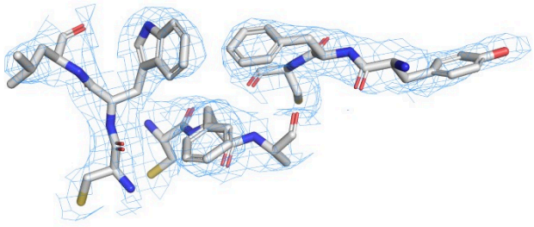

ACVR2A – Activin A

Figure S2.1: 2Fo-Fc map of hydrophobic hot spot residues. The density ofBMPR2 is consistent with a low-resolution structure and a moiety that exhibits a high average B-factor.

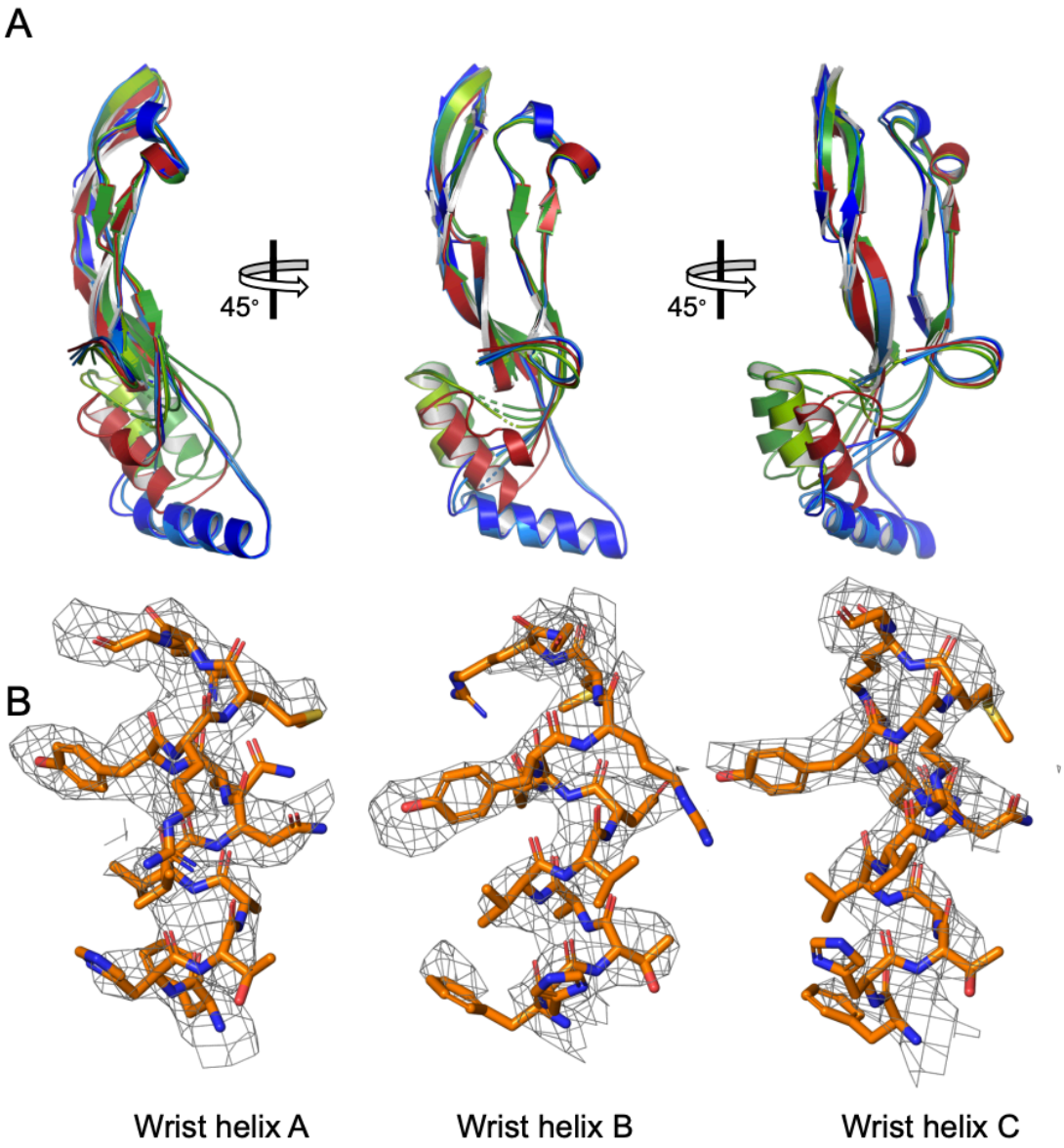


Figure S2.2: A) Superposition of GF Protomers. The three activin B protomers in the structure are colored blue, three activin A protomers in the structure are colored green, the AlphaFold model used for MR is colored red. Note the significant shift in the wrist helix between the AlphaFold model and the activin B structure after refinement. B) Simulated annealing $F_o$-$F_c$ map superimposed over the refined activin B wrist helices, corresponding to the three activin B protomers.

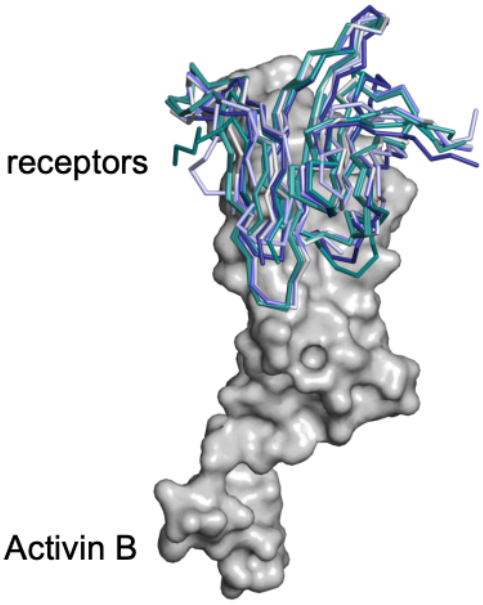


Figure S2.4: Superposition of all GF protomers. One Activin Band all non-crystallographic receptor protomers. Receptors are placed in a nearly identical position on the GF. The small differences observed betweenBMPR2 protomers could reflect the low resolution of the structure, structural flexibility of BMPR2, and/or the low affinity of the complex.

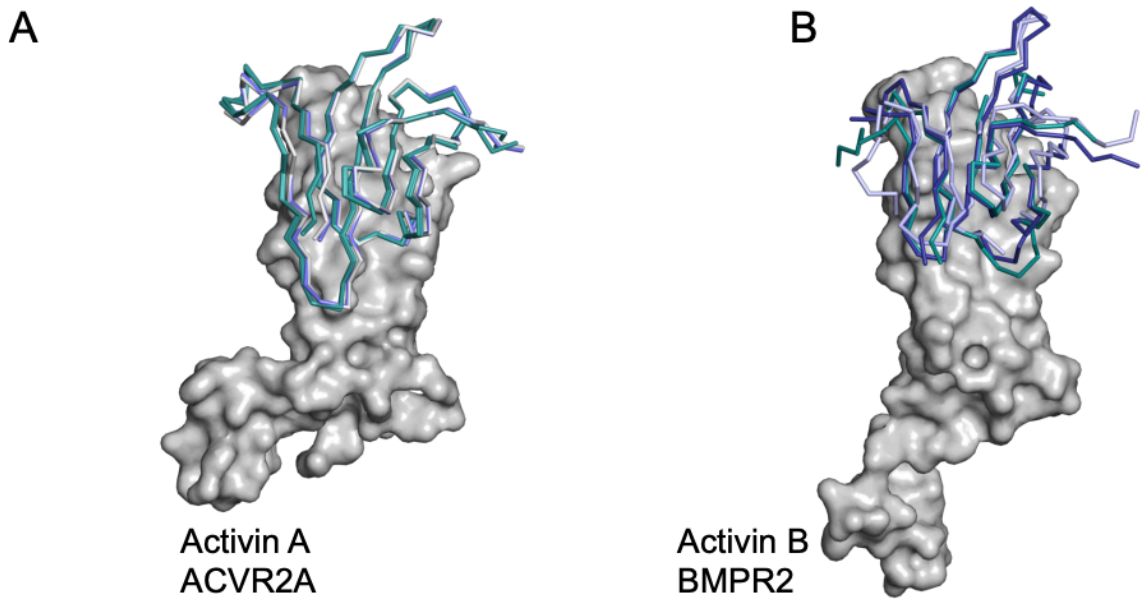


Figure S2.5: A) Superposition of Activin A protomers. B) Superposition of Activin B protomers. One GF and all non-crystallographic receptor protomers are shown as indicated. Structural plasticity of BMPR2 outside of receptor binding regions can be noted.

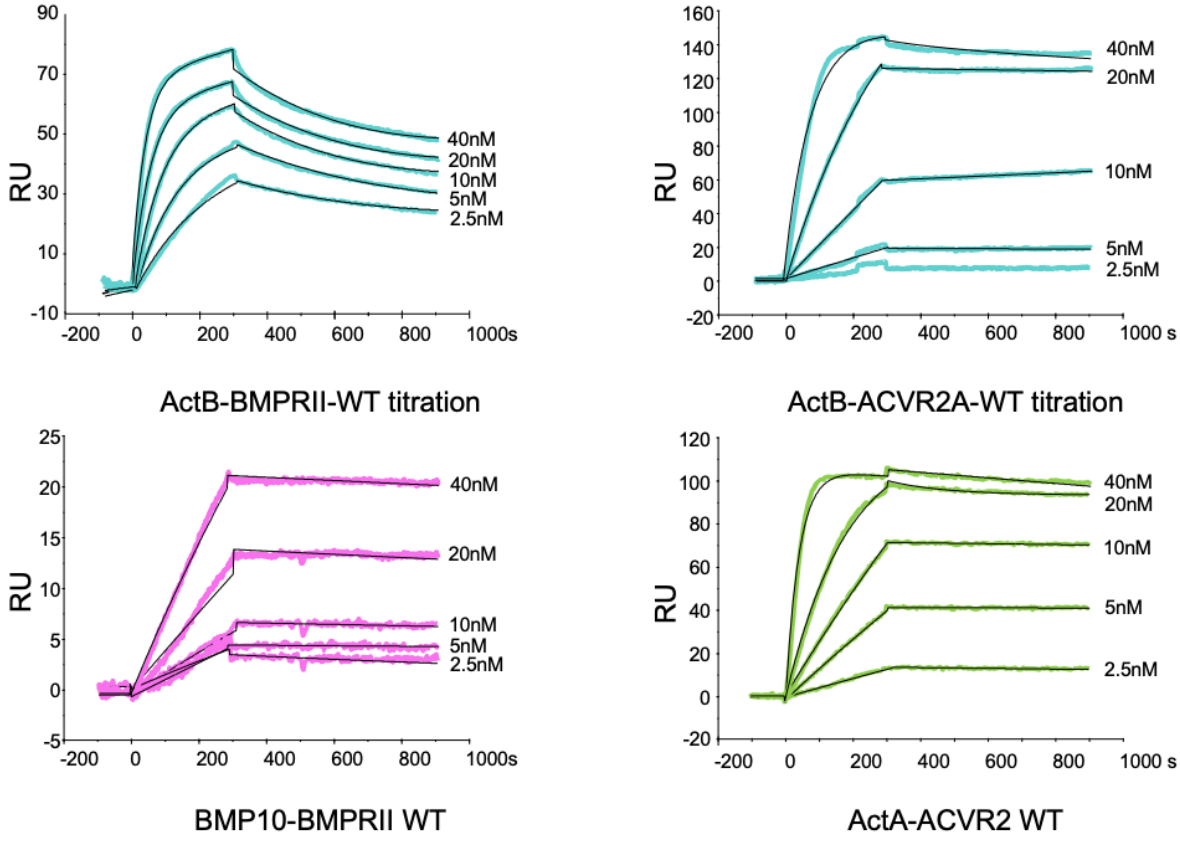


Figure S2.6: SPR titration of various GFs vs wild-type receptors as noted. Concentrations are shown on the side of each panel. Kinetic parameters are shown in the tables.

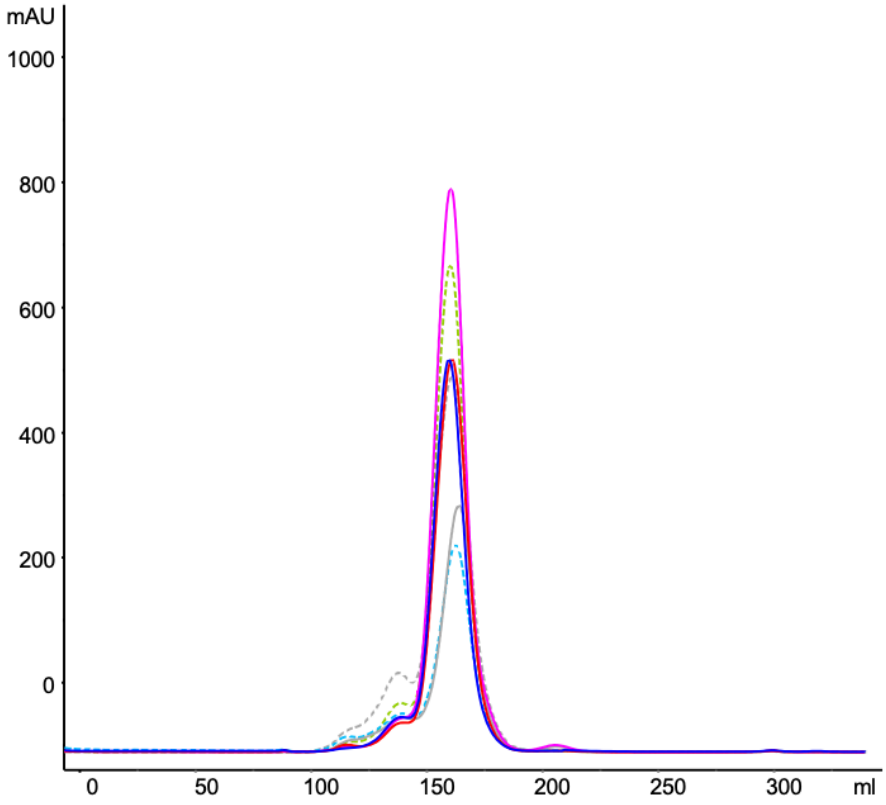


Figure S2.7: SEC chromatograms of BMPR2$^{VAR}$-FC. All BMR2-Fc fusion variants can be purified to homogeneity by size exclusion chromatography, indicating all constructs are properly folded and correspond to the dimeric form.

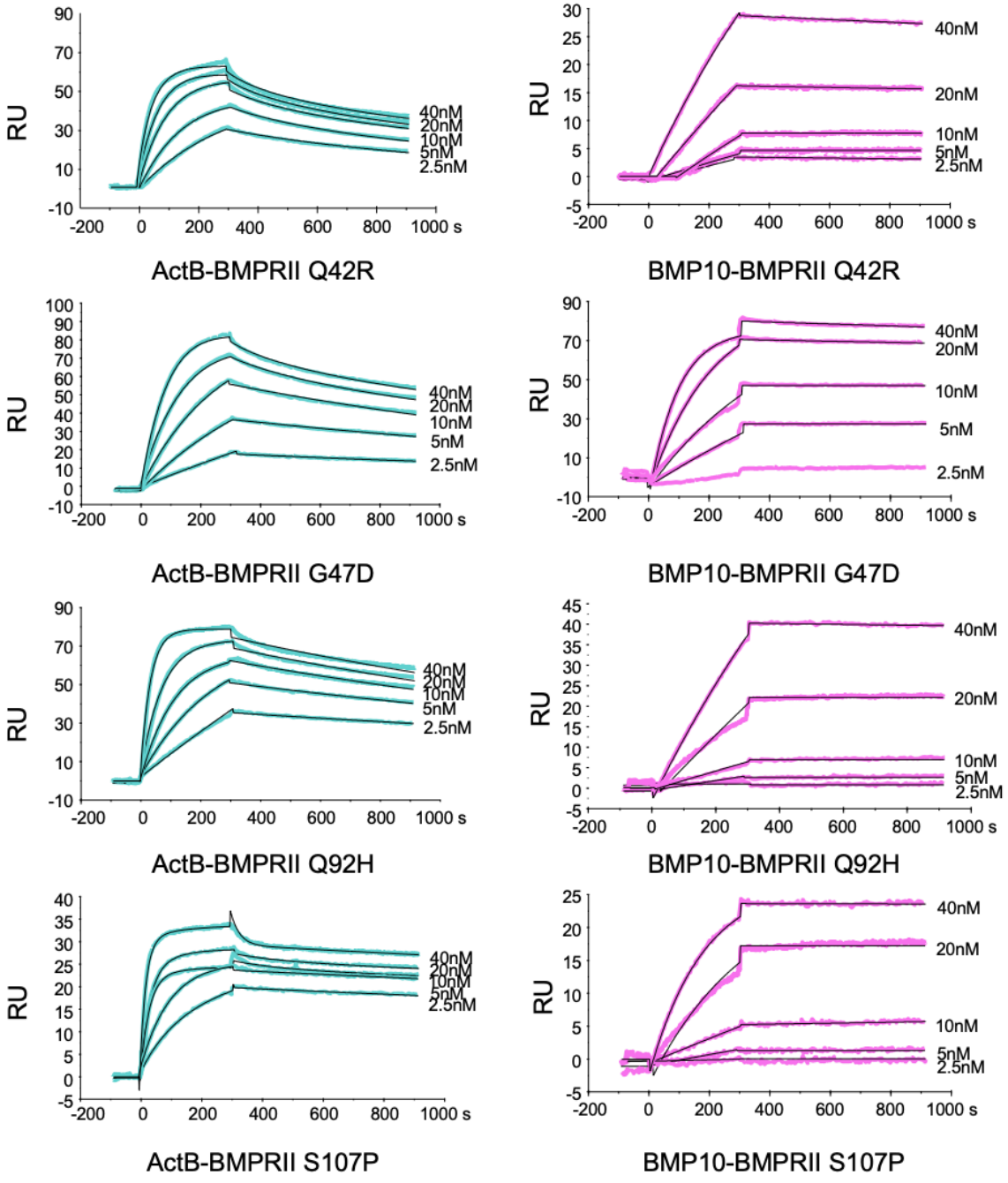


Figure S2.8: SPR titration of various Activin B (green) and BMP10 (pink vs PAH variants. Concentrations are shown on the side of each panel. Kinetic parameters are shown in the tables.

# CHAPTER 3

# UNRAVELLING THE EFFECT OF TGF-β GROWTH FACTORS AND THEIR SIGNALING ON PROLIFERATION IN PULMONARY ARTERIAL ENDOTHELIAL CELLS

**ABSTRACT**

Transforming growth factor-beta (TGF-β) growth factors are a large family of multifunctional cytokines that regulate various cellular processes, including cell proliferation, migration and tissue homeostasis. In pulmonary arterial hypertension (PAH), an imbalance in the TGF-β signaling pathway results in the excessive proliferation of pulmonary arterial endothelial cells (PAECs) and pulmonary arterial smooth muscle cells (PASMCs). Studies have shown a reduction in SMAD1/5/8 signaling and an increase in SMAD2/3 signaling. However, how this imbalance leads to the proliferative phenotype of pulmonary vascular cells in PAH remains unclear. Here, we show that BMP9 and BMP10, two of the TGF-β GFs, induce PAECs proliferation, however, they have no effect on PASMCs proliferation. Then, we further explore the signaling that causes PAECs proliferation. We found that even though BMP9 and BMP10 can bind to three TGF-β type II receptors, including BMPR2, ActRIIA and ActRIIB, BMP9 and BMP10 specifically signal via BMPR2 to activate SMAD 1/5/8 signaling, leading to the induction of PAECs proliferation. Moreover, when we knocked down BMPR2 in PAECs, we observed that Bimagrumab (BiMab), an antibody that blocks the ectodomains of ActRIIA and ActRIIB, was able to reduce BMP9- and BMP10-induced SMAD 1/5/8 signaling. In contrast, BiMab had no effect on BMP9 and BMP10 signaling in healthy PAECs. This suggests that BMP9 and BMP10 specifically signal through BMPR2 to induce SMAD 1/5/8-mediated PAEC proliferation. When BMPR2 expression is reduced, BMP9 and BMP10 may bind to ActRIIA to initiate SMAD 1/5/8 signaling in PAECs. Notably, BMP10 can compete with BMP9 for receptor binding in PAECs. In conclusion, with decreased BMPR2 levels, BMP9 and BMP10 may shift their binding preference to ActRIIA, potentially contributing to the aberrant cell growth observed in PAH.

## INTRODUCTION

Transforming growth factor beta (TGF-β) is known to play a major role in cell regulation, homeostasis, proliferation and differentiation [1-3]. It is also associated with many diseases It a large family consists of structurally conserved growth factors (GFs), transmembrane serine/threonine kinases receptors (Type I and Type II receptor), R-SMAD transcription factors, coreceptors and inhibitors. There are over 33 different growth factors identified including TGF-βs, activins, inhibins, Nodal, Lefty, bone morphogenetic proteins (BMPs), growth and differentiation factors (GDFs) and anti-Müllerian hormone (AMH), 7 type I receptors (ALK1-7) and 5 type II receptors (TGFβRII, BMPR2, ActRIIA, ActRIIB or AMHRII). These growth factors signal by forming a complex with a heterocomplex of two Type II receptors and two Type I receptors which initiates two intracellular signaling cascades: SMAD 1/5/8 and SMAD 2/3 [4]. It is generally acknowledged that BMPs and some GDFs signal through SMAD 1/5/8 and TGF-β, Activins, and Nodal signals through SMAD 2/3 [5,6]. This seemingly straightforward signaling pathway is complicated by having many overlapping interactions between GFs and receptors. For example, BMPR2 can bind to BMP9, BMP10, GDF 15, Activin A or Activin B, and likewise, ActRIIA can bind to BMP9, BMP10, Activin A or Activin B [7,8]. TGF-β signaling can be further convoluted by the accessory factors like coreceptors and endogenous antagonists [9]. TGF-β growth factors are secreted by many different cell types (i.e endothelial cells, fibroblasts, immune cells, smooth muscle cells, etc) and their expression can vary dependent on the context, the tissue, and the physiological or pathological condition [10,11]. In addition, the GF-receptors ratio differs from cell type to cell type. This variability in receptor expression influences the responsiveness of cells to GFs and contributes to the fine-tuning of signaling pathways. The complexity and variability of TGF-β signaling have made it challenging to fully understand its mechanisms and roles in various

diseases. Strikingly, mutations in the BMPR2 gene are strongly related to pulmonary arterial hypertension (PAH), a severe, fatal disease characterized by the remodeling of pulmonary arteries [12-15]. In familial PAH, mutations of BMPR2 are inherited as an autosomal dominant trait with incomplete penetrance, and they are also found in 20% of the patients with idiopathic PAH as well. [16,17] Interestingly, even in the absence of BMPR2 mutations, there is a reduced level of BMPR2 as well as an increased level of circulatory Activin A and GDF11 [18,19]. Nonetheless, the functional consequences brought by these changes for the pathogenesis of PAH are still unclear. Notably, the hyperproliferation of pulmonary arterial endothelial cells (PAECs) and smooth muscle cells (PASMCs) is strongly implicated in the development of plexiform lesions and vascular remodeling [20,21]. Hence, deciphering the molecular mechanisms driving cell proliferation in both cell types under normal conditions is crucial for comprehending the pathological processes involved in PAH. In order to identify which TGF-β GFs are involved in PAECs proliferation, we screened TGF-β GFs and their signaling in relation to stimulating PAECs proliferation. To determine if the corresponding GFs signal via BMPR2 to initiate their downstream signaling, we examined the impact of Bimagrumab (BiMab), an antibody that blocks the ectodomain of ActRIIA and ActRIIB, on the signaling of these GFs and their capacity to induce PAECs proliferation. To investigate whether there is a signaling change under the reduced level of BMPR2, we assessed the impact of BiMab on GFs' signaling and their proliferation effects in BMPR2 knockdown PAECs. To dissect the interaction of GF-receptors specificity, we investigate their signaling in HEK 293 cells. Finally, to explore the differences in BMP9 and BMP10 signaling and assess whether these two GFs exhibit competition for receptor binding, we compared their activation of SMAD 1/5/8 signaling with respect to timing and concentration. Additionally, we examined both signaling and proliferative effect when both GFs were present in PAECs.

## RESULTS

### BMP9 and BMP10 induce PAECs proliferation

The central hypothesis proposed here is that the imbalance between TGF-β and BMP signaling is the key regulatory process of pulmonary vasculature remodeling in PAH [18]. Various SMAD 2/3 and SMAD 1/5/8 GFs, including BMP7, BMP9, BMP10, Activin A, Activin B, GDF11, and TGF-β1, are implicated in PAH pathogenesis. SMAD 1/5/8 GFs, including BMP9 and BMP10, bind to ALK1, which is the type I receptor that is predominantly expressed on PAECs, and their mutations in PAH patients suggest involvement in pulmonary vascular remodeling [22]. BMP7 is a potential biomarker for PAH patient prognosis [23]. SMAD 2/3 GFs, like TGF-β1, show increased expression in SuHx rat lungs and stimulate PASMCs proliferation [24, 25]. Activin A and GDF11 expressions increase in small arterioles of PAH patients and hypoxia-induced PH mouse blood vessels [19, 26-28]. Activin B, with significant structural similarity to Activin A, induces myogenic and fibrogenic gene expression in PASMCs and triggers macrophage inflammatory responses, indicating a role in PAH progression [29,30]. To investigate the effects of these GFs on healthy human PAECs proliferation by treating PAECs with 10 ng/mL of the selected GFs (Fig 3.1B), we found that BMP9 and BMP10 induce PAEC proliferation, while the other GFs have no effect. Upon examining their signaling in PAECs, we discovered that only BMP9 and BMP10 activate SMAD 1/5/8 signaling, whereas the other GFs do not activate either SMAD 1/5/8 or SMAD 2/3 signaling (Fig 3.1A). This finding suggests that BMP9 and BMP10 are needed for PAECs proliferation and the other GFs do not signal in PAECs. (Fig 3.1A).

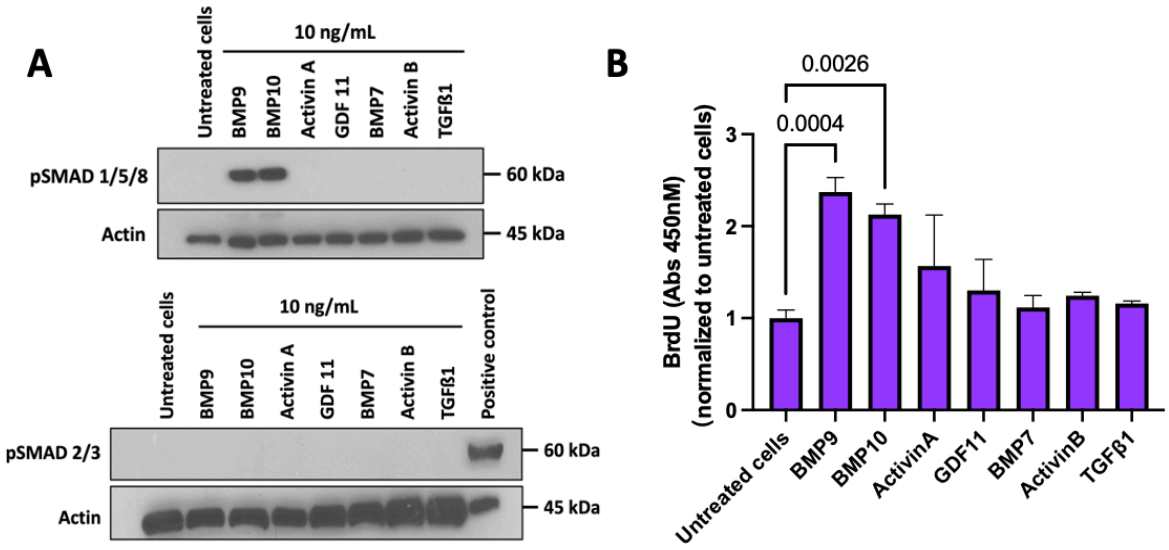


Figure 3.1: GFs screening for signaling activation and proliferation effects on PAECs. A, Anti-p-SMAD Western blots of whole cell lysate display SMAD signaling phosphorylation (top panel: p-SMAD 1/5/8, bottom panel: p-SMAD2/3) in samples treated with 10 ng/mL of BMP9, BMP10, Activin A, GDF11, BMP7, Activin B, TGFβ1, or vehicle (assay medium). BMP9 and BMP10 induce SMAD 1/5/8 signaling. The other tested GFs did not induce any SMAD signaling in PAECs. B, PAECs proliferation was measured by treating the PAECs with 10 ng/mL of BMP9, BMP10, Activin A, GDF11, BMP7, Activin B, TGFβ1, or vehicle (assay medium). BrdU levels were measured at an absorbance of 450 nm. Absorbance values were normalized to untreated cells. BMP9 and BMP10 increased cell proliferation, while the other GFs had no effect on proliferation. The average of four biological replicates is shown, with error bars representing SD. Statistical significance was determined by two-way ANOVA using Prism 9.

## BMP9 and BMP10 induce PAECs proliferation through SMAD 1/5/8 signaling

BMPs can activate SMAD 1/5/8 signaling and other non-canonical pathways. Prior research has shown that BMP9 induces Akt and MAPKs in osteoblasts and HepG2 cells [31,32]. Given the versatile signaling that BMP9 and BMP10 may activate in PAECs, we sought to determine if their induced PAECs proliferation is mediated through SMAD 1/5/8 signaling using the small molecule inhibitor LDN-193189. LDN-193189, a Dorsomorphin derivative, inhibits BMP-induced SMAD 1/5/8 phosphorylation with high specificity for BMP receptors at low concentration [33]. To minimize non-specific effects, we used the lowest possible LDN concentration, so we titrated 500 nM LDN-193189 in a two-fold decrease down to 31.2 nM in BMP10-treated PAECs (Fig 3.2A). LDN-193189 progressively diminished SMAD 1/5/8

phosphorylation, with complete inhibition at 500 nM. To ensure complete SMAD 1/5/8 signaling inhibition in PAECs and following previously used lab concentrations [34], we selected 1 μM LDN-193189 for the cell proliferation assay. PAECs were treated with 10 ng/mL BMP9 and BMP10, with or without 1 μM LDN-193189, and cell proliferation was measured (Fig 3.2B). The presence of LDN-193189 reduced BMP9 and BMP10-induced cell proliferation, indicating that these GFs induce proliferation by activating the SMAD 1/5/8 signaling pathway.

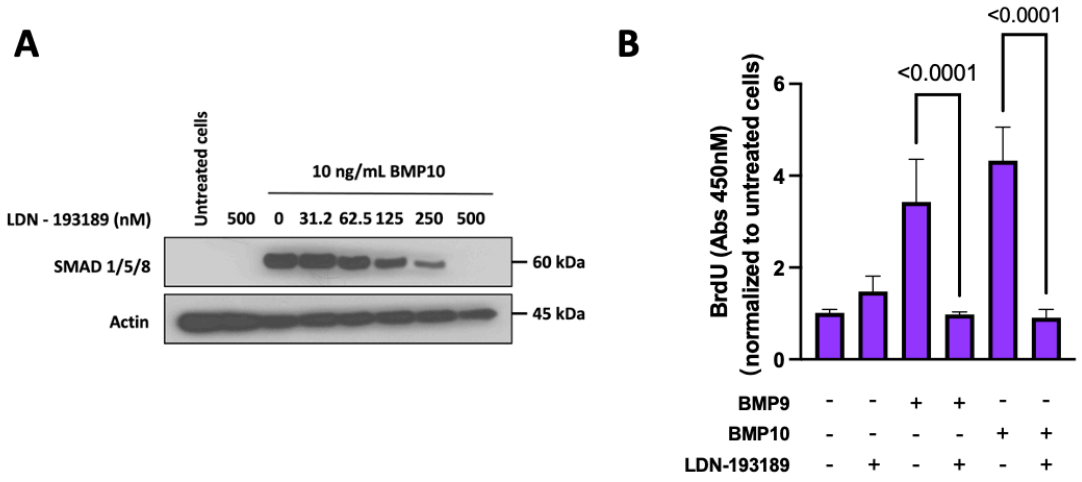


Figure 3.2: LDN-193189 inhibits BMP9 and BMP10-induced PAECs proliferation. A) 0-500 nM of LDN-193189 is titrated against 10 ng/mL of BMP10, 500 nM LDN-193189 effectively suppressing SMAD 1/5/8-mediated BMP10 signaling. B) PAECs were treated with 10 ng/mL of BMP9 or BMP10, with or without 1 μM LDN-193189. BrdU level were measured at an absorbance of 450 nm. LDN-193189 inhibits BMP9 and BMP10-mediated PAECs proliferation. Data were normalized to untreated cells, and the average of four biological replicates is presented, with error bars representing SD. Statistical significance was determined using two-way ANOVA with Prism 9.

## BMPR2 is the preferred type II receptor for BMP9 and BMP10 mediated PAEC proliferation

Many TGF-β GFs can bind to multiple Type I receptors, as well as Type II receptors. BMP9 and BMP10 can bind to then Type II receptors BMPR2, ActRIIA, and ActRIIB with considerable affinity [7,8]. Western blot showed that in PAECs, BMPR2 and ActRIIA, but not ActRIIB, were expressed, while in human embryonic kidney cells (HEK 293), all three receptors were expressed

(Fig 3.3A). To determine which Type II receptor BMP9 and BMP10 bind to activate SMAD 1/5/8 signaling for inducing PAEC proliferation, we investigated the effect of Bimagrumab (BiMab) on cell proliferation and signaling. BiMab is a Monoclonal antibody developed as a therapeutic that binds to the extracellular domain of ActRIIA and ActRIIB [35]. We treated PAECs with 10 ng/mL BMP9 and BMP10 with or without 300 nM BiMab. Interestingly, BiMab did not inhibit BMP9 and BMP10-mediated SMAD 1/5/8 signaling (Fig 3.3B). This indicated that BMP9 and BMP10 stimulate SMAD 1/5/8 signaling via BMPR2 in PAECs. Consistent with this finding, BiMab had no effect on BMP9 and BMP10-induced cell proliferation (Fig 3.3C). These findings demonstrate that although PAECs express both BMPR2 and ActRIIA, BMP9 and BMP10 preferentially signal through BMPR2-mediated to activate SMAD 1/5/8 signaling and promote PAEC proliferation.

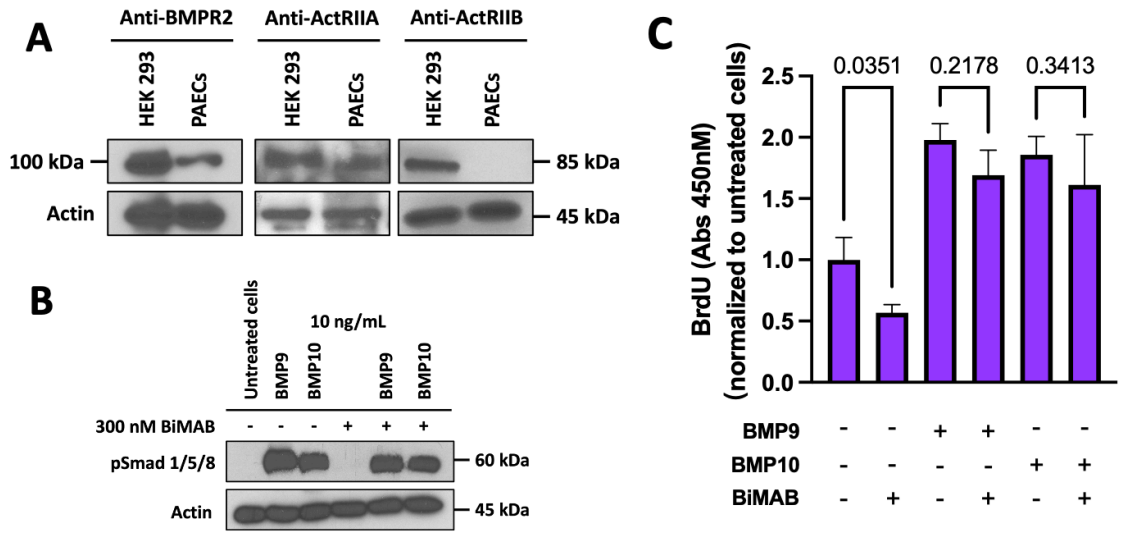


Figure 3.3: BiMab does not affect BMP9 and BMP10 signaling or their induced cell proliferation. A, Type II receptor expression levels in PAECs and HEK 293 cells were determined by Western blots. BMPR2 (100 kDa) and ActRIIA (85 kDa) were expressed in PAECs, while all three receptors were expressed in HEK 293 cells. B, SMAD 1/5/8 signaling was measured by Western blots; cells were treated with 10 ng/mL BMP9 or BMP10 with or without BiMab. BiMab did not affect BMP9 and BMP10-mediated signaling. C, Similarly, the same treatments were applied for the cell proliferation assay. BiMab did not affect BMP9 and BMP10-induced cell proliferation. Data was normalized to untreated cells, and the average of four biological replicates is shown, with error bars representing SD. Statistical significance was determined by two-way ANOVA using Prism 9.

**BMP9 and BMP10 might divert binding to ActRIIA for SMAD 1/5/8 signaling under reduced BMPR2 expression**

In PAH, heterozygous BMPR2 mutations are identified in both idiopathic and familial cases, with a haploinsufficiency inheritance pattern [36,37]. However, the effect of reduced BMPR2 levels on TGF-β signaling in pulmonary vasculature remains unclear. To elucidate the role of BMPR2 mediated BMP9 and BMP10 signaling and its effect on proliferation, we knocked down BMPR2 in PAECs. Due to the presence of BMPR2 and ActRIIA in PAECs (Fig 3.3A) and their high affinity for BMP9 and BMP10, it is worth investigating GF-receptor binding changes and cell proliferation under reduced BMPR2 signaling. Here, we adopted a similar approach using BiMab to determine the utilized receptor for BMP9 and BMP10-mediated signaling. First, we knocked down BMPR2 using pooled siRNA in PAECs, achieving a reduction in BMPR2 expression level of about 50% (Fig 3.4A). Then, we treated PAECs with 10 ng/mL of BMP9 or BMP10 with or without 300 nM BiMab. We found that siRNA knockdown of BMPR2 reduced BMP9 and BMP10-mediated SMAD 1/5/8 signaling approximately 1.8-fold. BiMab, does not inhibit SMAD 1/5/8 signaling in the non-targeting siRNA transfected PAEC cells. However, in the BMPR2 siRNA transfected PAECs, BiMab blocked the BMP9 and BMP10-mediated SMAD 1/5/8 signaling, indicating that the loss of BMPR2 results in BMP9/10 signaling via ActRIIA. Thus, BMP9 and BMP10 might divert their receptor interaction from BMPR2 to ActRIIA when there is a reduced level of BMPR2 in PAECs. To examine cell proliferation in BMPR2 siRNA knockdown PAECs, we showed that there was a decrease in BMP9 and BMP10-induced proliferation when BMPR2 expression levels were reduced. Additionally, BiMab further reduced BMP9 and BMP10-induced PAEC proliferation, supporting the conclusion that BMP9 and BMP10 switch their receptor utilization and signal through ActRIIA to induce cell proliferation.

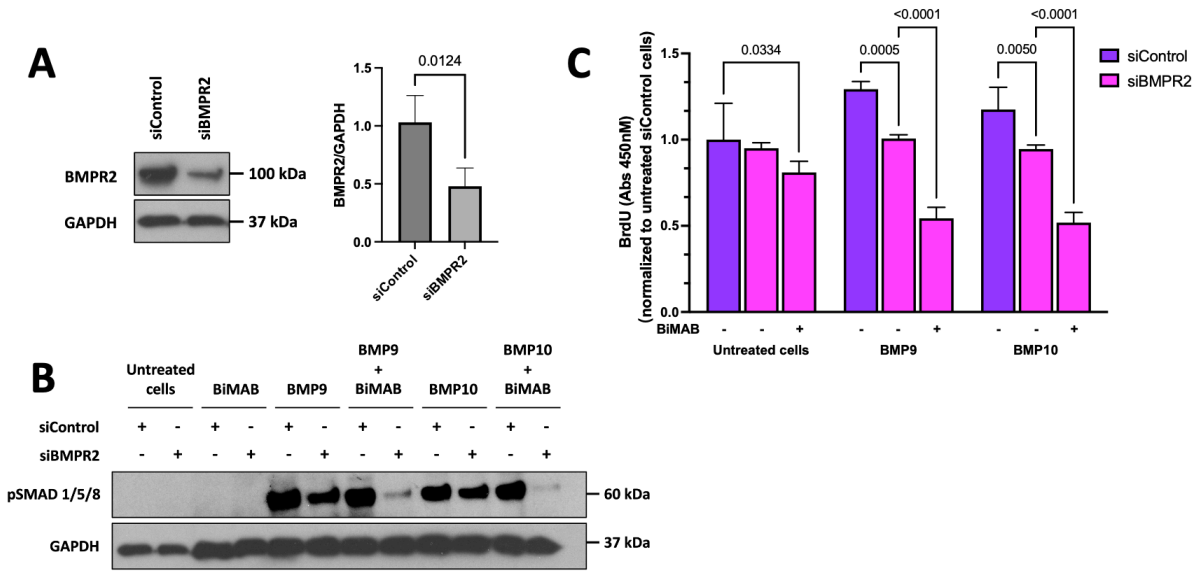


Figure 3.4: BiMab attenuates BMP9 and BMP10-mediated SMAD 1/5/8 signaling in BMPR2 knockdown PAECs. A, Validation of BMPR2 siRNA knockdown in PAECs by western blot; cells were transfected with Dharmafect transfection reagent, pooled BMPR2 siRNA (siBMPR2), or control siRNA (siControl). The results show a ~50% reduction in BMPR2 expression level. B, SMAD 1/5/8 signaling activation is measured by western blots; cells were treated with 10 ng/mL of BMP9 or BMP10 with or without 300 nM BiMab in siBMPR2 or siControl transfected cells. BiMab effectively blocks BMP9 and BMP10 signaling in the siBMPR2 knockdown cells but not in the siControl knockdown cells. C, The same treatment was applied for the cell proliferation assay; in siBMPR2 knockdown PAECs, BMP9 and BMP10-induced cell proliferation decreased. Additionally, BiMab further reduced BMP9 and BMP10-induced proliferation. Data were normalized to untreated siControl cells. The average of four biological replicates is shown, with error bars representing SD. Statistical significance was determined by two-way ANOVA using Prism 9.

## BMP9 and BMP10 have greater specificity toward BMPR2, among the type II receptors

In BMP signaling, three BMP type II receptors are involved: BMPR2, ActRIIA, and ActRIIB. Many BMPs, such as BMP2, BMP4, BMP9, and BMP10, presumably bind all three Type II receptors [7,8,38]. However, a key question in this area of investigation is whether the GFs can signal through all three receptors or whether they have a preference for one receptor over the others. To address these questions, we studied BMP10 signaling using stably transfected human embryonic kidney (HEK293) reporter cells. We found that increasing concentrations of BMPR2-Fc, ActRIIB-Fc, and ActRIIA-Fc inhibited BMP10 signaling (Fig 3.5A). Interestingly, ActRIIB-Fc inhibited 5 nM BMP10 signaling with the greatest potency (1.33 nM), followed by BMPR2-Fc

and ActRIIA-Fc, being the least potent (35 nM and 187 nM, respectively, Table 3.1). These findings show that the three receptors bind BMP10 with significant affinity. We then examined BMP10 signaling when by blocking the receptor binding interface of ActRIIA and ActRIIB using BiMab. Increasing concentration of BiMab inhibited Activin B signaling, however, BiMab could only partially inhibit BMP10 signaling (38.1 nM and 3.5 nM, respectively, Table 3.2), as indicated by the reduced SMAD 2/3 and SMAD 1/5/8 responses (Fig 3.5B). We further investigated BMP10 signaling by overexpressing ALK1 in combination with either of the three type II receptors in HEK 293 BRE reporter cells. High concentrations of BiMab can only minimally reduce BMP10 signaling, regardless of which type II receptors we overexpressed (Fig 3.5C, D). By contrast, BiMab inhibited Activin B completely, revealing the distinct receptor utilization of the two GFs. This leads us to conclude that BMP10 preferentially activates the SMAD 1/5/8 signaling pathway via BMPR2 .

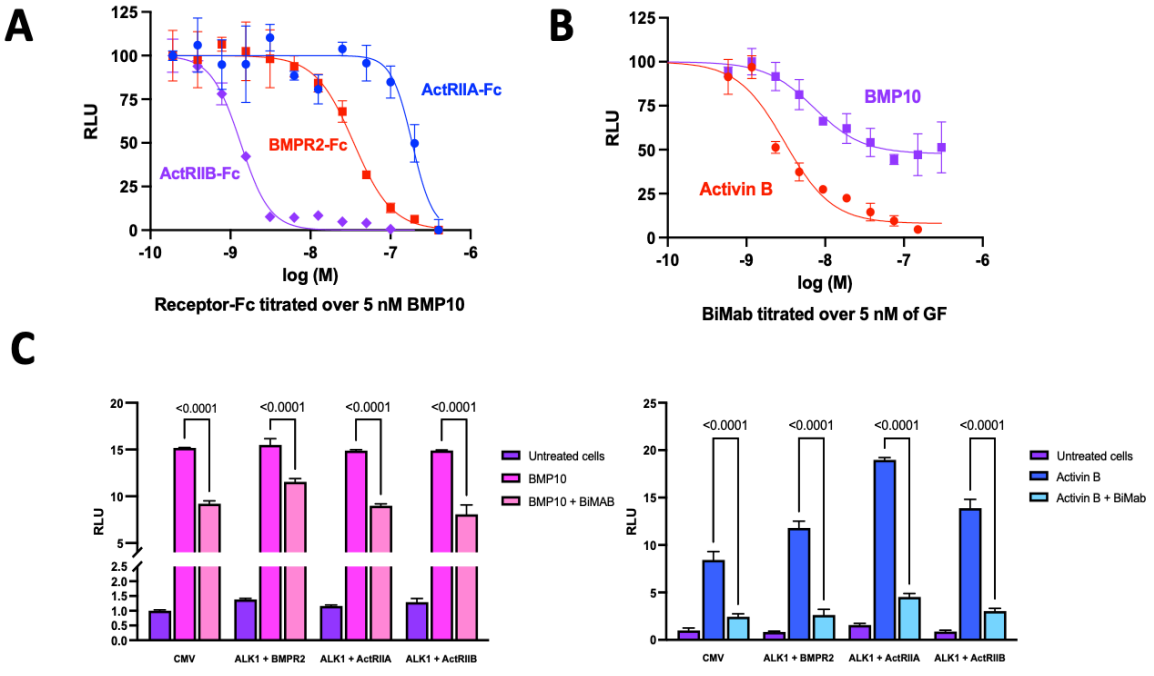


Figure 3.5: BMP10 binds preferably to BMPR2 for its signaling. Stably transfected HEK293 reporter cells were induced with 5 nM GFs. A, Increasing concentrations of BMPR2-Fc (Red), ActRIIA-Fc (Blue), and ActRIIB-Fc

Figure 3.5 (cont'd).
(Purple) were added; all three receptor-Fc inhibited BMP10 signaling. B, Increasing concentrations of BiMab were added; BiMab could inhibit Activin B signaling (Red) but only partially blocked BMP10 signaling (Purple). Stably transfected HEK293 BRE reporter cells were transfected with CMV or ALK1 + BMPR2/ActRIIA/ActRIIB and induced with either 5 nM BMP10 or 20nM Activin B +/- 300 nM BiMab. C, BiMab inhibits Activin B signaling significantly, but not BMP10. Luciferase units were normalized to GF control (Relative Luciferase Unit, RLU). The average of three biological replicates is shown, with error bars representing SD. Statistical significance was determined by two-way ANOVA using Prism 9.

Table 3.1: Inhibitory potency of Receptor-Fc Fusions

| Type II receptor –Fc fusion | BMP10 |
|---|---|
| BMPR2-Fc | 3.5E-8 |
| ActRIIA-Fc | 18.7E-8 |
| ActRIIB-Fc | 0.13E-8 |

$IC_{50}$ (M)

Table 3.2: Inhibitory potency of Bimagrumab

| | BMP10 | Activin B |
|---|---|---|
| BiMAB | 3.81E-8 | 0.35E-8 |

$IC_{50}$ (M)

## Receptor-binding competition can occur between BMP9 and BMP10

After we exploited the specificity of BMP10 choosing its receptor for forming functional signaling complex, it is worthwhile to explore the competition between growth factors (GFs) for receptor binding. Previous studies have shown that TGF-β family receptors bind to overlapping GFs with different affinities at the same recognition site [7,8,39,40]. Often, GFs compete for the same receptor. Numerous examples of GF-receptor competition exist, such as BMP2 competing with Activin A, Activin B, and GDF11 for ActRIIA and ActRIIB, or BMP7 competing with Activin A, GDF8, and Inhibin [7,41,42]. This leads us to ask if BMP9 and BMP10 compete with each other to cross-regulate their activities. BMP9 and BMP10 are closely related members of the BMP family [43,44], sharing many structural and functional similarities. Both GFs exhibit a high

degree of amino acid sequence identity in their mature form (approximately 68%) (Fig 3.6A) and serve as key regulators of vascular homeostasis, bone formation, and liver metabolism [44-47]. They are expressed in various tissues throughout the body, including the liver, heart, and lungs, with some overlapping expression patterns [48-51]. After expressing in those organs, they circulate in the bloodstream [52,53]. The question arises: why does the human body require two similar growth factors? In PAECs, both GFs induce SMAD 1/5/8 signaling for cell proliferation. Here, we wanted to determine the duration each GF takes to induce SMAD 1/5/8 signaling and the time required for the signaling to disappear, as well as the amount of BMP9 and BMP10 needed to activate SMAD 1/5/8 signaling. Our Western blots showed that both 10 ng/mL BMP9 and BMP10 induce SMAD 1/5/8 signaling as early as 30 minutes. BMP9-mediated signaling begins to diminish around 24 hours (Fig 3.6B, left panel), whereas BMP10-mediated signaling persists at 48 hours (Fig 3.6B, right panel). Interestingly, BMP9 signaling decreases with increasing concentration (Fig 3.6C, left panel), which may be due to BMP9's ability to compete with itself for the BMPR2 binding site. Meanwhile, BMP10 signaling only begins at 10 ng/mL (Fig 3.6C, right panel). To investigate whether BMP9 and BMP10 compete for SMAD 1/5/8 signaling, we treated PAECs with 10 ng/mL BMP9 while increasing the concentration of BMP10. Intriguingly, increasing concentrations of BMP10 reduced BMP9-mediated signaling, suggesting they might compete for BMPR2 binding sites (Fig 3.6D). In conclusion, BMP9 and BMP10 signal through SMAD 1/5/8 at different durations and concentrations in PAECs. To assess the phenotypic consequences, we replicated the experimental setup for immunoblotting and conducted a cell proliferation assay. We demonstrated that BMP10 can reduce BMP9-mediated PAEC proliferation (Fig 3.6E). Collectively, these findings suggest that BMP9 and BMP10 exhibit receptor-binding competition when present in the same spatial context, potentially affecting their functionality in PAECs.

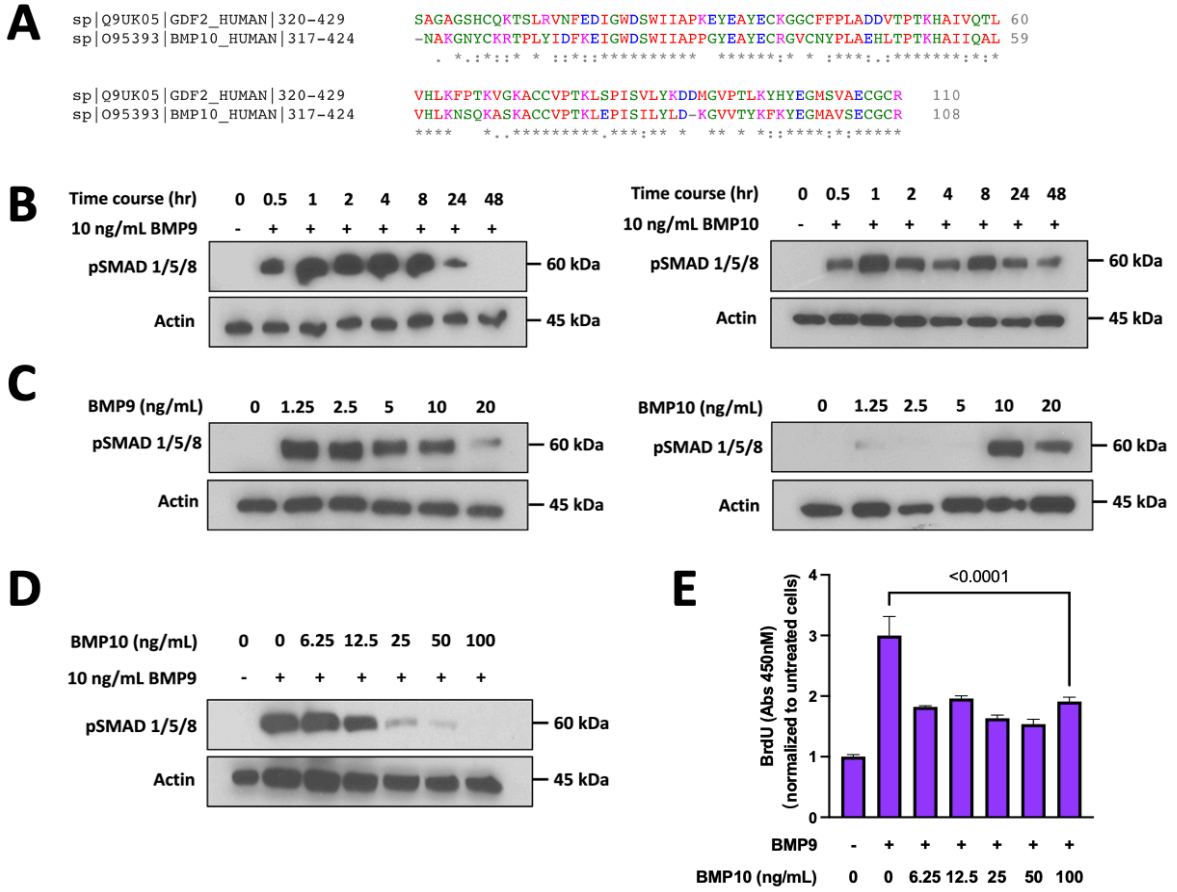


Figure 3.6: BMP9 and BMP10 exhibit differences in SMAD 1/5/8 signaling activation and compete for receptor binding. A) Sequence alignment of BMP9 and BMP10, where "*" denotes a single, fully conserved residue, ":" represents conservation of residues with highly similar properties, and "." indicates conservation of residues with moderately similar properties. B) PAECs were treated with 10 ng/mL of BMP9 or BMP10, and cell lysates were collected at various time points (0.5, 1, 2, 4, 8, 23, and 48 hrs). BMP9 signaling began to diminish at 24 hrs, while BMP10 signaling persisted at 48 hrs. C) PAECs were treated with increasing concentrations of BMP9 or BMP10, and cell lysates were collected after 30 mins. BMP9 induced SMAD 1/5/8 signaling at 1.25 ng/mL, but signaling decreased with higher concentrations. BMP10 did not induce SMAD 1/5/8 at concentrations of 5 ng/mL or less, but it did at 10 ng/mL or higher. PAECs were treated with 10 ng/mL BMP9 and increasing concentrations of BMP10 were added. D) As BMP10 concentrations increased, BMP9 signaling decreased. E) BMP10 inhibited BMP9-induced cell proliferation starting at 6.25 ng/mL. Data was normalized to untreated cells, and the average of four biological replicates is shown with error bars representing the standard deviation. Statistical significance was determined using two-way ANOVA in Prism 9.

## DISCUSSION

Pulmonary arterial hypertension is a progressive condition characterized by increased blood pressure in the pulmonary arteries, which can eventually lead to right heart failure and death.

The pathogenesis of PAH is complex and multifactorial, involving various molecular pathways and cellular processes that contribute to pulmonary vascular remodeling and dysfunction. TGF-β family being one of the key signaling pathways implicated in PAH, it is essential to target TGF-β signaling for offering potential therapeutic strategies for treating PAH. However, due to its multifunctional and redundant nature, it is challenging in understanding and modulate its effects on the disease.

To investigate the role of TGF-β signaling in PAH, researchers have employed various experimental models, ranging from in *vitro* to in *vivo*. Here, we aimed to study TGF-β signaling using primary pulmonary artery endothelial cells, as they are one of the cell types that recapitulate molecular pathways involved in PAH pathogenesis. We also dissected TGF-β signaling using HEK 293 cells. These models help elucidate the intricate interactions between TGF-β family members and their downstream signaling components.

Initially, we screened the proliferative effects and signaling of several TGF-β growth factors on PAECs. This enabled us to identify which TGF-β GFs contribute to PAEC proliferation, thus establishing a foundation for understanding the role of TGF-β signaling in PAEC proliferation. Among the seven selected TGF-β GFs, we discovered that BMP9 and BMP10 can induce PAEC proliferation and activate the SMAD 1/5/8 signaling pathway. None of the SMAD 2/3 activating GFs signaled in PAECs, suggesting the potential absence of essential components for their signaling. For instance, we observed that ActRIIB is not present in PAECs.

To elucidate the proliferative mechanisms of BMP9 and BMP10 in PAECs, we investigated their impact on SMAD 1/5/8 signaling activation. Our anti-p-SMAD 1/5/8 western blot results indicated that the SMAD1/5/8 pathway was necessary for BMP9- and BMP10-induced PAEC proliferation. This finding was supported by the SMAD 1/5/8 signaling inhibitor LDN-

193189, which suppressed PAEC proliferation when treated with BMP9 and BMP10. To identify the type II receptors that BMP9 and BMP10 utilize for SMAD 1/5/8 signaling activation in PAEC proliferation, we employed Bimagrumab to differentiate between BMPR2 and ActRIIA/ActRIIB within the cells. We observed that BiMab did not inhibit BMP9- and BMP10-mediated SMAD 1/5/8 signaling or their induced PAEC proliferation. Intriguingly, when BMPR2 was knocked down using siRNA in PAECs, BiMab was able to suppress BMP9- and BMP10-mediated SMAD 1/5/8 signaling and inhibit the proliferative effects of BMP9 and BMP10. Based on these findings, we propose that under reduced BMPR2 expression levels in PAECs, BMP9 and BMP10 may preferentially bind to ActRIIA to induce SMAD 1/5/8 signaling pathways.

We further examined the specificity of receptor binding for the GFs to form functional signaling complexes. Using stably transfected HEK 293 reporter cells, we discovered that increasing concentrations of BiMab only partially blocked BMP10 signaling, even in cells that are overexpressing ALK1 with ActRIIA or ActRIIB. This finding indicates that the majority of BMP10 signaling occurred through BMPR2-mediated signaling. This is consistent with BMP10 signaling in PAECs, as high concentrations of BiMab do not inhibit BMP9- and BMP10-induced SMAD 1/5/8 signaling or their proliferative effects on PAECs. We hypothesize that under normal BMPR2 levels, BMP9 and BMP10 exhibit specificity towards BMPR2 in forming functional signaling complexes. However, when BMPR2 expression levels are low, BMP9 and BMP10 preferentially bind to ActRIIA in PAECs for signaling.

In various studies, BMP9 and BMP10 have often been studied together due to their structural and functional similarities. Despite activating the same downstream signaling, we found that they differ in the timing and concentration at which they activate SMAD 1/5/8 signaling in PAECs. Interestingly, as the concentration of BMP9 in PAECs increased, its signaling decreased.

Additionally, increasing BMP10 concentration in BMP9-induced PAECs reduced BMP9-mediated SMAD 1/5/8 signaling and its proliferative effect. This finding is intriguing since one study demonstrated that plasma BMP10 levels are significantly higher than plasma BMP9 levels in PAH patients [54], this might suggest that receptor binding competition exists and BMP10 can compete with BMP9 for type II receptor binding.

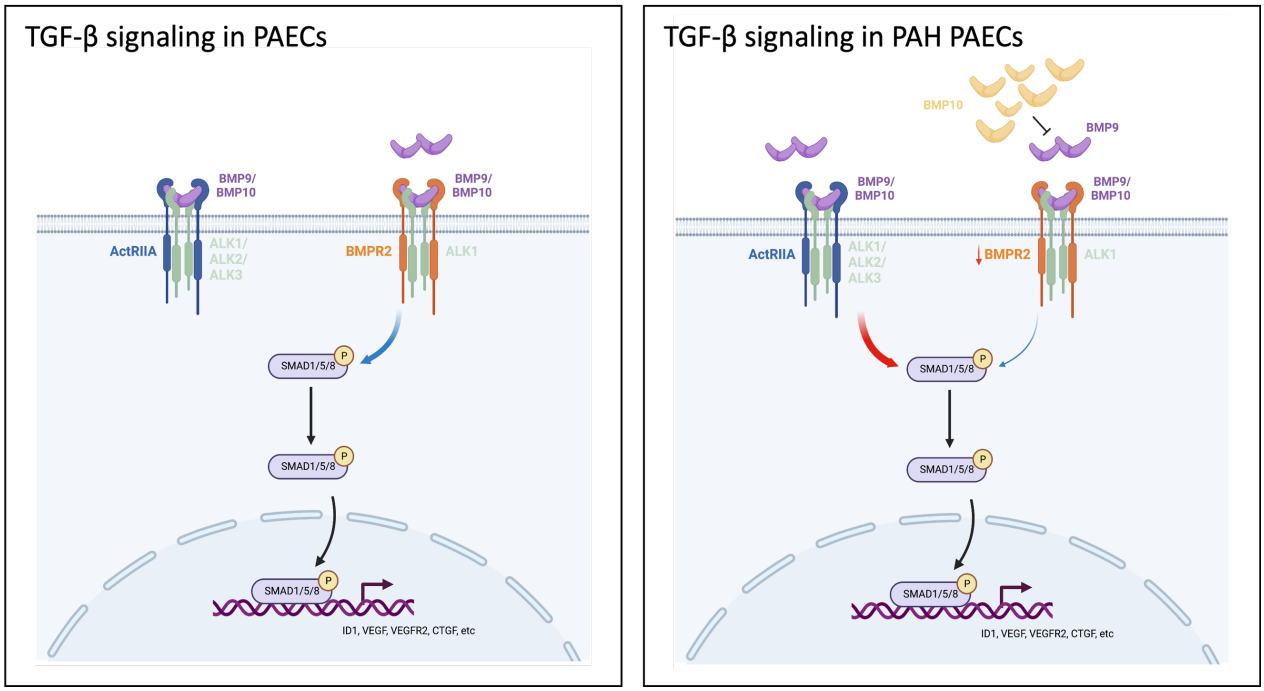


Figure 3.7: Proposed model for TGF-β signaling in PAH PAECs. In healthy PAECs (right), BMP9 and BMP10 specifically signal via BMPR2/ALK1 to induce SMAD 1/5/8 signaling and may potentially form a non-signaling complex with ActRIIA. In PAH PAECs (left), where BMPR2 expression levels are reduced, BMP9 and BMP10 shift their binding preference to ActRIIA for SMAD 1/5/8 signaling activation. Furthermore, excess BMP10 can function as a competitive inhibitor of BMP9 signaling, potentially further diminishing BMPR2-mediated signaling while enhancing ActRIIA-mediated signaling.

Based on our findings, we propose that BMP9 and BMP10 induce PAEC proliferation mainly through binding to BMPR2 for SMAD 1/5/8 signaling activation. However, ActRIIA takes over when BMPR2 levels are reduced. Furthermore, with an imbalance in plasma BMP9 and BMP10 levels, and higher BMP10 levels, BMP10 might potentially dominate SMAD 1/5/8 signaling via ActRIIA (Fig 3.7). This disruption of vascular homeostasis could lead to aberrant

PAEC proliferation in PAH.

## EXPERIMENTAL PROCEDURES

### Growth factors

Human TGFβ1 (P01137), BMP7 (P18075), BMP9 (Q9UK05) and GDF11 (O95390) were obtained from R&D Systems. Activin A (Q53T31), Activin B (Q53T31), and BMP10 (O95393) were produced in-house using stably transfected CHO cells. Activin A was captured from condition medium (CM) by Protein A affinity chromatography. BMP10 was captured from CM by Metal affinity chromatography (Excel, Cytiva). Both GF moieties were separated from the prodomain using Reversed Phase Chromatography (Resource RPC, Cytiva). Activin B was purified as described [55]. GFs were lyophilized and stored at −80 C.

### Receptor Fc fusions

Human BMPR2 cDNA (Q13873) and synthetic genes for human ActRIIA (P27037), ActRIIB (Q13705), ALK1 (P37023) and Bimagrumab (BiMab) were fused to human IgG1-Fc. Receptor-Fc fusion constructs included signal peptide and extracellular domains of human ActRIIA(1–120), ActRIIB(1–120), BMPRII(1–136), or ALK1(1-118). Extracellular domains were linked to a C-terminal human IgG1-Fc via a 22-amino acid-long linker containing TEV and enterokinase cleave sites. Fusion proteins and BiMab were expressed in stably transfected CHO cells and purified from CM using Protein A affinity chromatography as described followed by size exclusion chromatography in phosphate-buffered saline, pH 7.5. Purified proteins were stored at −80 °C. Purity of receptor-Fc fusion proteins was determined by SDS-PAGE under reducing and non-reducing conditions. NCBI-protein accession numbers are shown in parentheses.

**Small Molecule Inhibitors**

LDN-193189 was purchased from Biovision. Samples were reconstituted in DMSO according to the manufactures' instructions.

**Cell lines**

Human primary pulmonary arterial endothelial cells (CC-2530) were obtained from LONZA (Basel, Switzerland). Cells were maintained as per supplier's instructions. PAECs were grown in American Type Culture Collection (ATCC) vascular cell basal medium (PCS-100-030) supplemented with Endothelial Cell Growth Kit-VEGF (PCS-100-041) and 1% penicillin/streptavidin. Passage 2-10 were used for conducting experiments. Human embryonic kidney cells (CRL-1573) were obtained from ATCC. Cells were grown in Eagle's minimum essential medium (EMEM) supplemented with 10% fetal bovine serum and 1% penicillin/streptavidin. Passage 5 cells were transfected with the SMAD2/3 responsive reporter plasmid pGL4.48 (luc2P/SMAD binding element (SBE)/HYGRO) or the SMAD1/5/8 responsive reporter plasmid pGL4 (luc2P/2X BMP responsive element (BRE)/PURO) using lipofectamine 2000 and subjected to hygromycin B (50 μg/ml) or puromycin (0.5 μg/ml) selection. Passage 8 SBE reporter cell pools were cryopreserved. BRE reporter cells were subjected to clonal selection and single clones were cryopreserved at passage 11. Both cells were grown at 37 °C under a humidified 5% CO2 atmosphere. All freshly thawed cells were passaged twice before performing assays.

**Reporter assays**

50,000 SBE or 10,000 BRE reporter cells per well were seeded in 96-well plates and grown overnight in complete EMEM medium. After 24hr incubation, medium was replaced by assay medium (serum-free EMEM, 5 nM GFs and 0–300 nM receptor-Fc fusion or BiMab). GFs with

receptor-Fc fusion was incubated at room temperature for 1hr before addition to cells. Or cells were pre-treated with BiMab for 30min at 37 °C, followed by the addition of GFs with BiMab. For receptor overexpression transfections, assay medium containing growth medium without penicillin/streptavidin, in addition of 0.3 μL/well of TransIT®-293 Transfection Reagent (Mirus) with combination of 50 ng myc tagged ALK1, ALK2, or ALK3 plasmid and 50 ng HA-tagged BMPR2, ActRIIA, or ActRIIB plasmid were added in the cells. Control cells were transfected with 100 ng CMV vector. After 24hrs, cells were washed with free serum EMEM, and then treated with tested proteins in free serum EMEM. Luciferase expression was measured using a luciferase assay reagent after cells were incubated 16hr in assay medium. Firefly luciferase activity was measured using a FLUOstar Omega plate reader. Reporter gene assays were performed in triplicates and were repeated multiple times. Data presented is the mean of three independent measurements. Error bars represent the SD from three independent measurements. GraphPad Prism 9.3 was used for data fitting, analysis, and for generating graphs.

**Cell proliferation assay**

For the assessment of PAEC proliferation, cells were seeded at ~35,000 cells/well in 24 wells plates and grown overnight in complete medium as described in the **cell line** section. Cells were serum-restricted in vascular basal medium with Endothelial Cell Growth Kit-BBE (PCS-100-040) containing 0.5% FBS overnight. Cells were then treated with 10ng/mL BMP7, BMP9, BMP10, Activin A, Activin B, GDF11, or TGF-β1. For SMAD 1/5/8 signaling inhibition study, cells were treated with 10ng/mL of BMP9 or BMP10, with or without 1uM of LDN-193189. For receptor specificity studies, cells were pre-incubated with 300 nM BiMab in the corresponding wells for 30mins, and then treated with 10ng/mL of BMP9 or BMP10, with or without 300nM BiMab. Cells were incubated at 37°C overnight and cell proliferation was evaluated using the

BrdU Cell Proliferation Asssay Kit (#6813, Cell Signaling Technology). Briefly, cells were incubated with 1X bromodeoxyuridine (BrdU) for 24hr at 37 °C and fixed for 30 mins the next day at room temperature (RT). The fixing solution is removed and cells were incubated with 1X detection antibody solution for 1hr at RT. Cells were washed three times and incubated with 1X HRP-conjugated secondary antibody solution for 30 mins at RT, cells were washed again three times and TMB Substrate was added until the addition of STOP solution after 30 mins of incubation. Absorbance at 450nM was measured using a FLUOstar Omega plate reader. Cell proliferation assays were performed in three biological replicates and repeated multiple times. Error bars represent the SD from three independent measurements. GraphPad Prism 9.3 was used for data fitting, analysis, and for generating graphs.

**SiRNA transfection**

PAECs were seeded at ~ 40,000 cells/well in 24 wells plates and grown overnight in complete medium. After 24hr incubation, cells were maintained in Optimem serum free medium (Life Technologies) for 2 hours prior to the addition of Dharmafect 1 transfection reagent with or without siRNAs for BMPR2 or ON-TARGETplus Non-targeting Control siRNAs 1 (Dharmafect) for 4 hours. After transfection, cells were returned to complete medium with 10% FBS without penicillin/streptavidin. For signaling assays, cells were starved in assay medium (vascular basal medium with BBE kit containing no FBS and no penicillin/streptavidin) for 2hrs until the cells were treated with tested proteins in assay medium or 30 mins at 37 °C. Cells lysates were collected for immunoblotting. For proliferation study, it follows the protocol for BrdU cell proliferation assay protocol as described.

**Immunoblotting**

For signaling and expression studies, PAECs were seeded at ~200,000 cells/well in 6 wells

plates and grown overnight in complete medium as described in the **cell line** section. Cells were serum-starved in assay medium (vascular basal medium with Endothelial Cell Growth Kit-BBE without FBS) overnight. Cells were treated under the same conditions as the cell proliferation assay. After 30mins at 37°C, cells were lysed in ice-cold RIPA lysis buffer containing 150 mm NaCl, 1% Nonidet P-40, 0.1% SDS, 0.5% sodium deoxycholate, 50 mm Tris, pH 8.0, 1× "Recom Protease Arrest" protease inhibitor mixture (G-Biosciences) and 2× "Phosphatase Arrest" phosphastase inhibitor mixture (G-Biosciences). Cell lysates were stored at −80 °C. Protein concentration of lysates was determined using BCA assay. For Western blot, equal amounts of protein (5 μg) were separated under reducing conditions on TGS-polyacrylamide gels (Bio-Rad) and transferred to Hybond-P membranes (GE Healthcare). Membranes were blocked with Membranes were blocked with Superblock (Thermofisher) and incubated with primary antibodies at a 1:1000 dilution, including mouse monoclonal anti-BMPR2 (1F12, Abcam), goat polyclonal anti-ActRIIA (AF340), anti-ActRIIB (AF339, all R&D system), rabbit monoclonal anti-phospho-SMAD2 (138D4), or anti-phospho-SMAD1/5 (41D10, all Cell Signaling Technology), and followed by incubation with Horseradish peroxidase conjugated secondary antibody at 1:5000 dilution. As a loading control, all blots were re-probed with a monoclonal antibody towards either anti-β-actin (8H10D10) or anti-GAPDH (D16H11, Cell Signaling Technology), Western Bright ECL HRP substrate was used for detection (Advansta). Blots were visualized using autoradiography film. Densitometry was performed using ImageJ software.

## REFERENCES


1. Zhang, Y., P.B. Alexander, and X.F. Wang, *TGF-beta Family Signaling in the Control of Cell Proliferation and Survival.* Cold Spring Harb Perspect Biol, 2017. **9**(4).

2. Kubiczkova, L., et al., *TGF-beta - an excellent servant but a bad master.* J Transl Med, 2012. **10**: p. 183.

3. Dong, M. and G.C. Blobe, *Role of transforming growth factor-beta in hematologic malignancies.* Blood, 2006. **107**(12): p. 4589-96.

4. Miyazawa, K., et al., *Two major Smad pathways in TGF-beta superfamily signalling.* Genes Cells, 2002. **7**(12): p. 1191-204.

5. Goebel, E.J., et al., *Structural biology of the TGFbeta family.* Exp Biol Med (Maywood), 2019. **244**(17): p. 1530-1546.

6. Hinck, A.P., T.D. Mueller, and T.A. Springer, *Structural Biology and Evolution of the TGF-beta Family.* Cold Spring Harb Perspect Biol, 2016. **8**(12).

7. Aykul, S. and E. Martinez-Hackert, *Transforming Growth Factor-beta Family Ligands Can Function as Antagonists by Competing for Type II Receptor Binding.* J Biol Chem, 2016. **291**(20): p. 10792-804.

8. Chu, K.Y., et al., *Type II BMP and activin receptors BMPR2 and ACVR2A share a conserved mode of growth factor recognition.* J Biol Chem, 2022. **298**(7): p. 102076.

9. Chang, C., *Agonists and Antagonists of TGF-beta Family Ligands.* Cold Spring Harb Perspect Biol, 2016. **8**(8).

10. Xu, X., et al., *Transforming growth factor-beta in stem cells and tissue homeostasis.* Bone Res, 2018. **6**: p. 2.

11. Ma, J., et al., *TGF-beta-Induced Endothelial to Mesenchymal Transition Is Determined by a Balance Between SNAIL and ID Factors.* Front Cell Dev Biol, 2021. **9**: p. 616610.

12. Badesch, D.B., et al., *Diagnosis and assessment of pulmonary arterial hypertension.* J Am Coll Cardiol, 2009. **54**(1 Suppl): p. S55-S66.

13. Pousada, G., et al., *Mutational and clinical analysis of the ENG gene in patients with pulmonary arterial hypertension.* BMC Genet, 2016. **17**(1): p. 72.

14. Austin, E.D. and J.E. Loyd, *Heritable forms of pulmonary arterial hypertension.* Semin Respir Crit Care Med, 2013. **34**(5): p. 568-80.

15. Austin, E.D., J.A. Phillips, III, and J.E. Loyd, *Heritable Pulmonary Arterial Hypertension Overview*, in *GeneReviews((R))*, M.P. Adam, et al., Editors. 1993: Seattle (WA).

16. Welch, C.L. and W.K. Chung, *Genetics and Genomics of Pediatric Pulmonary Arterial Hypertension.* Genes (Basel), 2020. **11**(10).

17. Fessel, J.P., J.E. Loyd, and E.D. Austin, *The genetics of pulmonary arterial hypertension in the post-BMPR2 era.* Pulm Circ, 2011. **1**(3): p. 305-19.

18. Rol, N., et al., *TGF-beta and BMPR2 Signaling in PAH: Two Black Sheep in One Family.* Int J Mol Sci, 2018. **19**(9).

19. Yndestad, A., et al., *Elevated levels of activin A in clinical and experimental pulmonary hypertension.* J Appl Physiol (1985), 2009. **106**(4): p. 1356-64.

20. Boehme, J., et al., *Pulmonary artery smooth muscle cell hyperproliferation and metabolic shift triggered by pulmonary overcirculation.* Am J Physiol Heart Circ Physiol, 2016. **311**(4): p. H944-H957.

21. Jia, Z., et al., *Pulmonary Vascular Remodeling in Pulmonary Hypertension.* J Pers Med, 2023. **13**(2).

22. David, L., et al., *Identification of BMP9 and BMP10 as functional activators of the orphan activin receptor-like kinase 1 (ALK1) in endothelial cells.* Blood, 2007. **109**(5): p. 1953-61.

23. Liu, D., et al., *Elevated Levels of Circulating Bone Morphogenetic Protein 7 Predict Mortality in Pulmonary Arterial Hypertension.* Chest, 2016. **150**(2): p. 367-73.

24. Calvier, L., et al., *Chronic TGF-beta1 Signaling in Pulmonary Arterial Hypertension Induces Sustained Canonical Smad3 Pathways in Vascular Smooth Muscle Cells.* Am J Respir Cell Mol Biol, 2019. **61**(1): p. 121-123.

25. Lambers, C., et al., *The interaction of endothelin-1 and TGF-beta1 mediates vascular cell remodeling.* PLoS One, 2013. **8**(8): p. e73399.

26. Yung, L.M., et al., *ACTRIIA-Fc rebalances activin/GDF versus BMP signaling in pulmonary hypertension.* Sci Transl Med, 2020. **12**(543).

27. Ryanto, G.R.T., et al., *An endothelial activin A-bone morphogenetic protein receptor type 2 link is overdriven in pulmonary hypertension.* Nat Commun, 2021. **12**(1): p. 1720.

28. Joshi, S.R., et al., *Sotatercept analog suppresses inflammation to reverse experimental pulmonary arterial hypertension.* Sci Rep, 2022. **12**(1): p. 7803.

29. Namwanje, M. and C.W. Brown, *Activins and Inhibins: Roles in Development, Physiology, and Disease.* Cold Spring Harb Perspect Biol, 2016. **8**(7).

30. Ryanto, G.R.T., et al., *Inactivating the Uninhibited: The Tale of Activins and Inhibins in Pulmonary Arterial Hypertension.* Int J Mol Sci, 2023. **24**(4).

31. Garcia-Alvaro, M., et al., *BMP9-Induced Survival Effect in Liver Tumor Cells Requires p38MAPK Activation.* Int J Mol Sci, 2015. **16**(9): p. 20431-48.

32. Eiraku, N., et al., *BMP9 directly induces rapid GSK3-beta phosphorylation in a Wnt-independent manner through class I PI3K-Akt axis in osteoblasts.* FASEB J, 2019. **33**(11): p. 12124-12134.

33. Yu, P.B., et al., *BMP type I receptor inhibition reduces heterotopic [corrected] ossification.* Nat Med, 2008. **14**(12): p. 1363-9.

34. Aykul, S., et al., *Smad2/3 Activation Regulates Smad1/5/8 Signaling via a Negative Feedback Loop to Inhibit 3T3-L1 Adipogenesis.* Int J Mol Sci, 2021. **22**(16).

35. Morvan, F., et al., *Blockade of activin type II receptors with a dual anti-ActRIIA/IIB antibody is critical to promote maximal skeletal muscle hypertrophy.* Proc Natl Acad Sci U S A, 2017. **114**(47): p. 12448-12453.

36. Machado, R.D., et al., *BMPR2 haploinsufficiency as the inherited molecular mechanism for primary pulmonary hypertension.* Am J Hum Genet, 2001. **68**(1): p. 92-102.

37. Thomson, J., et al., *Familial and sporadic primary pulmonary hypertension is caused by BMPR2 gene mutations resulting in haploinsufficiency of the bone morphogenetic protein tuype II receptor.* J Heart Lung Transplant, 2001. **20**(2): p. 149.

38. Nickel, J. and T.D. Mueller, *Specification of BMP Signaling.* Cells, 2019. **8**(12).

39. Martinez-Hackert, E., A. Sundan, and T. Holien, *Receptor binding competition: A paradigm for regulating TGF-beta family action.* Cytokine Growth Factor Rev, 2021. **57**: p. 39-54.

40. Mueller, T.D. and J. Nickel, *Promiscuity and specificity in BMP receptor activation.* FEBS Lett, 2012. **586**(14): p. 1846-59.

41. Piek, E., et al., *Functional antagonism between activin and osteogenic protein-1 in human embryonal carcinoma cells.* J Cell Physiol, 1999. **180**(2): p. 141-9.

42. Rebbapragada, A., et al., *Myostatin signals through a transforming growth factor beta-like signaling pathway to block adipogenesis.* Mol Cell Biol, 2003. **23**(20): p. 7230-42.

43. Katagiri, T. and T. Watabe, *Bone Morphogenetic Proteins.* Cold Spring Harb Perspect Biol, 2016. **8**(6).

44. Desroches-Castan, A., et al., *BMP9 and BMP10: Two close vascular quiescence partners that stand out.* Dev Dyn, 2022. **251**(1): p. 178-197.

45. Wang, P., et al., *Bone Morphogenetic Protein-9 Enhances Osteogenic Differentiation of Human Periodontal Ligament Stem Cells via the JNK Pathway.* PLoS One, 2017. **12**(1): p. e0169123.

46. Yuan, Y.M., et al., *BMP10 suppresses hepatocellular carcinoma progression via PTPRS-STAT3 axis.* Oncogene, 2019. **38**(48): p. 7281-7293.

47. Pascale, R.M., F. Feo, and D.F. Calvisi, *The complex role of bone morphogenetic protein 9 in liver damage and regeneration: New evidence from in vivo and in vitro studies.* Liver Int, 2018. **38**(9): p. 1547-1549.

48. Liu, W., et al., *Highly expressed BMP9/GDF2 in postnatal mouse liver and lungs may account for its pleiotropic effects on stem cell differentiation, angiogenesis, tumor growth and metabolism.* Genes Dis, 2020. **7**(2): p. 235-244.

49. Song, J.J., et al., *Bone morphogenetic protein-9 binds to liver cells and stimulates proliferation.* Endocrinology, 1995. **136**(10): p. 4293-7.

50. Neuhaus, H., V. Rosen, and R.S. Thies, *Heart specific expression of mouse BMP-10 a novel member of the TGF-beta superfamily.* Mech Dev, 1999. **80**(2): p. 181-4.

51. Tillet, E., et al., *A heterodimer formed by bone morphogenetic protein 9 (BMP9) and BMP10 provides most BMP biological activity in plasma.* J Biol Chem, 2018. **293**(28): p. 10963-10974.

52. Herrera, B. and G.J. Inman, *A rapid and sensitive bioassay for the simultaneous measurement of multiple bone morphogenetic proteins. Identification and quantification of BMP4, BMP6 and BMP9 in bovine and human serum.* BMC Cell Biol, 2009. **10**: p. 20.

53. Wang, L., et al., *BMP9 and BMP10 Act Directly on Vascular Smooth Muscle Cells for Generation and Maintenance of the Contractile State.* Circulation, 2021. **143**(14): p. 1394-1410.

54. Llucia-Valldeperas, A., et al., *Increased Bone Morphogenetic Protein 10 in Pulmonary Hypertension.* Circulation, 2022. **146**.

55. Schmelzer, C.H., et al., *Purification and characterization of recombinant human activin B.* Biochim Biophys Acta, 1990. **1039**(2): p. 135-41.

# CHAPTER 4

# CONCLUSION AND FUTURE DIRECTIONS

## FROM LIGAND TO SIGNALING: THE IMPORTANCE OF RECEPTOR BINDING IN BIOLOGICAL SIGNALING

Biological signaling is a fundamental process that enables cells and organisms to communicate, respond to their environment, and maintain homeostasis. Remarkably, a diverse array of signaling pathways cooperate to regulate numerous physiological functions in human cells. Examples include the Wnt/β-catenin, Notch, MAPK, JAK-STAT, NF-κB, and TGF-β pathways, among many others. These pathways engage in intricate crosstalk, contributing to the complexity of the biological signaling system.

Signaling pathways consist of a multitude of molecules, such as receptors, ligands, enzymes, and transcription factors, which collaboratively transmit and decode information in a highly coordinated manner. In general, a signaling pathway transmits signals through several stages: 1) initiation, during which growth factors (GF) bind to specific receptors on the target cell surface; 2) transduction, where the signal is relayed from the receptors to intracellular signaling molecules, typically via phosphorylation; and 3) integration, in which the cell processes multiple signaling inputs to generate an appropriate response.

Often, research has predominantly focused on downstream signaling, neglecting the crucial first step: signaling initiation. Examining receptor-binding interactions is just as important as investigating the downstream effects of signaling pathways. From a biochemical perspective, this enables us to understand how growth factors interact with receptors to activate signaling cascades. From a biological standpoint, this knowledge enhances our comprehension of pathophysiology and how alterations in pathway activation affect the dynamics of the entire signaling ecosystem, promoting disease progression. Overall, understanding the molecular mechanisms that underlie various physiological and pathological processes is crucial for identifying novel therapeutic targets

and developing innovative treatment strategies for a wide range of diseases. When we turn our attention to pulmonary arterial hypertension again, we encounter a highly intricate condition with unclear pathophysiology. Because of its complex etiology, PAH is probably caused by a variety of environmental and genetic factors. In Chapter 1, I mentioned that being female is considered one of the risk factors associated with PAH. Estrogen is thought to play a role in the development and progression of PAH. Women are more susceptible to PAH due to the fluctuation of estrogen levels throughout their lives, which are generally higher compared to men. According to a study, variations in estrogen metabolism, regulated by CYP1B1 polymorphism, may elevate the risk of familial PAH development in female carriers of BMPR2 mutations. It has been discovered that certain estrogen metabolites, particularly 4-OHE, have pro-proliferative effects. Therefore, an increased level of 4-OHE resulting from CYP1B1 alterations will raise the likelihood of PAH development in females [1]. It is crucial to enhance awareness regarding the diagnosis of PAH in females. Furthermore, through continued research efforts, there is potential to personalize treatments specifically for females with PAH.

In PAH, more than 400 mutations have been identified in the BMPR2 gene. Exploring the fact that missense mutations tend to have a worse prognosis compared to nonsense mutations is an intriguing topic. This observation can be explained by several factors. Firstly, proteins carrying missense mutations are often less stable and exhibit more structural defects compared to proteins truncated by nonsense mutations. Secondly, missense mutations may interfere with the normal function of the wild-type protein, exerting a dominant negative effect. A third possibility is that nonsense mutations are more likely to trigger nonsense-mediated decay, a process that degrades mRNA with premature stop codons. This limits the production of mutant proteins, whereas missense mutations are less effective in activating this protective mechanism, resulting in a higher

number of potentially disruptive variants. It's important to note that the location of the mutations also plays a significant role in affecting protein function. Although numerous missense mutations at GBD have been identified, their specific consequences remain unknown. In Chapter 2, we investigated eight GBD variants and tested their ability to bind and interact with BMP10 and Activin B. Variants within the hydrophobic hotspot fail to bind to both growth factors indicating that mutations of these residues interrupt the shape of the GF-binding interface and therefore hindered GF binding. In contrast, variants in peripheral loop areas remained active. Consequently, there is a potential for a gain of function. One hypothesis is that these peripheral mutations influence the stability of BMPR2 and enhance the affinity of a specific GF to the receptor, thereby facilitating abnormal PAEC proliferation. To test this hypothesis, one possible approach is to transfect PAECs with BMPR2 mutant plasmids and compare them to non-transfected cells. Subsequently, the cells can be treated with different GFs, such as Activin A, Activin B, BMP9, BMP10, and TGF-β1. By examining the resulting signaling alterations and the proliferative capacity of GFs in PAECs with overexpressed BMPR2 variants, we can gain further insights into the effects of these mutations. In Chapter 3, I focused on the role of BMPR2-mediated signaling in PAH. The proliferation of PAECs and PASMCs is one of the major factors contributing to pulmonary vasculature remodeling in PAH. This abnormal cell growth can lead to the narrowing and obstruction of blood vessels, increased pulmonary vascular resistance, and ultimately, right heart failure [2]. The general proposed mechanism is that endothelial cell dysfunction can lead to the activation of several cellular signaling pathways in the endothelium along with other stress factors, resulting in the uncontrolled proliferation of PAECs and PASMCs [3]. And the imbalance of TGF-β signaling and BMP signaling may be the main culprit for this aberrant cell growth in PAH [4, 5]. In Chapter 3, a couple of questions have been addressed, including what growth factors

are involved in PAEC proliferation, which receptors and the downstream SMAD signaling are associated with the GF-induced PAEC proliferation and whether there are any signaling changes with reduced levels of BMPR2 in PAEC. Some results may appear counterintuitive, leading to more questions arise. The common belief suggests that most BMPR2 mutations are associated with loss of function. However, my findings have demonstrated that BMP9 and BMP10 actually stimulate the proliferation of PAECs through BMPR2 signaling. This raises the question: why do BMPR2 mutations contribute to the hyper-proliferation of PAECs in PAH? One hypothesis is that BMPR2 mutations might trigger a compensatory upregulation of other receptors or pathways that promote PAEC proliferation. Since BMPR2 mutation is heterozygous, it could lead to an increase in its expression. Consequently, more wild-type BMPR2 is produced, exacerbating the proliferation of PAECs. Another hypothesis is that BMP9 and BMP10 may activate signaling through ActRIIA when BMPR2 expression is reduced, as discussed in Chapter 3. This suggests that alternative pathways or receptors could be involved in mediating the proliferative effects of BMP9/10 when BMPR2 function is compromised. Remarkably, we found that BMP10 can act as a competitive inhibitor for BMP9 signaling. Since one study demonstrated that plasma BMP10 levels are significantly higher than plasma BMP9 levels in PAH patients [6], this might suggest that receptor binding competition exists and BMP10 can compete with BMP9 for type II receptor binding. This suggests the existence of receptor binding competition, wherein BMP10 competes with BMP9 for binding to the type II receptor. However, the situation becomes perplexing when we consider that treating PAECs with BMP10 alone induces proliferation while inhibiting BMP9 signaling and BMP9-induced proliferation. Consequently, based on this information, one would expect that increasing BMP10 levels would decrease cell proliferation rather than enhance it.

Currently, the role of BMP10 in cell proliferation lacks sufficient research. The conundrum

may be attributed to the context-dependent and pleiotropic effects of BMP10. While BMP10 can inhibit BMP9 signaling *in vitro*, within the intricate *in vivo* environment of the diseased pulmonary artery, BMP10 might activate other pathways to promote proliferation. Additionally, there could be a temporal aspect to BMP10's effects. It is plausible that initially, BMP10 inhibits BMP9-induced proliferation. However, over time, BMP10 accumulates and initiates proliferation through its own signaling pathway. Notably, according to my observation, while BMP10's signal persists even after 48 hours, BMP9's signal diminishes after 24 hours. This temporal difference suggests that, with time, BMP10 takes over the role of BMP9 in PAEC proliferation. Further studies need to be done to elicit the relationship between BMP9 and BMP10.

The goal of most research is eventually to develop effective treatments. Sotatercept, a recombinant fusion protein that consists of the extracellular domain of ActRIIA linked to the Fc portion of human IgG, is currently undergoing phase 3 clinical trial for PAH. As a ligand trap, it sequesters specific TGF-β growth factors, preventing their binding to cell surface receptors and inhibiting their signaling. However, the exact mechanism by which it reverses pulmonary vascular remodeling in PAH remains uncertain. Studies have shown Sotatercept reduces pulmonary vascular resistance among PAH patients and improves their outcomes, like exercise capacity. Nonetheless, there are some adverse effects including an increase in hemoglobin levels, telangiectasia and epistaxis [7]. These side effects can be associated with a related condition called hereditary hemorrhagic telangiectasia (HHT), which can be caused by mutations in multiple genes, including BMP9. Mutations in BMP9 can result in various symptoms, including nosebleeds, skin telangiectasis, and arteriovenous malformations, due to abnormal blood vessel formation and remodeling [8]. Therefore Sotatercept may induce a phenocopy of BMP9 mutation. Several experiments can be conducted to test this hypothesis. For instance, the effects of Sotatercept on

BMP9-induced proliferation can be examined in wild-type PAECs or in BMPR2 knockdown cells. Additionally, mouse models with BMP9 mutations can be generated, and wild-type mice can be treated with Sotatercept to compare phenotypes such as pulmonary pressure and vessel remodeling. Furthermore, PAECs can be isolated from these mice to compare the transcription levels of BMP9 target genes. If this hypothesis holds true, it could provide valuable insights into the pathophysiology of PAH. Sotatercept's ability to trap BMP9 and impair its signaling under conditions of reduced BMPR2 levels suggests a potential mechanism of action. However, since Sotatercept can also trap other TGF-β growth factors, further studies are necessary to investigate its effects on different growth factors that may be associated with the pathophysiology of PAH. Overall, further research is crucial to advance the development of personalized therapeutics for PAH patients with improved safety profiles compared to Sotatercept.

**FUTURE DIRECTIONS**

The work presented in this thesis demonstrated that TGF-beta family ligands BMP9 and BMP10 bind to BMPR2 to induce SMAD 1/5/8 signaling, promoting PAEC proliferation. However, numerous questions remain unanswered regarding how they induce PAEC proliferation, as well as the mechanism underlying aberrant cell growth in PAH. A few key questions to consider include: What downstream cell proliferation genes do BMP9 and BMP10 activate for transcription? Is SMAD 2/3 signaling activated in BMPR2 knockdown PAECs by growth factors that are well known to activate this pathway, or is SMAD 2/3 signaling activated by growth factors that typically stimulate SMAD1/5/8 signaling instead? Are there any non-canonical signaling pathways activated by BMP9 and BMP10, other than the SMAD 1/5/8 signaling pathway, in both PAECs and BMPR2 knockdown PAECs, which contribute to vascular cell proliferation in PAH?

To answer these questions, more studies should be carried out. To investigate the potential

activation of downstream cell proliferation genes by BMP9 and BMP10, we can perform gene expression profiling by treating PAECs with these proteins and conducting mRNA seq to measure the mRNA levels of proliferation-associated genes, such as Cyclin D1, c-Myc, epidermal growth factor receptor (EGFR), vascular endothelial growth factor (VEGF) and platelet-derived growth factor (PDGF). Additionally, we can explore the change in the expression of these genes upon BMPR2 knockdown in PAECs treated with BMP9 and BMP10 using immunoblotting. Furthermore, using LDN-193189 to inhibit SMAD 1/5/8 signaling will allow us to examine the direct effect of canonical signaling on the expression of these cell proliferation target genes. To address the second proposed question, which asks if and how SMAD 2/3 signaling is activated in BMPR2 knockdown PAECs, we can first knockdown BMPR2 in PAECs and investigate the pathway activation by examining the phosphorylation of SMAD 2/3 using immunoblotting. We can treat the BMPR2 knockdown PAECs with BMP9, BMP10, and SMAD 2/3 growth factors, such as Activin A, Activin B, TGF-β1, Nodal, and GDF11. In normal PAECs, we observed no activation of SMAD 2/3 signaling upon treatment with Activin A, Activin B, TGF-β1, and GDF11. However, with reduced BMPR2 levels, these factors may induce SMAD 2/3 signaling, and we can investigate their proliferation effects on PAECs. Moreover, one study has demonstrated that BMP9 can induce SMAD 2/3 signaling in human microvascular endothelial cells (HMVEC-LBl), suggesting that it might bind to ActRIIA and activate SMAD 2/3 signaling in siBMPR2-transfected PAECs [9, 10]. We can further investigate whether BMP9 and BMP10 activate any non-canonical signaling pathways, aside from the SMAD 1/5/8 pathway, in PAEC as well as in BMPR2 knockdown PAEC. To do this, we can utilize kinase array assays, a high-throughput technique that detects the activation of multiple kinases in cells via phosphorylation, to identify potential non-canonical signaling pathways that BMP9 and BMP10 might activate in PAECs. It is a very

powerful tool since it is capable of detecting the phosphorylation of over 40 kinases, including Akt, c-Jun, Erk, JNK, MAPKs, and mTOR. To further examine the impact of BMP9 and BMP10 activated non-canonical signaling pathways on PAEC proliferation, we can use specific inhibitors, such as SB203580 to target the p38 pathway or U0126 to target the ERK signaling pathway. If these pathways are involved in BMP9 and BMP10-induced PAEC proliferation, we expect to observe a decrease in proliferation in the presence of these inhibitors. Overall, the three proposed questions contribute to elucidating the specific molecular targets and mechanisms by which BMP9 and BMP10 contribute to pulmonary vascular remodeling, revealing the impact of BMPR2 deficiency on SMAD2/3 signaling to potentially uncover the involvement of other TGF-β family members, and expanding our knowledge of the interplay between canonical and non-canonical signaling pathways in PAH development and progression. These research directions aim to deepen our understanding of the role of TGF-β signaling in PAH-associated cell proliferation, potentially leading to the identification of novel therapeutic targets and strategies for managing this debilitating disease.

## CLOSING REMARKS

It's truly fascinating how the molecular basis of a signaling pathway can be linked to the pathophysiology of a disease, leading to remarkable advancements in treatment options. This link underscores the importance of biochemical studies, transitioning from in vitro experiments to in vivo research, progressing through clinical trials and ultimately, turning into bedside patient care.

## REFERENCES


1. Austin, E.D., et al., *Alterations in oestrogen metabolism: implications for higher penetrance of familial pulmonary arterial hypertension in females.* Eur Respir J, 2009. **34**(5): p. 1093-9.

2. Shimoda, L.A. and S.S. Laurie, *Vascular remodeling in pulmonary hypertension.* J Mol Med (Berl), 2013. **91**(3): p. 297-309.

3. Kurakula, K., et al., *Endothelial Dysfunction in Pulmonary Hypertension: Cause or Consequence?* Biomedicines, 2021. **9**(1).

4. Gore, B., et al., *Key role of the endothelial TGF-beta/ALK1/endoglin signaling pathway in humans and rodents pulmonary hypertension.* PLoS One, 2014. **9**(6): p. e100310.

5. Rol, N., et al., *TGF-beta and BMPR2 Signaling in PAH: Two Black Sheep in One Family.* Int J Mol Sci, 2018. **19**(9).

6. Llucia-Valldeperas, A., et al., *Increased Bone Morphogenetic Protein 10 in Pulmonary Hypertension.* Circulation, 2022. **146**.

7. Humbert, M., et al., *Sotatercept for the treatment of pulmonary arterial hypertension: PULSAR open-label extension.* Eur Respir J, 2023. **61**(1).

8. Wooderchak-Donahue, W.L., et al., *BMP9 mutations cause a vascular-anomaly syndrome with phenotypic overlap with hereditary hemorrhagic telangiectasia.* Am J Hum Genet, 2013. **93**(3): p. 530-7.

9. Star, G.P., M. Giovinazzo, and D. Langleben, *Bone morphogenic protein-9 stimulates endothelin-1 release from human pulmonary microvascular endothelial cells: a potential mechanism for elevated ET-1 levels in pulmonary arterial hypertension.* Microvasc Res, 2010. **80**(3): p. 349-54.

10. Holtzhausen, A., et al., *Novel bone morphogenetic protein signaling through Smad2 and Smad3 to regulate cancer progression and development.* FASEB J, 2014. **28**(3): p. 1248-67.